

FINAL REPORT
For the Florida Department of Transportation

Effects of Aggregate Gradation, Aggregate Type, and SBS Polymer-Modified Binder on Florida HMAC Fracture Energy Properties

FDOT Research Contract No.: BD-543-20

FSU Research Project No.: OMNI 021037

by

Principal Investigator: W. V. Ping, P.E.

Research Assistant: Yuan Xiao

Department of Civil & Environmental Engineering
Florida A&M University – Florida State University
COLLEGE OF ENGINEERING
Tallahassee, FL 32310

March 2009

DISCLAIMER

The opinions, findings and conclusions expressed in this publication are those of the authors and not necessarily those of the State of Florida Department of Transportation or the U.S. Department of Transportation. This report is prepared in cooperation with the State of Florida Department of Transportation and the U.S. Department of Transportation.

METRIC CONVERSIONS

inches = 25.4 millimeters

feet = 0.305 meters

square inches = 645.1 millimeters squared

square feet = 0.093 meters squared

cubic feet = 0.028 meters cubed

pounds = 0.454 kilograms

poundforce = 4.45 newtons

poundforce per square inch = 6.89 kilopascals

pound per cubic inch = 16.02 kilograms per meters cubed

1 psi = 6.89475 kPa

1/psi = 0.145×10^6 /GPa

				Technical Report Documentation Page	
1. Report No.		2. Government Accession No.		3. Recipient's Catalog No.	
4. Title and Subtitle Effects of Aggregate Gradation, Aggregate Type, and SBS Polymer-Modified Binder on Florida HMAC Fracture Energy Properties		5. Report Date March 2009		6. Performing Organization Code	
7. Author(s) W. V. Ping and Yuan Xiao		8. Performing Organization Report No. FSU C&G No. OMNI 021037			
9. Performing Organization Name and Address FAMU-FSU College of Engineering Department of Civil & Environmental Engineering 2525 Pottsdamer Street Tallahassee, Florida 32310-6046		10. Work Unit No. (TRAIS)		11. Contract or Grant No. FDOT BC-543-20	
12. Sponsoring Agency Name and Address Florida Department of Transportation Research Center, MS30 605 Suwannee Street Tallahassee, Florida 32399-0450		13. Type of Report and Period Covered Final Report April 2007 - March 2009		14. Sponsoring Agency Code	
15. Supplementary Notes Prepared in cooperation with the Federal Highway Administration, U.S. Department of Transportation					
16. Abstract The primary objective of this research study was to evaluate the fracture mechanics properties of HMA concrete for Superpave mixtures. An experimental program was performed on asphalt mixtures with various types of materials. The laboratory testing program was developed by applying the viscoelastic fracture mechanics-based framework that appeared to be capable of describing the whole mechanical properties of HMA according to past research studies at University of Florida. The goals for these experiments are to evaluate the effect of aggregate type, the effect of coarse aggregate gradation adjustment to control mix designs, and the effect of SBS polymer on fracture mechanics properties of HMA mixtures. Two standard coarse mixes were selected as control levels for fracture mechanics tests: one granite mixture and one limestone mixture. Each control mix design was modified to two different gradation levels with the control asphalt binder (PG 67 22) and three SBS polymer content levels (3.0%, 4.5%, and 6.0%) with the original aggregate gradation. Evaluation of the test results indicated the increase of nominal maximum aggregate amount by 5% to 15% to the standard coarse mix designs had negligible effect on HMA fracture mechanics properties. The SBS polymer-modified asphalt binder improved the fracture mechanics behavior of asphalt mixtures comprehensively. The limestone materials seemed to hold advantages over the granite materials in improving the performance of thermal cracking at low service temperatures and the rutting resistance at high service temperatures.					
17. Key Words hot mix asphalt, gradation, SBS polymer, resilient modulus, creep, tensile strength, fracture energy		18. Distribution Statement This document is available to the public through the National Technical Information Service, Springfield, Virginia, 22161			
19. Security Classif. (of this report) Unclassified		20. Security Classif. (of this page) Unclassified		22. Price	
21. No. of Pages					
Form DOT F 1700.7 (8-72) PF V2.1, 12/13/93		Reproduction of completed page authorized			

ACKNOWLEDGEMENTS

Funding for this research was provided by the Florida Department of Transportation (FDOT) and Federal Highway Administration (FHWA) through the Research Center of the FDOT. This research was initiated by Bruce Dietrich, State Pavement Design Engineer, with the FDOT.

Engineers and staff at the Pavement and Bituminous Section of the FDOT State Materials Office provided significant support to this research study. Mariani Asphalt Company, through the assistance of Kevin Hardin and his associates, provided the SBS polymer-modified asphalt binders without charge and also provided classification results to the research. The FDOT Research Center, through the assistance of Richard Long and his staff, provided financial and contractual support.

The laboratory testing program was carried out by Ed Mallory. The base asphalt binder was provided without charge by C. W. Roberts Contracting Company.

TABLE OF CONTENTS

LIST OF TABLES.....	viii
LIST OF FIGURES	ix
EXECUTIVE SUMMARY	xii
CHAPTER 1 INTRODUCTION.....	1
1.1 Background	1
1.2 Objectives	2
1.3 Report Outline	3
CHAPTER 2 LITERATURE REVIEW	4
2.1 Introduction	4
2.2 Asphalt Cement Properties.....	4
2.3 Hot Mix Asphalt (HMA) Mixture Design.....	19
2.4 Mechanical Tests for Characterization of Asphalt Mixtures.....	31
2.5 HMA Fracture Mechanics Concepts	36
CHAPTER 3 MATERIALS AND EXPERIMENTAL PROGRAM.....	42
3.1 General	42
3.2 Mix Designs and Aggregate Gradation Modifications.....	42
3.3 SBS Polymer-modified Asphalt Binder	43
3.5 Specimen Preparation and Volumetric Properties.....	47
3.6 Test Procedures	48
3.7 Testing Program	52
CHAPTER 4 FRACTURE MECHANICS PROPERTIES FROM IDT	55
4.1 Resilient Modulus Testing Procedures and Results	55
4.2 Creep Compliance Testing Procedures and Results.....	61
4.3 Tensile Strength Testing Procedures and Results	61
CHAPTER 5 EVALUATION OF FRACTURE MECHANICS PROPERTIES	68
5.1 Aggregate Gradation Effects	68
5.2 SBS Polymer-modified Binder Effects	81
5.3 Effect of Aggregate Type	101
5.4 Summary of Analysis and Findings from Fracture Mechanics Tests.....	106
CHAPTER 6 SUMMARY AND CONCLUSIONS.....	109

6.1 Summary	109
6.2 Findings and Conclusions	110
6.3 Recommendations	112
APPENDIX A LABORATORY ANALYSIS REPORTS	113
APPENDIX B CREEP COMPLIANCE TEST RESULTS	118
REFERENCES.....	128

LIST OF TABLES

Table 2-1: Generic classification of asphalt additives and modifiers (Roberts et al. 1996)	7
Table 2-2: Chosen unit weight ranges by mix type	26
Table 2-3: Recommended aggregate ratios.....	28
Table 3-1: Number of specimens prepared.....	47
Table 3-2: Specimens tested for fracture mechanics properties	48
Table 3-3: Specific gravities and air voids of the mixtures	48
Table 4-1: Resilient modulus test results at -10°C (SI units).....	57
Table 4-2: Resilient modulus test result at -10°C (English units)	57
Table 4-3: Resilient modulus test results at 5°C (SI units).....	58
Table 4-4: Resilient modulus test result at 5°C (English units).....	58
Table 4-5: Resilient modulus test results at 25°C (SI units).....	59
Table 4-6: Resilient modulus test result at 25°C (English units).....	59
Table 4-7: Resilient modulus test results at 40°C (SI units).....	60
Table 4-8: Resilient modulus test result at 40°C (English units).....	60
Table 4-9: Tensile strength test results for F2 series mixtures (SI units)	64
Table 4-10: Tensile strength test results for F2 series mixtures (English units).....	65
Table 4-11: Tensile strength test results for F4 series mixtures (SI units)	66
Table 4-12: Tensile strength test results for F4 series mixtures (English units).....	67
Table 5-1: Power law regression coefficients for modified gradation mixes	70
Table 5-2: Power model regression coefficients for modified gradation tests	73
Table 5-3: Power model regression coefficients for PMA mixture tests.....	85
Table A-1: Lab analysis report for 0.0% polymer base asphalt (Graded as PG67-22).....	113
Table A-2: Lab analysis report for 3.0% polymer asphalt (Graded as PG76-22).....	114
Table A-3: Lab analysis report for 4.5% polymer asphalt (Graded as PG82-22).....	115
Table A-4: Lab analysis report for 6.0% polymer asphalt (Graded as PG82-28).....	116
Table A-5: Gradations for F2C and its adjustments	117
Table A-6: Gradations for F4C and its adjustments	117
Table B-1: Creep compliance test results at -10°C (1/GPa)	118
Table B-2: Creep compliance test results at -10°C (1/psi).....	118
Table B-3: Creep compliance test results at 5°C (1/GPa).....	119
Table B-4: Creep compliance test results at 5°C (1/psi).....	119
Table B-5: Creep compliance test results at 25°C (1/GPa).....	120
Table B-6: Creep compliance test results at 25°C (1/psi).....	120
Table B-7: Creep compliance test results at 40°C (1/GPa).....	121
Table B-8: Creep compliance test results at 40°C (1/psi).....	121

LIST OF FIGURES

Figure 2-1: Polymer classifications based on link structure	9
Figure 2-2: SBS polymer modifier structure	9
Figure 2-3: Complex modulus of styrene-butadiene-styrene-modified asphalt at 60°C (Chen et al. 2002)	11
Figure 2-4: Relationship between the observed critical cracking temperature (T_{cr}) and SBS polymer concentration (Collins et al. 1991)	13
Figure 2-5: Comparison of the rut depths measured on sections with PMA and the companion sections without PMA mixtures (van Quintus et al. 2007).....	14
Figure 2-6: Components of complex modulus G^*	16
Figure 2-7: Viscous and elastic behavior of asphalt binders	16
Figure 2-8: Dynamic shear rheometer	17
Figure 2-9: Stress-strain response of viscoelastic material.....	17
Figure 2-10: Typical aggregate gradations.	21
Figure 2-11: The four principles of Bailey method for coarse-graded mix	26
Figure 2-12: Combined blend evaluation for coarse-graded mixes.....	27
Figure 2-13: Combined blend evaluation for fine-graded mixes.....	27
Figure 2-14: Illustration of gradation requirements for 12.5 mm (1/2 in.) nominal size.....	31
Figure 2-15: Indirect diametral test during loading and at failure	33
Figure 2-16: Theoretical stress distribution on horizontal diametral plane for indirect tensile test (After Yoder et al. 1975).....	35
Figure 2-17: Theoretical stress distribution on vertical diametral plane for indirect tensile test (After Yoder et al. 1975).....	35
Figure 2-18: Illustration of potential loading condition (Roque et al. 2002).....	38
Figure 2-19: Determination of fracture energy and dissipated creep strain energy	38
Figure 3-1: Gradation curves for F2 and its trial adjustments	45
Figure 3-2: Gradation curves for F4 and its trial adjustments	45
Figure 3-3: Change of percent retained on top 3 sieves for F2 series.....	46
Figure 3-4: Change of percent retained on top 3 sieves for F4 series.....	46
Figure 3-5: Cutting of raw specimen	46
Figure 3-6: Indirect diametral resilient modulus test setup	50
Figure 3-7: Load & deformations in a typical resilient modulus test	50
Figure 3-8: Load and deformation curves of creep compliance test.....	51
Figure 3-9: Specimen fails after tensile strength test.....	53
Figure 3-10: Flowchart of the experimental program for measuring fracture mechanics properties of HMA mixtures.....	54
Figure 4-1: Instantaneous and total resilient deformations.....	56
Figure 4-2: Determination of fracture energy and dissipated creep strain energy	63
Figure 5-1: Power law regression for F2 gradation series	69
Figure 5-2: Power law regression for F4 gradation series	70
Figure 5-3: Resilient modulus for mixtures with modified gradations (GPa)	71
Figure 5-4: Resilient modulus for mixtures with modified gradations (ksi)	71
Figure 5-5: Comparison of resilient modulus between control and modified gradations.....	72
Figure 5-6: Power model parameter D_1 for modified gradations	73
Figure 5-7: Power model parameter m for modified gradations.....	74

Figure 5-8: Comparison of creep compliance for granite gradation series.....	74
Figure 5-9: Comparison of creep compliance for limestone gradation series	75
Figure 5-10: Tensile strength for control and modified gradation mixes (MPa).....	76
Figure 5-11: Tensile strength for control and modified gradation mixes (psi).....	77
Figure 5-12: Comparison of TS between control and modified gradation mixes.....	77
Figure 5-13: Fracture energy for modified gradation mixes (KPa)	78
Figure 5-14: Fracture energy for modified gradation mixes (psi).....	78
Figure 5-15: DCSE for modified gradation mixes (KPa).....	79
Figure 5-16: DCSE for modified gradation mixes (psi)	79
Figure 5-17: Comparison of fracture energy for modified gradation mixtures	80
Figure 5-18: Comparison of DCSE for modified gradation mixtures	80
Figure 5-19: Comparison of resilient modulus for F2 SBS PMA mixes (GPa).....	82
Figure 5-20: Comparison of resilient modulus for F2 SBS PMA mixes (ksi)	82
Figure 5-21: Comparison of resilient modulus for F4 SBS PMA mixes (GPa).....	83
Figure 5-22: Comparison of resilient modulus for F4 SBS PMA mixes (ksi)	83
Figure 5-23: Comparison of M_R between control and PMA mixtures	84
Figure 5-24: Power model parameter D_1 for mixes with SBS PMA	86
Figure 5-25: Power model parameter m for mixes with SBS PMA	86
Figure 5-26: Creep compliance master curves for granite PMA mixtures	87
Figure 5-27: Creep compliance master curves for limestone PMA mixtures.....	87
Figure 5-28: Comparison of creep compliance at -10°C for F2 series.....	88
Figure 5-29: Comparison of creep compliance at 5°C for F2 series.....	88
Figure 5-30: Comparison of creep compliance at 25°C for F2 series.....	89
Figure 5-31: Comparison of creep compliance at 40°C for F2 series.....	89
Figure 5-32: Comparison of creep compliance at -10°C for F4 series.....	90
Figure 5-33: Comparison of creep compliance at 5°C for F4 series.....	90
Figure 5-34: Comparison of creep compliance at 25°C for F4 series.....	91
Figure 5-35: Comparison of creep compliance at 40°C for F4 series.....	91
Figure 5-36: Tensile strength for granite PMA mixes (MPa).....	93
Figure 5-37: Tensile strength for granite PMA mixes (psi).....	93
Figure 5-38: Tensile strength for limestone PMA mixes (MPa)	94
Figure 5-39: Tensile strength for limestone PMA mixes (psi)	94
Figure 5-40: Comparison of tensile strength between control and PMA mixes.....	95
Figure 5-41: Fracture energy for granite PMA mixes (KPa)	95
Figure 5-42: Fracture energy for granite PMA mixes (psi)	96
Figure 5-43: Fracture energy for limestone PMA mixes (KPa).....	96
Figure 5-44: Fracture energy for limestone PMA mixes (psi).....	97
Figure 5-45: DCSE for granite PMA mixes (KPa).....	97
Figure 5-46: DCSE for granite PMA mixes (psi)	98
Figure 5-47: DCSE for limestone PMA mixes (KPa)	98
Figure 5-48: DCSE for limestone PMA mixes (psi)	99
Figure 5-49: Comparison of fracture energy between control and PMA mixes.....	99
Figure 5-50: Comparison of fracture energy between control and PMA mixes.....	100
Figure 5-51: Relationship between the observed failure strain and SBS polymer content..	100
Figure 5-52: Gradation curves for control mixes and the modified gradation mixes.....	102
Figure 5-53: Comparison of resilient modulus for granite and limestone mixtures.....	103
Figure 5-54: Comparison of CP between granite and limestone mixes at -10°C	103

Figure 5-55: Comparison of CP between granite and limestone mixes at 5°C.....	104
Figure 5-56: Comparison of CP between granite and limestone mixes at 25°C.....	104
Figure 5-57: Comparison of CP between granite and limestone mixes at 40°C.....	105
Figure 5-58: Comparison of tensile strength between granite and limestone mixes	105
Figure 5-59: Comparison of fracture energy between granite and limestone mixes	106
Figure B-1: Creep compliance of F2 control and all polymer-modified levels at -10°C.....	122
Figure B-2: Creep compliance of F4 control and all polymer-modified levels at -10°C.....	122
Figure B-3: Creep compliance of F2 control and all polymer-modified levels at 5°C.....	122
Figure B-4: Creep compliance of F4 control and all polymer-modified levels at 5°C.....	123
Figure B-5: Creep compliance of F2 control and all polymer-modified levels at 25°C.....	123
Figure B-6: Creep compliance of F4 control and all polymer-modified levels at 25°C.....	123
Figure B-7: Creep compliance of F2 control and all polymer-modified levels at 40°C.....	124
Figure B-8: Creep compliance of F4 control and all polymer-modified levels at 40°C.....	124
Figure B-9: Creep compliance of F2 control and modified gradation levels at -10°C.....	124
Figure B-10: Creep compliance of F4 control and modified gradation levels at -10°C.....	125
Figure B-11: Creep compliance of F2 control and modified gradation levels at 5°C.....	125
Figure B-12: Creep compliance of F4 control and modified gradation levels at 5°C.....	125
Figure B-13: Creep compliance of F2 control and modified gradation levels at 25°C.....	126
Figure B-14: Creep compliance of F4 control and modified gradation levels at 25°C.....	126
Figure B-15: Creep compliance of F2 control and modified gradation levels at 40°C.....	126
Figure B-16: Creep compliance of F4 control and modified gradation levels at 40°C.....	127

EXECUTIVE SUMMARY

Hot mix asphalt (HMA) is a viscoelastic material and has been broadly used in pavement structures. It is important to understand the mechanism of complex behavior of HMA mixtures in field for improving pavement mechanical performance. Aggregate gradation and asphalt binder are two key factors that influence the engineering properties of HMA. The asphalt binder plays a significant role in elastic properties of HMA and it is the essential component that determines HMA's viscous behavior. Many research studies suggest that the Styrene-Butadiene-Styrene (SBS) polymer is a promising modifier to improve the asphalt binder, and hence benefit the HMA viscoelastic properties. The specific beneficial characteristics and appropriate polymer concentration need to be identified. In addition, aggregate gradation requirements have been well defined in Superpave mix design criteria. However, a potentially sound coarse mixture with the gradation curve passing below the coarse size limit may be disqualified from being used. There is a need to evaluate the Superpave gradation requirements by studying mixtures purposely designed exceeding the coarse aggregate control limits.

The primary objective of this research study was to evaluate the fracture mechanics properties of HMA concrete for Superpave mixtures. An experimental program was performed to evaluate the engineering properties of the asphalt mixtures with various types of materials. The laboratory testing program was developed by applying a viscoelastic fracture mechanics-based framework that appeared to be capable of describing comprehensive mechanical properties of HMA according to past research studies. The goals for these experiments are to evaluate the effect of aggregate type, the effect of coarse aggregate gradation adjustment to mix designs, and the effect of SBS polymer content on fracture mechanics properties of HMA concrete.

To achieve the objectives and goals, a complete dynamic testing system was acquired to perform the temperature controlled dynamic tests to determine the engineering properties for all selected asphalt concrete mixtures. The laboratory experimental program for fracture mechanics properties involved two standard asphalt mix designs as control levels: one granite mixture and one limestone mixture. Each control mix design was modified to two different gradation levels with the control asphalt binder (PG 67-22) and three SBS polymer

content levels (3.0%, 4.5%, and 6.0%) with the original aggregate gradation. The volumetric properties of all the mixtures were verified to ensure that the specimens' air voids are as close to the optimum (4.0%) as possible.

The SHRP IDT test procedure was generally followed to perform the indirect diametral tensile test. The measurement and analysis system developed for SHRP IDT was also applied. Three types of IDT test, the resilient modulus test, the creep compliance test, and the tensile strength test, were performed to determine the fracture mechanics properties of asphalt concrete at four temperature levels: -10, 5, 25, and 40°C (14, 41, 77, and 104°F). Evaluation of the test results indicated the following characteristics: 1) the increase of nominal maximum aggregate amount to the standard mix designs in this study had negligible or slightly adverse effect on HMA fracture mechanics properties; 2) The SBS polymer-modified asphalt binder improved the fracture mechanics behavior of asphalt mixtures. The resilient modulus values of polymer-modified asphalt (PMA) mixtures decreased with an increase of SBS polymer content throughout the concentration range tested. At the high testing temperature of 40°C, an optimum SBS content appeared to exist around 4.5% to make the HMA stiffest, which suggested that limiting the concentration within an optimal range is especially important at high service temperatures. The SBS polymer also helped the HMA obtain an upgraded creep performance. The mixtures with SBS polymer modifiers were more compliant at the low temperature level (-10°C) and became less compliant at the high testing temperature (40°C), which should lead to improved resistance to rutting and thermal cracking of HMA. At a specific temperature level, a higher SBS polymer concentration generally resulted in higher creep compliance values. Furthermore, the SBS polymer modifier improved the asphalt mixture fracture properties by increasing the fracture energy (FE) limit or dissipated creep strain energy (DCSE) limit which were indicators of mixtures' resistance to fatigue cracking. The failure strain of PMA mixtures tended to increase with an increase of SBS polymer content at low temperatures (-10°C and 5°C).

It was found that the limestone mixtures were more compliant than the granite mixtures at low temperatures and turned to be less compliant than granite at high temperature (40°C). Therefore limestone materials appeared to hold advantages over granite materials in improving the performance of thermal cracking at low service temperatures and the rutting resistance at high service temperatures.

CHAPTER 1

INTRODUCTION

1.1 Background

The Superpave asphalt mix design method has been increasingly accepted, and the system has been implemented in Florida. The current Superpave mix design approach is based on meeting certain asphalt binder, aggregate and volumetric properties such as the asphalt binder performance grading (PG) specification, aggregate gradation control limits, gradation restricted zone, asphalt mix air voids, voids in mineral aggregate (VMA), voids filled with asphalt (VFA), etc. The Superpave mix design system has continuously been under evaluation to search for further improvements.

Gradation is perhaps the most important property of an aggregate. It affects almost all the important properties of hot mix asphalt (HMA) mixtures including stiffness, stability, durability, permeability, workability, fatigue resistance, frictional resistance, and resistance to moisture damage. Therefore, gradation is a primary consideration in asphalt mix design, and the Superpave specifications place limits on the aggregate gradations that can be used in HMA mixtures. The gradation of the aggregate is important to ensure that 1) the maximum aggregate size is not too large or too small, 2) VMA requirements are met, and 3) a satisfactory aggregate skeleton is obtained. According to the Superpave, the aggregate gradation must be within the control limits to meet the Superpave requirements. For example, if a 19-mm (3/4-inch) maximum aggregate size is specified, then 100 % of the aggregate must pass the 25-mm (1-inch) sieve size. At least 90-100 % of the aggregate must be finer than the nominal maximum size (19 mm). Less than 90% of the aggregate must pass the 12.5-mm sieve. In order to meet the Superpave requirements, a coarse graded aggregate will have to be *gap-graded* to be within the nominal size control limits. However, a *smoother* coarse gradation passing below the lower control limit may provide similar results to the *gap-graded* curve. Research is needed to evaluate the Superpave gradation control limits and to propose improved coarse gradation limits for Florida asphalt mixes.

In addition, polymer-modified binders have been used in Superpave mixtures of many state agencies in an effort to improve the mixtures. SBS (styrene-butadiene-styrene) polymer has been

used to modify the asphalt binders. Some laboratory and full-scale field tests have been performed to evaluate the beneficial effects of adding the SBS polymer to asphalt binders and modified asphalt mixtures. SBS polymer modifiers appear to provide greater benefit to open graded mixtures than to dense graded mixtures. It has been recommended that asphalt binder modified with 3% SBS polymer is an effective way of treating the Superpave mixtures. However, modifiers with higher percentage of SBS polymer have been successfully used in Europe. It appears that research is needed to evaluate the beneficial effect of using higher dosages of SBS polymer. The fracture mechanics concept/approach has been proposed and studied extensively (Roque et al. 2002, 2004). The approach has been verified by some field sections and cores related to the top-down cracking mode of failure in Florida. The fracture mechanics approach may be adopted as a basis to evaluate the performance of modified HMA mixtures.

1.2 Objectives

The primary objectives of this study were to evaluate the effects of aggregate gradation, aggregate type, and SBS polymer-modified binder on the engineering properties of HMA mixtures. Specifically, the research goals were to evaluate the coarse aggregate gradation limits specified in the Superpave mix design criteria, to evaluate the benefits of using higher dosages of SBS polymer modifier in HMA mixtures, and to evaluate the effect of aggregate type on fracture mechanics properties of asphalt mixtures.

The scope of this study included the following tasks:

Task 1 Literature review of Superpave aggregate gradation requirements, the performance and benefits of polymer-modified binders, and fracture energy approach

Task 2 Laboratory evaluation of Florida HMAC mixtures: An experimental program was developed to evaluate the following factors:

- Aggregate type: granite and limestone
- Aggregate gradation: control level, and two levels of smooth coarse gradation
- SBS polymer-modified binder: control level and three SBS polymer content levels (3%, 4.5%, and 6%)

1.3 Report Outline

This report summarizes the study to evaluate the HMA coarse aggregate gradation effect, to study the SBS polymer-modified binder effect, and to evaluate the effect of aggregate type. The report is organized as the following structures:

Chapter 1 introduces the background, objective, and scope of the study.

Chapter 2 gives a comprehensive literature review of the aggregate gradation effect and SBS polymer modifier effect on HMA. The fracture mechanics model developed by Roque et al. (2004) is introduced to evaluate the engineering properties of asphalt concrete.

Chapter 3 introduces the materials and develops a whole experimental program. Detailed testing methods and procedures are specified.

Chapter 4 presents the results from IDT sweep set of tests for the two control mixes, four modified gradation mixes, and six mixes with SBS polymer-modified asphalt binders at different concentrations (3%, 4.5%, and 6%).

Chapter 5 analyzes the IDT test results in detail to account for the gradation effect and SBS polymer modifier effect on the HMA mixtures.

Chapter 6 summarizes the complete research study. Conclusions and recommendations are presented based on the test results and findings of this study.

CHAPTER 2

LITERATURE REVIEW

2.1 Introduction

The purpose of this study is to evaluate the engineering properties of asphalt concrete mixtures obtained from laboratory tests. Asphalt concrete pavement performance is influenced by a great number of factors. HMA mixtures are essentially made up of various kinds of aggregates in appropriate size combinations and different types of asphalt binders. This research study is focused on the material effects of aggregate gradation and Styrene-butadiene-styrene (SBS) polymer-modified asphalt binders. There are many laboratory test methods developed for measuring the mechanical properties of asphalt concrete over the past twenty years. The most common ones are the indirect diametral tensile (IDT) test and the dynamic modulus test (DMT). They were introduced in the AASHTO flexible pavement design guide in 1993 and 2004 respectively. In this chapter the following are to be discussed:

- To conduct a comprehensive literature review on publications related to aggregate gradation effect and SBS polymer-modified asphalt binder effect on flexible asphalt mixture characteristics
- To introduce test methods, procedures, and corresponding comparisons of testing methodologies that have been used to evaluate mechanical responses of asphalt concrete mixtures
- To review the fracture mechanics and energy models that were developed and used to evaluate cracking performance of HMA mixtures

The following sections provide an explanation of the basic material mechanisms and approaches used to evaluate the performance of asphalt pavement.

2.2 Asphalt Cement Properties

Asphalt cement is bituminous material that is either naturally occurring or produced by distillation process from crude petroleum using different refining techniques. It is widely used throughout the world in roadway paving applications. Asphalt cement is a black, sticky and

highly viscous material at ambient temperatures. It is also resistant to the action of most acids, alkalis and salts. The largest use of asphalt cement is in the production of hot mix asphalt (HMA) for construction of flexible pavements. By applying heat to the asphalt cement, it can be liquefied for mixing with mineral aggregates; it adheres to aggregate particles and binds them to form HMA. After cooling to ambient temperature, with asphalt cement's excellent adhesive and waterproofing characteristics, HMA become a very strong and durable paving material which can sustain heavy traffic loads.

Three methods, based on penetration, viscosity and performance are used to classify asphalt cements into different standard grades. The penetration grading of asphalt cement is specified in ASTM D946 and is primarily controlled by the penetration test. The viscosity grading is specified in ASTM D3381. It is based on either the viscosity of the original asphalt cement or on the viscosity of the asphalt cement after aging in the rolling thin film oven (RTFO) test. The performance-based method of classifying asphalt binders was developed in the Strategic Highway Research Program (SHRP).

2.2.1 Chemical Properties of Additives and Polymer Modifiers

Asphalt modifiers have been used for over 60 years. They were more commonly used in Europe compared to the United States in the 20th century. A greatly increased effort has been dedicated to the research and application of asphalt modifiers over the past 20 years in the United States. The Superpave asphalt binder specifications based on SHRP require the asphalt binders to meet stiffness criteria at both high and low pavement service temperatures. However, most regular asphalt binders are not qualified for the requirements in areas with extreme climate conditions. In the meantime, traffic volume and loads have increased significantly in recent years. This has caused lots of premature rutting and cracking of HMA pavement constructed with neat asphalt binders. Modifications of asphalt binders become of considerable interest in the improvement of pavement performance and service life. Although high initial cost discourages the use of modifiers, some state highway agencies started to specify modified asphalt binders and to be willing to pay a higher initial cost for pavements with a longer service life and reduced risk of premature distress, and therefore, lower life cycle costs. Additionally, the disposal of waste

materials and industrial byproducts, such as tires, glass, sulfur, etc., used as additives in HMA is economical and benefits the environment.

Some specific technical reasons for using additives and modifiers in HMA are listed as follows (Roberts et al. 1996):

1. Obtaining stiffer mixtures at high service temperatures to minimize rutting
2. Obtain softer mixtures at low service temperatures to minimize thermal cracking
3. Improve fatigue resistance of HMA mixtures
4. Improve asphalt-aggregate bonding to reduce stripping or moisture susceptibility
5. Improve resistance to aging or oxidation; rejuvenate aged asphalt binders
6. Permit thicker asphalt films on aggregate for increased mix durability
7. Improve abrasion resistance of mixture to reduce raveling
8. Reduce flushing or bleeding; reduce structural thickness of pavement layers
9. Reduce life cycle costs and improve overall performance of HMA pavements

Additives and modifiers can be classified in different ways. A generic classification system was first suggested by Terrel and Walter (1986). A modified version of the system (Table 2-1) and a discussion of each additive or modifier were given by Roberts et al. (1996).

It can be seen in Table 2-1 that polymers are comprised of rubber, plastic and their combination materials. Elastomers (rubber) and plastomers (plastic) are the two basic categories. Elastomers resist deformation from applied stress with their high extensibility and contractibility and rapidly recover upon removal of the load. The initial modulus is usually low but they stiffen when stretched. Plastomers resist deformation by their tough and rigid three-dimensional network. Earlier research showed that elastomers (rubbers) increase asphalt binders' tensile strength with elongations whereas little additional strength is obtained from the rubbers by asphalt binders until they are stretched. On the other hand, plastomers exhibit quick early strength on loading but may fracture under strain (Hines 1993). Therefore, when elastomers are used for modifying asphalt cements, HMA pavements generally get more flexible and resilient. In contrast, asphalt binders modified with plastomers usually improve the stiffness moduli of HMA pavement.

Table 2-1: Generic classification of asphalt additives and modifiers (Roberts et al. 1996)

Type	Generic Examples	
1. Filler	<ul style="list-style-type: none"> • Mineral Filler: crusher fines lime Portland cement fly ash • Carbon black 	
2. Extender	<ul style="list-style-type: none"> • Sulfur • Lignin 	
3. Polymers	Rubber: <ul style="list-style-type: none"> a. Natural latex b. Synthetic latex c. Block copolymer d. Reclaimed rubber 	<ul style="list-style-type: none"> • Natural rubber • Styrene-butadiene or SBR • Polychloroprene latex • Styrene-butadiene-styrene (SBS), Styrene-isoprene-styrene (SIS) • Crumb rubber modifier
	Plastic	<ul style="list-style-type: none"> • Polyethylene/Polypropylene • Ethylene acrylate copolymer • Ethyl-vinyl-acetate (EVA) • Polyvinyl chloride (PVC) • Ethylene propylene or EPDM • Polyolefins
	Combination	Blends of polymers above
4. Fiber	<ul style="list-style-type: none"> • Natural: asbestos rock wool • Man-made: polypropylene polyester fiberglass mineral cellulose 	
5. Oxidant	Manganese salts	
6. Antioxidant	<ul style="list-style-type: none"> • Lead compounds • Carbon • Calcium salts 	
7. Hydrocarbon	<ul style="list-style-type: none"> • Recycling and rejuvenating oils • Hard and natural asphalts 	
8. Anti-stripping Agent	<ul style="list-style-type: none"> • Amines • Lime 	
9. Waste Materials	<ul style="list-style-type: none"> • Roofing shingles • Recycled tires • Glass 	
10. Miscellaneous	<ul style="list-style-type: none"> • Silicones • Deicing calcium chloride granules 	

A polymer molecule is produced by the reaction of many monomers, which are smaller molecules, with one another in long chains or clusters. The term “poly” means many as opposed to “mono.” Homopolymers are made up of only one kind of repeating monomer in the polymer

molecular chain. Copolymers are composed of the combination of two or more different monomers in a random or block arrangement. The types of polymers are listed below.

- Homopolymer: only one monomer is used along the chain.



- Random Copolymer: the repeating units are in random sequence.



- Alternating Copolymer: the two units repeat in an ordered manner.



- Block Copolymer: the chain consists of long sequence (blocks) of repeating units.



- Grafted Copolymer: branched copolymer in which the side chains are structurally distinct from the main chain.



- Periodic copolymers: with A and B units arranged in a repeating sequence, e.g.



The physical properties of polymers vary remarkably depending on the sequence, structure, and chemical process for the composing monomers (Usmani 1997). Polymers can also be categorized into linear polymers, branched polymers, and cross-linked polymers as shown in Figure 2-1 according to their structures.

Polymers may also be classified as thermosets and thermoplastics. Thermosets are usually rigid and tightly cross-linked. When mixed with asphalt at high temperatures, the thermoset's particles may swell to more than twice the original volume as a result of chemical interaction which leads to a remarkable increase in mixture viscosity. Thermoplastic elastomers are commonly applied in the modification of asphalt binders. They are usually linear or branched in types of block copolymer $(\text{SB})_n\text{X}$, where 'S' denotes the styrene block, 'B' denotes the butadiene block, and 'X' denotes the coupling agent, as shown in Figure 2-2. It was found that a separation takes place between butadiene (soft block) and the styrene (hard block) because they are mutually

incompatible; as a result, the styrene remains dispersed in a continuous elastomeric matrix (Diani et al. 1997).

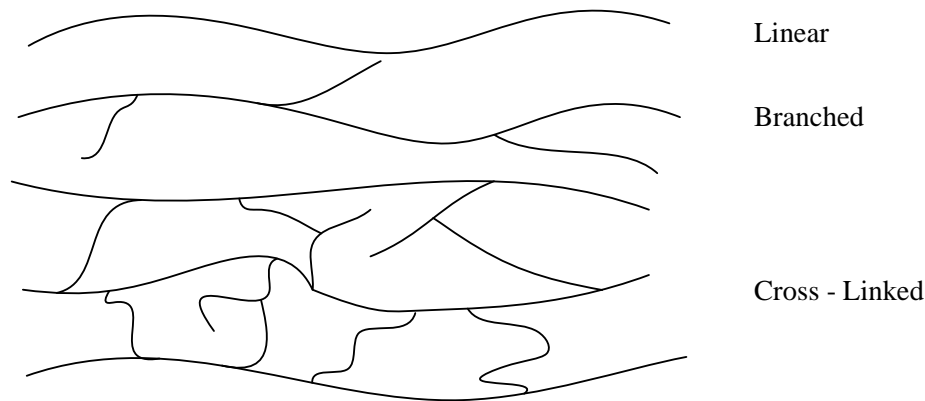


Figure 2-1: Polymer classifications based on link structure

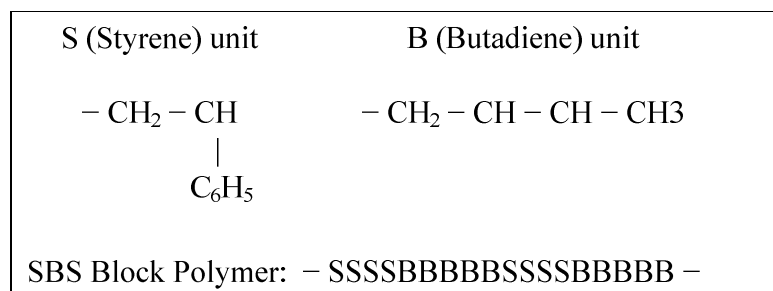


Figure 2-2: SBS polymer modifier structure

As listed in Table 2-1, Elastomers or rubbers used as asphalt modifiers include natural rubber, styrene-butadiene latexes (SBR), polychloroprene latex, styrene-butadiene-styrene block polymers (SBS), styrene-isoprene-styrene block polymers (SIS), and crumb rubber modifiers (ground tires). SBS block copolymers are usually in the solid forms of pellets, crumbs, or ground material in bags or bulk. The common concentration level is about 3% to 5% by weight of asphalt cement in the HMA industry. High shear mixing equipment is used for blending the SBS modifier with hot asphalt cement maintained at 350-380°F (177-193°C). Since the asphalt binder must be within specified viscosity ranges for workability purposes during mixing and compaction, it is probably necessary to increase the mixing and compaction temperatures while conducting laboratory work and testing.

Polymer modifiers have complex characteristics and their effects on asphalt binders depend on quite a few factors such as polymer concentration, molecular weight, chemical composition, and molecular structure. Other important things include the source of original asphalt binder, production process, binder grade, reaction between binder and modifier, etc. Special properties can be obtained through various combinations of elastomers and plastomers to meet desired requirements. However, it should be noted that it is very difficult to predict whether a particular combination will be able to provide improvements in the desired property. Sometimes polymer properties may get diluted or even changed when blended with asphalt binders. The structures of the pure polymer-modified binder generally are different from those of the PMB in the asphalt mixture. Therefore, it is necessary to test the polymer-modified asphalt binder; or in more practical situations, it would be more advisable to evaluate the performance of actual HMA produced with modified asphalt binder (Wegon and Brule 1999). It is hoped that polymer modifiers can be used in Superpave mix design and evaluation procedures to obtain a stiffer HMA at high service temperatures to minimize rutting, a more elastic HMA to resist fatigue cracking at intermediate temperatures, and a softer HMA at low service temperatures to resist thermal cracking.

Chen et al. (2002, 2003) investigated the morphology of the SBS modified binders described by the concentration and the presence of the microstructure of the copolymer. As the polymer content increases, the dispersed polymer particles gradually swell to form local SBS networks which highly enhance the mechanical properties of the asphalt binder (viscosity, softening point, toughness and complex modulus, etc). A continuous polymer structure was observed to begin at an SBS content between about 5% and 6%, yet the minimum percentage depends more on the base asphalt and the polymer itself. An optimum SBS content is based on the formation of the critical network between asphalt and polymer, which appeared to be slightly higher than the phase inversion content that occurs when the SBS entered the continuous matrix phase. However, once the critical networks begin to form, increases in polymer content have less significant effect on PMA property improvement (Figure 2-3), or may even lead to the separation of polymer and bitumen. Recent work by Chen and Huang (2007) showed that the SBS-asphalt blended with sulfur resulted in improved rheological characteristics.

Brule et al. (1988) studied the relationship between the composition, structure, and properties of asphalt binders incorporated with SBS block copolymers. It was found that

increasing the agitation time made the microstructure finer, which led to a greater deformability. They also found that the amount of polymer required for matrix inversion and for obtaining highly modified practical properties depended significantly on the asphalt itself. However, the value of this inversion threshold was not predictable. The extent of swelling in asphalt-SBS blends was not highly dependent on content for high polymer concentrations, but increased substantially as the amount of polymer decreased; it also appeared to be independent of temperature in the high-level range (80-160°C). In addition, the SBS polymer was no longer swollen in the binder but dissolved beyond a colloidal instability index value.

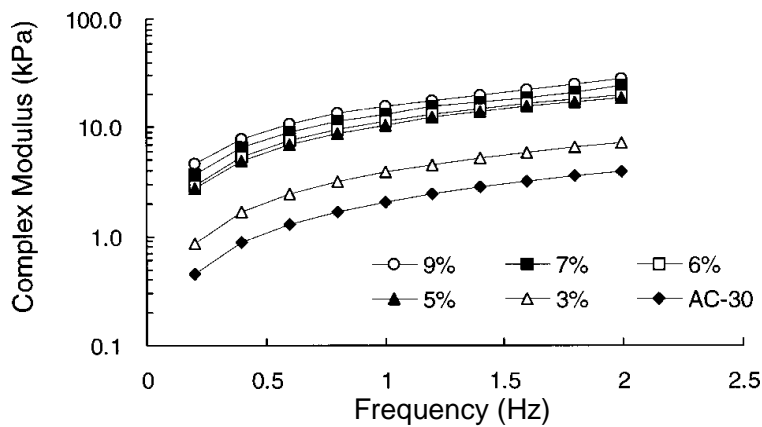


Figure 2-3: Complex modulus of styrene-butadiene-styrene-modified asphalt at 60°C (Chen et al. 2002)

Lu et al. (1998) reported that SBS polymer modification improves the low-temperature properties of bitumen. The polymer modification reduces the creep stiffness and limiting stiffness temperature of bitumen. The changes generally increase with SBS content and are influenced slightly by SBS structure.

Many studies (Huffman 1980; Lalwani et al. 1982; Scofield 1989) have reported that the polymer-modified asphalt can lower temperature susceptibility, which is the primary drawback of regular asphalt, reduce binder penetration, increase the viscosity and softening point, and improve resistance to aging and oxidation. These effects should lead to increased resistance to deformation (rutting) and thermal cracking in practice. King et al. (1986) documented a correlation between styrene-butadiene elastomer-modified asphalt and pavement durability. The

addition of polymer improves stiffness, rutting resistance, fatigue life, adhesion and stripping resistance to the bituminous mix.

Carpenter et al. (1987) conducted a series of lab tests on asphalt mixtures including the diametral resilient modulus test, indirect tensile test at temperatures ranging from 72°F to -20°F (22.2°C to -28.9°C), and permanent deformation testing at 72°F (22.2°C) and 100°F (37.8°C). The testing indicated that the polymer additives reduced stiffness at low temperatures yet maintained adequate stiffness at elevated temperatures. The low-temperature performance was greatly improved over that of untreated asphalt cements of all grades, whereas the permanent deformation characteristics were greatly improved at elevated temperatures. Carpenter et al. (2006) conducted further tests and showed that the healing/recovery rate of the polymer-modified binders is significantly greater than the neat binder. Button (1992) drew a summary of asphalt additive performance which indicated positive influences by polymer addition in bitumen.

Collins et al. (1991) studied the performance of paving asphalt modified by SB polymers. The modification resulted in a substantial improvement of fatigue life by reducing flexural fatigue cracking and a dramatic increase of strength and resistance to creep at high temperatures. They also found that the actual critical cracking temperature was significantly lower than that of the base asphalt and decreased with increasing polymer content (Figure 2-4). The poly-butadiene chains in polymer contribute to the flexibility of the binder and the elastomeric lattice between asphalt molecules and SBS polymer improves the elastic characteristics of the binder without increasing the stiffness binders at low service temperatures. Similar findings were reported by many other researchers. Verhaeghe et al. (1994) conducted studies on asphalt binder modified with Ethylene Vinyl Acetate (EVA) which improves the compressive strength and rutting resistance of asphalt mixes. Pradhan (1993) reported that the addition of commercial SBR modifiers improves the physical properties related to rutting problems on Montana asphalt pavements. Testing programs conducted by Kennedy et al. (1992) showed that SBS and SBR polymers generally increase the mixture's tensile strength at high temperatures and tensile strain at failure at low temperatures. The permanent deformation resistance was also improved, indicated by indirect creep testing.

King et al. (1993) studied a type of standard mixture containing four control bitumens with styrene-butadiene polymer of three different contents (x%, 1.5x% and 2x%). They found that the softer the base asphalt, the lower the cracking temperature; and that increasing the polymer

content generally lowered the cracking temperature. Shih (1996) conducted testing studies to compare the effects of different additives on typical Florida asphalt mixtures. Test results showed that the addition of modifiers generally benefits the rutting resistance of pavement and the SBR-modified asphalt mixtures have lower resilient moduli at low temperatures; thus, the addition of modifiers would be beneficial to the resistance of thermal cracking.

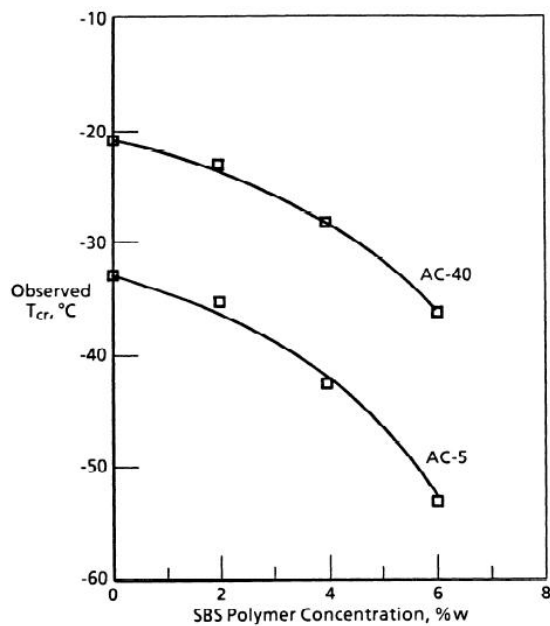


Figure 2-4: Relationship between the observed critical cracking temperature (T_{cr}) and SBS polymer concentration (Collins et al. 1991)

Aglan (1997) analyzed the fatigue tests and electron microscopic scans on polymer modification for asphalt mixtures. The binder-rich areas were observed to contain ridges produced by the micro-stretching of the SBS modified binder on the fracture surface, and the mixture test results showed a superior resistance to fracture.

Jones et al. (1998) performed Superpave IDT creep and strength tests on five different modified mixtures. Higher tensile strength was observed at intermediate temperatures, yet it appeared that there was no noticeable difference at low temperatures (around and below 0°C). Khattak and Baladi (1998, 2001) evaluated the effects of SBS polymer-modified binder on mechanical properties of mixtures. The measurement results showed increased fatigue life and tensile strength at intermediate temperature whereas low temperature elastic properties were

almost the same. They also found that the fatigue life and permanent deformation were strongly related to the rheological properties of polymer-modified binders. Kim et al. (2003) investigated the use of SBS modifier in asphalt pavement mixtures through lab testing for cracking resistance and healing characteristics. Although the SBS does not show an influence on healing of the asphalt mixture, it appears to reduce the rate of micro-damage accumulation which justified the benefits of SBS modification on creep and failure properties of the mixtures. More recently, van Quintus et al. (2007) conducted an investigation of a large amount of real-world pavement sections to quantify the benefits of using PMA mixtures. It was found that the PMA significantly enhanced the rutting performance of asphalt pavement (Figure 2-5) and its fatigue and fracture performance.

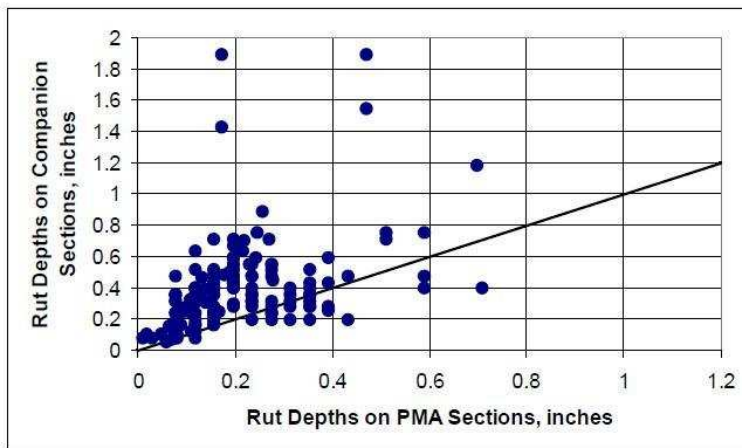


Figure 2-5: Comparison of the rut depths measured on sections with PMA and the companion sections without PMA mixtures (van Quintus et al. 2007)

2.2.2 Mechanical Properties of Asphalt Cement

The Strategic Highway Research Program (SHRP) was launched in 1987. The program made a research effort to develop performance-based tests and specifications for asphalt binders and HMA mixtures. The Superpave (Superior Performing Asphalt Pavements) binder tests and specifications have a few prominent features (McGennis et al. 1994; Warren et al. 1994; Asphalt Institute 1994) compared with the old physical testing system for asphalt cement.

The rolling thin film oven (RTFO) test is specified in AASHTO T240 and ASTM D2872. The RTFO simulates the asphalt binder aging during the manufacture and construction of HMA pavements. It continually exposes fresh binder to heat and air flow during rolling. This test mode does not allow any asphalt surface skin to be formed, this inhibits aging. And modifiers, if used in asphalt cement, usually remain dispersed due to rolling action, which makes the modified binder age more sufficiently. The RTFO test determines the mass of volatiles lost from the binder, which indicates the amount of aging that occurs during HMA production and construction. However, some asphalt binders gain weight during the RTFO aging due to the oxidative products formed during the test. The Dynamic Shear Rheometer (DSR) Test is used to characterize the viscous and elastic behavior of asphalt binders at high and intermediate service temperatures. The DSR measures the complex shear modulus G^* and phase angle δ of asphalt binders at the desired temperature and loading frequency. Complex modulus G^* can be considered as the total resistance of the binder to deformation at repeated shear load. Complex modulus G^* consists of two components as shown in Figure 2-6: (a) elastic modulus G' , also known as the storage or recoverable part; (b) loss modulus G'' , also known as the viscous or non-recoverable part (McGennis et al. 1994).

The values of G^* and δ for asphalt binders are affected by both service temperature and loading frequency. Most asphalt binders are viscoelastic at usual pavement service temperatures. They behave like elastic solids as well as viscous fluids simultaneously. The magnitude G^* and phase angle δ define a complete picture of the behavior of asphalt binders in certain conditions, as shown in Figure 2-7. The elastic component or storage modulus is related to the amount of energy stored in the sample during each testing cycle. The viscous component or loss modulus is related to the energy lost during each testing cycle through permanent flow or deformation (ASTM 1994).

The DSR test procedure is given in AASHTO TP5. The asphalt cement sample is sandwiched between a fixed plate and an oscillating plate or spindle as shown in Figure 2-8. Two types of oscillatory shear rheometer are usually used: constant stress and constant strain. Constant stress rheometers use a fixed torque to oscillate the top spindle and the strain will vary. Constant strain rheometers move the spindle with a fixed distance (e.g., from point A to B) and measure the torque resulting from this movement. All Superpave DSR tests are conducted in constant stress mode which uses a fixed torque to oscillate the top plate at a frequency of 10

radians per second (about 1.59 Hz). When torque is applied to the oscillating plate, it starts at point A and moves to point B, and then the spindle moves back and goes to point C passing point A. From point C it returns back to point A. This movement comprises one cycle of oscillation. When the spindle is oscillated back and forth with constant stress, the resulting strain is monitored.

The relationship between the applied stress and the resulting strain is used to compute complex modulus G^* and phase angle δ , which is the time lag between the applied stress and resulting strain. Theoretically, the phase angle δ is zero for a perfect elastic material because the strain response is instant. For an ideal viscous fluid, the time lag is 90 degrees. In reality, asphalt binders behave like viscoelastic materials with a stress-strain response between the two extreme conditions at certain service temperatures as shown in Figure 2-9, in which the resulting phase angle is between 0 and 90 degrees.

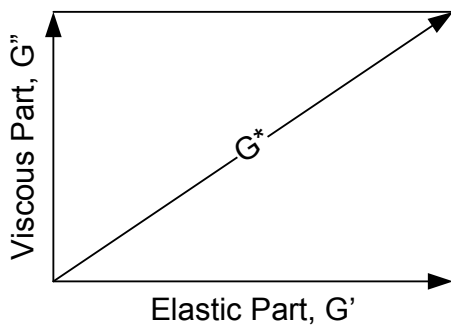


Figure 2-6: Components of complex modulus G^*

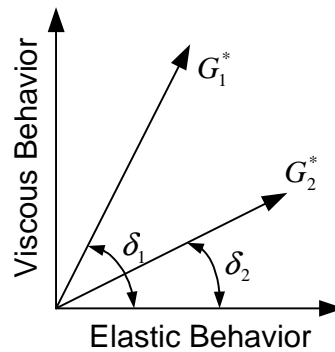


Figure 2-7: Viscous and elastic behavior of asphalt binders

G^* is the ratio of maximum shear stress (τ_{\max}) to maximum shear strain (γ_{\max}), which is calculated by the following formulas:

$$G^* = \frac{\tau_{\max}}{\gamma_{\max}} \quad (2-1)$$

$$\tau_{\max} = \frac{2T}{\pi r^3} \quad (2-2)$$

$$\gamma_{\max} = \frac{\theta \cdot r}{h} \quad (2-3)$$

Where,

T = maximum applied torque,

r = radius of binder specimen/plate (either 12.5 or 4 mm),

θ = deflection (rotation) angle,

h = specimen height (either 1 or 2 mm).

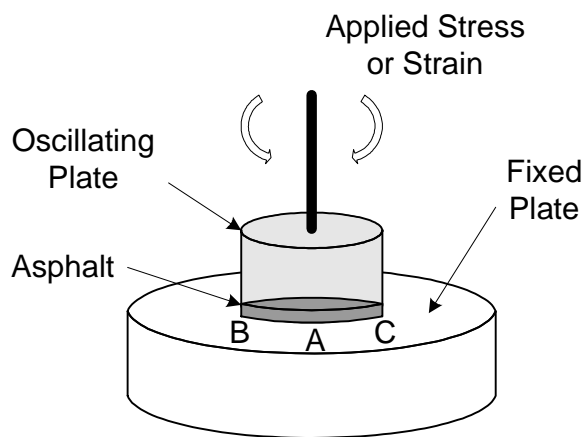


Figure 2-8: Dynamic shear rheometer

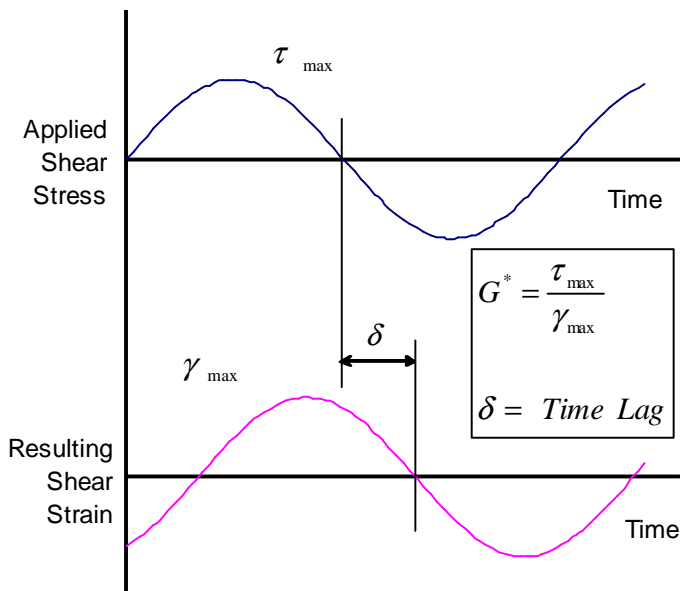


Figure 2-9: Stress-strain response of viscoelastic material

The SHRP researchers considered rutting to be a stress-controlled, cyclic loading phenomenon. Work is being done to deform the HMA pavement surface with each traffic loading cycle. A part of this work is recoverable in elastic rebound mode while some is dissipated in the form of permanent deformation and heat energy. The amount of dissipated work must be minimized in order to minimize rutting. The work dissipated per loading cycle at a constant stress can be expressed as follows (Bahia and Anderson 1995):

$$W_c = \pi \times \sigma_0^2 \left[\frac{1}{G^* / \sin \delta} \right] \quad (2-4)$$

Where,

W_c = work dissipated per load cycle,

σ_0 = stress applied during the load cycle,

G^* = complex modulus,

δ = phase angle.

The work dissipated per loading cycle is inversely proportional to G^*/δ , as indicated from the equation. A high complex modulus G^* value and low phase angle δ are both desirable for rutting resistance. This relationship appears logical because the asphalt binder will be stiffer with higher G^* value; the lower the δ value, the more elastic the asphalt binder will be, and thus the more resistant to rutting and permanent deformation. Therefore, the G^*/δ parameter was chosen as a Superpave asphalt binder specification.

Fatigue cracking is typically considered a strain-controlled phenomenon in thin HMA pavement layers and a stress-controlled phenomenon in thick ones. The SHRP researchers assumed that fatigue cracking should be considered mainly a strain-controlled phenomenon since it is known to be more prevalent in thin pavement layers (Bahia and Anderson 1995). The work dissipated per loading cycle at a constant strain can be expressed as follows:

$$W_c = \pi \times \varepsilon_0^2 [G^* \times \sin \delta] \quad (2-5)$$

Where ε_0 is the strain and other variables are as described previously. The equation indicates that the dissipated work will increase as G^* and/or δ are increased. As G^* decreases, the asphalt binder becomes less stiff and thus able to deform without building up large stresses which might cause cracking. In addition, low δ values indicate more elastic asphalt binders which can regain

their original condition without dissipating work. Therefore, $G^*\delta$ was chosen in Superpave specifications to limit the total amount of energy dissipated for minimizing fatigue cracking.

The Superpave asphalt binder specification is given in AASHTO MP1-93. It is meant to be performance-based and thus addresses three primary performance parameters of HMA pavements: permanent deformation (rutting), fatigue cracking, and low temperature (thermal) cracking. Other common specification criteria include safety, pumping and handling, excessive aging, etc.

2.3 Hot Mix Asphalt (HMA) Mixture Design

2.3.1 Physical Properties of Aggregates

Aggregates for HMA are usually classified by size as coarse aggregates, fine aggregates, and mineral fillers. ASTM defines coarse aggregate as particles retained on a No. 4 (4.75 mm) sieve, fine aggregate as that passing a No. 4 sieve (4.75 mm), and mineral filler as material with at least 70% passing the No. 200 (75 μ m) sieve. Some agencies use another sieve size as the dividing line between coarse and fine aggregates. For example, the Asphalt Institute uses the No. 8 (2.36 mm) sieve as the dividing line.

Specifications for coarse aggregates, fine aggregates, and mineral fillers are given in ASTM D692, D1073 and D242, respectively. Aggregates for HMA are generally required to be strong, sound, and properly graded; to have a clean surface without deleterious materials; to consist of angular particles with low porosity and appropriate absorption for asphalt cement.

The specific gravity of an aggregate is a basic parameter for HMA mix design. It is used to make weight-volume conversions and to calculate the void content in a compacted HMA. The specific gravity is defined as the ratio of the weight of a unit of volume of the material to the weight of an equal volume of water at approximately 23°C (73.4°F). Two different aggregate specific gravities are often used for HMA based on the method used to define the volume of the aggregate particles: (a) bulk specific gravity; and (b) effective specific gravity.

When the sample aggregates consist of separate aggregate fractions of coarse aggregate, fine aggregate and mineral filler, the bulk specific gravity of total aggregate can be calculated from the following equation:

$$G_{sb} = \frac{P_1 + P_2 + \dots + P_n}{\frac{P_1}{G_1} + \frac{P_2}{G_2} + \dots + \frac{P_n}{G_n}} \quad (2-6)$$

Where,

- G_{sb} = bulk specific gravity for the total aggregates,
- P_i = individual percentages by mass of aggregate, $i = 1, 2, \dots, n$;
- G_i = individual bulk specific gravity of aggregate, $i = 1, 2, \dots, n$.

The effective specific gravity of aggregate, G_{se} includes all void spaces in the aggregate particles excluding voids permeable to asphalt. It is determined by the following equation:

$$G_{se} = \frac{P_{mm} - P_b}{\frac{P_{mm}}{G_{mm}} - \frac{P_b}{G_b}} \quad (2-7)$$

Where,

- G_{se} = effective specific gravity of the aggregate,
- G_{mm} = maximum specific gravity of the mixture,
- P_{mm} = % by mass of total loose mixture = 100,
- P_b = asphalt content,
- G_b = specific gravity of asphalt cement.

2.3.2 Aggregate Gradation

Aggregate gradation is the distribution of particle sizes expressed as a percent of the total weight. It is one of the most important properties of an aggregate. The gradation of an aggregate is normally expressed as total percent passing various sieve sizes. It affects the HMA performance in many respects including stiffness, durability, stability, permeability, workability, resistance to rutting and fatigue cracking, and frictional resistance. Therefore, gradation is a critical consideration in asphalt mix design. Aggregate gradations are described as dense (well-graded), open (uniformly-graded), and gap-graded, as shown in Figure 2-10. Most states place limits on the aggregate gradations for HMA. Fuller and Thompson (1907) proposed one of the best known gradations for maximum density. The equation for Fuller's maximum density curve is:

$$P = 100 \cdot (d / D)^n \quad (2-8)$$

Where d is the diameter of the sieve size in question, P is the total percent passing or finer than the sieve and D is the maximum size of the aggregate. Studies by Fuller and Thompson showed that a maximum density can be obtained for an aggregate when $n=0.5$. In the early 1960s, the Federal Highway Administration introduced an aggregate grading chart which is based on the Fuller gradation but uses a 0.45 exponent in the equation. The maximum density lines can be conveniently obtained by drawing a straight line from the origin at the lower left corner of the chart to the actual percentage point of the nominal maximum size, which was defined in the specification as the largest sieve size retaining any material. The maximum aggregate size is normally limited to about one-half of the lift thickness in construction. The use of large stone mixes has been increased in recent years in order to minimize rutting. However, large maximum aggregate size (e.g. greater than 1 inch, or 25.4 mm) usually results in segregation during placement of HMA. Special attention is required when these large stone mixes are used.

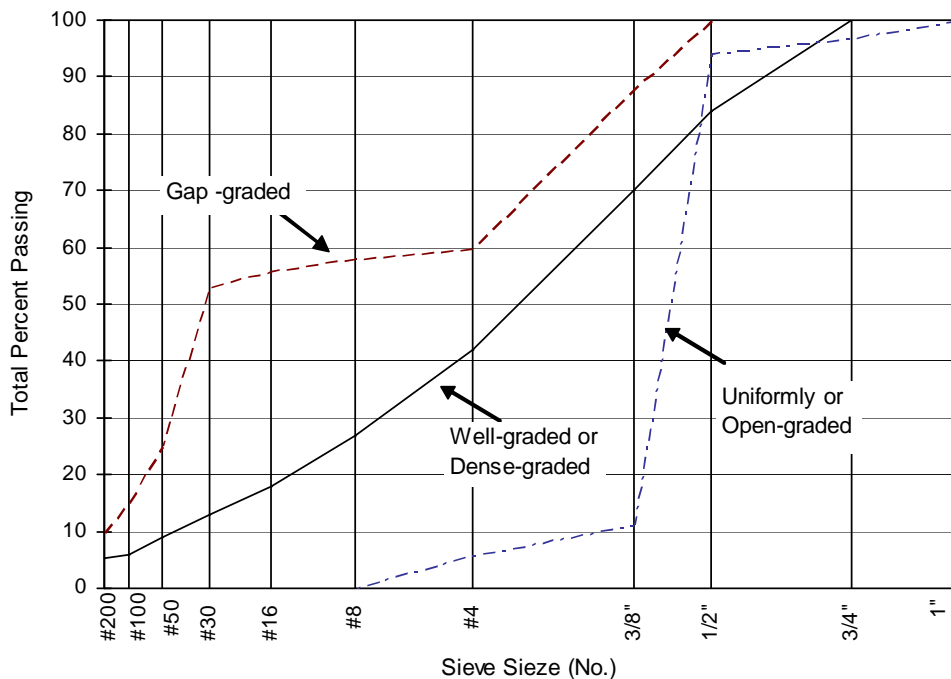


Figure 2-10: Typical aggregate gradations.

Some guidance for developing gradation limits and potential problem areas were proposed by Hveem in 1940. Theoretically, the gradation that gives the densest packing provides enhanced

stability and reduces void space in the mineral aggregate through increased interlocking between mixture particles. However, gradations of maximum density may not provide enough voids in the aggregate. There must be sufficient air void space in HMA to permit enough asphalt cement to be incorporated to provide adequate film thickness for maximum durability. In addition, appropriate HMA air voids content must be ensured in the mixture to avoid bleeding or rutting. Therefore, deviations from the maximum density curves are necessary in order to increase the total voids in the mineral aggregate (VMA). VMA is an important parameter and minimum values of VMA are required and suggested by most pavement agencies depending on the maximum nominal aggregate size of the mixture design. It is preferred that the gradation curve be approximately parallel to the maximum density line with a few percentage points offset, either above or below the line. Most specifications for HMA define aggregate gradation band and tolerance for each nominal maximum size mixture according to accumulated field experiences. In particular, the Superpave mix design developed by the Strategic Highway Research Program (SHRP) requires a selected number of control points on the gradation chart. The Superpave mix design system uses the following aggregate size definitions:

- Maximum size: one sieve size larger than the nominal maximum size.
- Nominal maximum size: one sieve size larger than the first sieve to retain more than 10%.

The maximum density line is obtained in Superpave by connecting the origin at the lower left of the 0.45 power gradation chart to the maximum aggregate size at the upper right of the chart (FHWA 1995).

Birgisson and Ruth (2001) developed a power law model to evaluate and classify gradation curves according to mixture performance. Ruth et al. (2002) expanded the parametric study and provided an experience-based methodology which introduced aggregate gradation factors based on regression analysis of power law constants (a_{ca} and a_{fa}) and exponents (n_{ca} and n_{fa}). These gradation factors were used to evaluate relationships with tensile strength, fracture energy, and failure strain of the mixtures. The findings appeared to imply that the gradation characterization factors relate well to mixture properties. Birgisson et al. (2004) and Ekingen (2004) established a correlation between dynamic modulus and aggregate gradation factors at high temperature (40°C) based on the power law model. The relationship between a low n_{fa} and a high dynamic modulus at 40°C has been identified, which indicates that power law parameters can be used to optimize mixture gradations for the dynamic modulus and the rate of change in the gradation on the fine

side affects the stiffness and rutting resistance of the mixture. In addition, it was also found that a high n_{ca} results in a low dynamic modulus when controlling for n_{fa} . More recently, Roque et al. (2006) developed a conceptual and theoretical approach to evaluate the relationship between coarse aggregate structure based on gradation and the pavement rutting performance. They found that the relative proportion of particles from two contiguous size ranges can be no greater than 70/30 and the porosity must be no more than 50% in order to form an interactive network.

2.3.3 HMA Mix Design

Most HMA produced before 1990s in the United States was designed using the Marshall or Hveem method. The Superpave mix design procedures were developed by the Strategic Highway Research Program (SHRP) and were adopted by a few states for some pavement projects starting in 1995. The key points for all three design methods are the same: to determine an appropriate asphalt content level with which to begin field construction.

The concept of the aggregate maximum density line for the densest packing of HMA was first validated by Nijboer (1948). Goode and Lufsey (1962) then proposed that aggregates should be graded using a mathematical concept of packing the void space between aggregates of large diameter with aggregates of smaller diameter. They noted that if the gradation corresponding to the exponent of 0.5 is used as proposed by Fuller in 1907, then the VMA may be too low to ensure both sufficient air void content and enough asphalt cement for durability and stability. Therefore, the FHWA included the suggested use of the 0.45 power curve as well as the maximum density line to evaluate and adjust aggregate gradations. Huber and Shuler (1992) presented the relationship of VMA to aggregate gradation and particle characteristics for a controlled experiment. They investigated different methods of drawing maximum density lines that produces the densest packing.

Hveem first noticed that there was a relationship between the gradation of the mineral aggregate and the amount of oil required to maintain a consistent color and appearance of the mixture. Then he realized that having the proper oil content did not guarantee good performance relative to rutting. This led to the development of Hveem stabilometer test to evaluate the ability of HMA mixtures to resist the shear forces applied by traffic loads. The basis for selecting the optimum asphalt content in the Hveem method is to use a well-graded aggregate with high

friction and appropriate amount of fines and add as much asphalt cement as the mixture will tolerate without losing stability. A detailed account of the evolution of the Hveem mixture design method was given by Vallerga and Lovering (1985). Details of specimen preparation and testing by Hveem apparatus are given in ASTM D1561 and D1560, respectively.

A detailed introduction of the Marshall mix design method is given by a few researchers (Foster 1982; White 1985). The acceptance tests on the aggregates and asphalt cement are conducted at the beginning. If the materials pass these tests, the test procedure for the Marshall method can be performed (The Asphalt Institute 1993). The test protocol calls for fabricating 18 test specimens for the volumetric analysis. Three loose mixture specimens are made near the optimum asphalt content to measure Rice specific gravity or theoretical maximum density (TMD). Three compacted specimens each are prepared at five different asphalt contents with 0.5% increments with at least two above the estimated optimum asphalt content and two below the estimated optimum. The approximate optimum asphalt content can be based on experience or specific guide.

The amount of compaction is selected based on traffic level. The test specimens are compacted using a Marshall hammer with 35, 50 or 75 blows per side for light, medium or heavy traffic, respectively. The bulk specific gravity is then measured for each specimen after proper handling. The Rice specific gravity (G_{mm}) is calculated for each of the asphalt content mixes using the equation (relationship between G_{mm} , G_{se} and P_b). Other volumetric parameters, including air voids (VTM), VMA, and VFA, are also calculated using the related equations presented earlier. The compaction procedure will produce specimens with decreasing air voids as a function of increasing asphalt binder content. The compacted specimens are usually 4 inches (100 mm) in diameter and 2.5 inches (63.5 mm) in height.

These specimens are then used for conducting the Marshall stability and flow test. The test is performed at 140°F (60°C), which is considered a critical temperature for permanent deformation. A load at 2 inches/minute (50.8 mm/min) is applied to the specimen until the maximum load is reached. The stability is the maximum load in pounds (Newtons) and the flow is the deformation in 0.01 inch (0.25 mm). The stability generally increases with increasing asphalt content, reaches a peak, and then decreases. The asphalt content at the peak stability value is a good indicator of optimum binder content based on the idea that constant compaction effort across varying asphalt content produces a maximum stability value near the optimum

asphalt content. In addition, the % VMA will decrease with increasing asphalt content, reach a minimum, and then increase. Since the mixture strength increases as the VMA decreases, the mix with minimum VMA should have the maximum strength or stability at the optimum asphalt content. Finally the optimum asphalt content is determined by averaging the three asphalt contents at maximum stability, maximum density and midpoint of the specified air voids range (typically 4 %). All parameters are checked at this optimum binder content for acceptability according to the Marshall mix design criteria.

2.3.3.1 Bailey Method

The Marshall mix design method was broadly used in the United States before the 1980s. It provides some guidance on the use of coarse and fine mixes. However, numerous trial and error process still have to be conducted to obtain a proper aggregate blend. The Bailey method gives a good starting point for mix design when adjustments are required to improve the volumetric properties of the mix (Vavrik et al. 2001; Asphalt Institute and the Heritage Group 2005). The detailed methodology is summarized herein.

The Bailey mix design method was originally developed by Robert. D. Bailey in the early 1980s. The primary purpose of this methodology is to control the mix properties during construction including volumetric properties, segregation, workability, and compatibility by focusing on aggregate packing. There are four key principles in the Bailey method:

1. Determine the coarse and fine aggregate. The coarse fraction creates voids and the fine fraction fills in the voids.
2. Analysis of coarse fraction which influences the packing of fine fraction.
3. Analysis of coarse part of the fine fraction, which relates to the packing of the overall fine fraction in the blend.
4. Analysis of fine part of the fine fraction, which relates to the packing of the fine portion of the gradation in the blend.

Figure 2-11 shows the four principles on a typical gradation curve for a coarse gradation mix. The Bailey method defines the break between coarse and fine fractions as the primary control sieve (PCS). The PCS is the closest sieve to the result of $0.22 \times \text{NMPS}$, where the NMPS denotes the nominal maximum particle size, which is equivalent to the nominal maximum

aggregate size (NMAS) used in the Superpave system. The Bailey method uses AASHTO T19 to determine the loose unit weight (LUW) and the rodded unit weight (RUW) of each individual aggregate used in the mix. The suggested chosen unit weight ranges for each mix type are shown in Table 2-2. It should be noted that stone mastic asphalt (SMA) references the RUW condition of coarse aggregate, while coarse-graded and fine-graded mixtures reference the LUW condition. The combined blend evaluation for coarse-graded and fine-graded mixes is shown in Figure 2-12 and Figure 2-13, respectively. SCS and TCS denote secondary control sieve and tertiary control sieve, respectively.

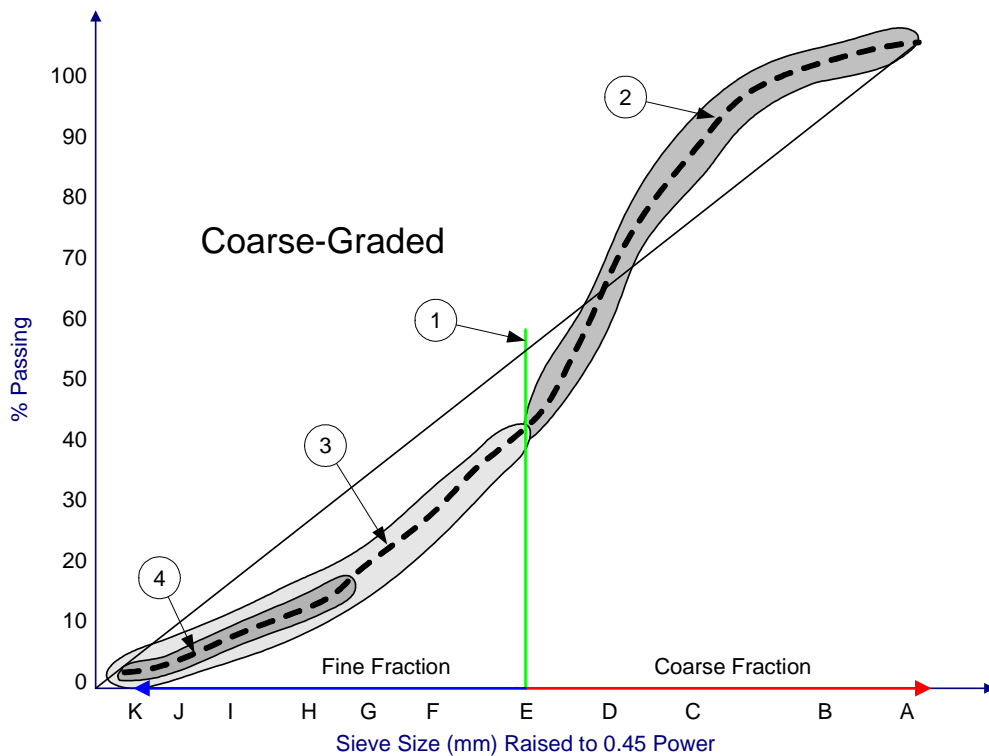


Figure 2-11: The four principles of Bailey method for coarse-graded mix

Table 2-2: Chosen unit weight ranges by mix type

Fine-Graded	Coarse-Graded	SMA
90% or less LUW	95% – 105% LUW	110% – 125% RUW

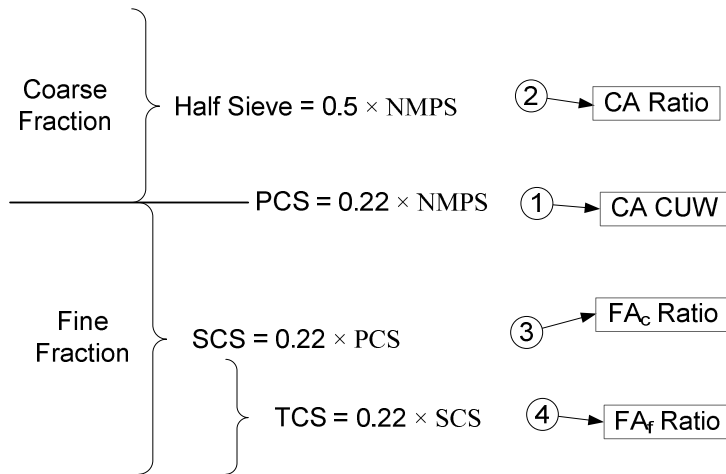


Figure 2-12: Combined blend evaluation for coarse-graded mixes.

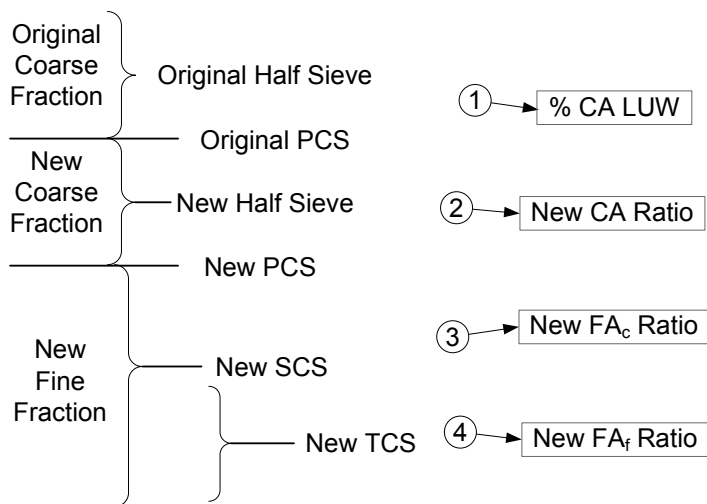


Figure 2-13: Combined blend evaluation for fine-graded mixes.

The coarse aggregate ratio (CA), coarse part of fine aggregate ratio (FA_c), and fine part of fine aggregate ratio (FA_f) can be calculated by the following equations:

$$\text{CA Ratio} = \frac{\% \text{ passing half sieve} - \% \text{ passing PCS}}{100 - \% \text{ passing half sieve}} \quad (2-9)$$

$$\text{FA}_c \text{ Ratio} = \frac{\% \text{ passing SCS}}{\% \text{ passing PCS}} \quad (2-10)$$

$$FA_f \text{ Ratio} = \frac{\% \text{ passing TCS}}{\% \text{ passing SCS}} \quad (2-11)$$

Table 2-3 shows the recommended values of the different ratios for coarse and fine mixes. The Bailey mix design method provides a useful and practical approach for evaluating volumetric properties and compactability and thus helps in better understanding the aggregate structure in asphalt mixtures as well as quality control at the plant or in the field.

Table 2-3: Recommended aggregate ratios

NMPS (mm)		37.5	25.0	19.0	12.5	9.5	4.75
CA Ratio	Coarse	0.80–0.95	0.70–0.85	0.60–0.75	0.50–0.65	0.40–0.55	0.30–0.45
	Fine	0.6 – 1.0					
FA _c Ratio	Coarse	0.35 – 0.50					
	Fine	0.35 – 0.50					
FA _f Ratio	Coarse	0.35 – 0.50					
	Fine	0.35 – 0.50					

2.3.3.2 Superpave Mix Design

Since the early 1980s, traffic volume and axle loads have been increasing remarkably in the United States. There emerged a need to develop an improved mix design method that could be used in various traffic conditions and environments. With this as a primary goal, the Strategic Highway Research Program (SHRP) was initiated in 1988 and completed in 1993 resulting in the Superior Performing Asphalt Pavement (Superpave) System. The Superpave system consists of the following components: new grading system for asphalt binder (performance graded (PG) grading system), consensus properties of aggregate, new mix design procedure, and mixture analysis procedures (FHWA 1995; Asphalt Institute 1995; TRB 1994).

The aggregate properties that are specified by the SHRP are the coarse and fine aggregate angularity, flat and elongated particles, and sand equivalent results. The angularity of aggregate is related to the shear strength of the HMA mix and thus influences the rutting performance of HMA pavement. The coarse aggregate angularity is determined by measuring the percentage of coarse aggregate particles with fractured faces, whereas the angularity for fine aggregate is measured by determining the amount of voids by the National Aggregate Association (NAA) flow test in accordance with AASHTO TP33 Method A. Flat or elongated particles tend to lie

flat or even break down during compaction, which may affect the workability of the mixtures. In addition, flat or broken aggregates will make the mixture VMA lower than designed or expected. The test procedure for flat or elongated particles is specified in ASTM D4791, “Flat or Elongated Particles in Coarse Aggregate.” The clay content is related to the stripping problem of the mixture. Excessive amounts of clay may result in a poor bond between the asphalt binder and aggregate. The clay content is measured by the sand equivalent test conducted in accordance with AASHTO T176 or ASTM D2419.

Aggregate blend is one of the most important factors to consider in HMA mix design to ensure that a satisfactory gradation skeleton is obtained and volumetric requirements are met. According to the definition given by Superpave, at least 90 – 100 % of the aggregate must be finer than the nominal maximum aggregate size. Control points are also set on the 2.36 mm (No. 8) and the 0.075 mm (No.200) sieve sizes. Superpave requires the aggregate gradation curve to be within the control limits. Another part of the Superpave specification for gradation curve is the restricted zone. The restricted zone provides a guide to help avoid too much natural rounded sand being used in the mixture and to help ensure minimum VMA requirements are met. However, Kandhal et al. (2001) showed that potential good mixes may get rejected because their gradations pass through the restricted zone. Chowdhury et al. (2001) found that there is no relationship between the restricted zone and permanent deformation when crushed aggregates are used in the mixture design. In practice, there are aggregate blends that pass through the restricted zone while not using an excessive amount of rounded aggregates that meet the minimum VMA requirements. A typical gradation curve along with the corresponding gradation limits is shown in Figure 2-14.

The Superpave gyratory compactor (SGC) is a key component of the Superpave mix design. The compaction equipment is designed to compact HMA samples to conditions similar to those obtained in the field under traffic loads. The compaction effort is controlled by three parameters: vertical pressure, angle of gyration, and number of gyrations. In the Superpave mix design procedure the vertical pressure is set at 600 kPa (87 psi), the angle of gyration is set at 1.25°, the rate of gyration is 30 revolutions per minute, and the number of applied gyrations depends on the design traffic level and average high air temperature. N_i , N_d , and N_m are three numbers of gyrations specified for the Superpave gyratory compactor. N_i is N-initial which measures the mixture compactibility to ensure that the mix will not compact too quickly. N_d is N-design and

represents the number of gyrations required to produce a density in the mixture similar to that ultimately obtained in the field when subjected to traffic. N_m is the N-maximum and is the number of gyrations that provides a compacted density which should not be exceeded in the field, for a too-densified mix will result in low VMA which may cause a rutting problem. Generally N_d is determined based on lab and field test data through comparison of in-place density and laboratory density at various numbers of gyrations. N_i and N_m are then given by the following equations:

$$N_i = (N_d)^{0.45} \quad (2-12)$$

$$N_m = (N_d)^{1.10} \quad (2-13)$$

Superpave defines the optimum asphalt content as the one that produces 4% air voids at N_d . An estimate of the optimum asphalt content is selected from aggregate blend trials. Three samples each are prepared at 0.5% below estimated optimum, at estimated optimum, at 0.5% above, and at 1.0% above estimated optimum. All samples are put into an oven to be aged at 135°C (275°F) allowing absorption of the asphalt cement into aggregate pores before compaction. Each sample is compacted up to N_m . The estimated bulk specific gravity at each number of gyrations is calculated by using the specimen weight, diameter (6 inches, or 150 mm) and height which is measured and recorded during the compaction process. This estimated density is slightly lower than the actual density because usually the raw compacted specimens have many surface voids on the top, bottom and cylindrical sides. The actual bulk specific density at N_m is measured by weighing the samples in air and water. The correction factor is calculated at N_m by the following equation:

$$CF = \frac{G_{mb} \text{ (actual)}}{G_{mb} \text{ (estimated)}} \quad (2-14)$$

The actual bulk specific gravity at N_i and N_d can be back-calculated using the correction factor and the estimated density at the corresponding number of gyrations. The theoretical maximum density (TMD) is measured from the rice test on loose mixtures. The air voids can then be determined by knowing the G_{mm} and the actual G_{mb} at various compaction levels. The air voids of three samples at each asphalt content level are averaged and plotted on a graph. The actual optimum asphalt content that provides 4 % air voids at N_d can be determined by

interpolation. It is required that the air voids be greater than 11% at N_i and greater than 2% at N_m . Other requirements that must be satisfied include VMA and VFA according to Superpave specifications.

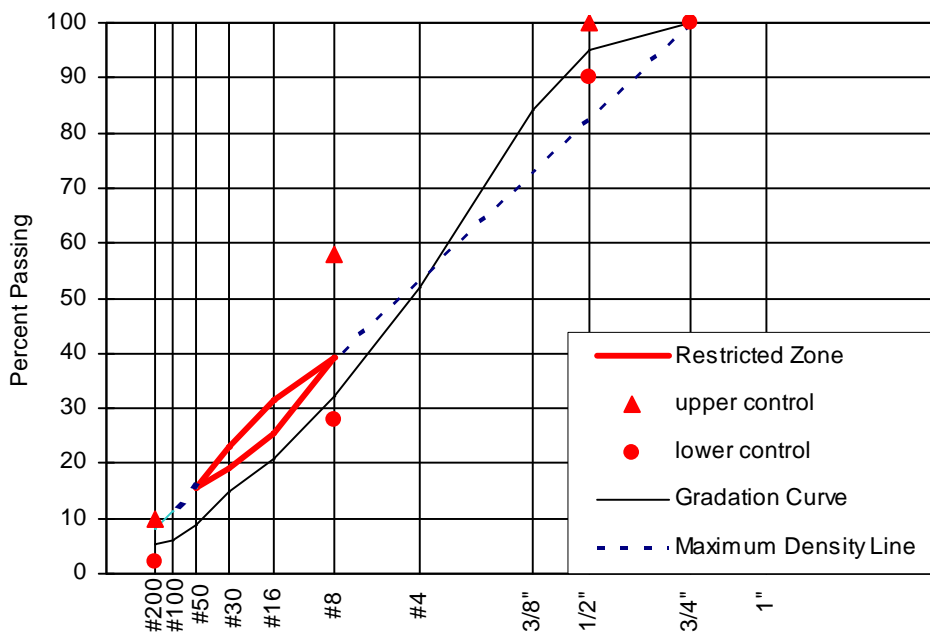


Figure 2-14: Illustration of gradation requirements for 12.5 mm (1/2 in.) nominal size

2.4 Mechanical Tests for Characterization of Asphalt Mixtures

2.4.1 Introduction

Flexible pavements constructed with asphalt mixtures are subjected to a wide range of traffic loads and environmental conditions. Characterization of HMA mixtures is the measurement and analysis of their response to these conditions. The performance of any HMA mixture is dependent upon the entire pavement structure, and the structural capacity of the pavement layers is dependent on the quality of materials and their compositions in the mixture. An understanding of fundamental engineering properties of HMA mixtures is required for satisfactory performance of pavement structures in service. There have been many testing protocols developed in the laboratory for measuring mixture properties related to thermal cracking, fatigue cracking, and permanent deformation over the past few decades. These test procedures are used to evaluate the

distress of HMA mixtures under various types of load at different loading rates and temperature levels similar to those encountered in the field.

The test methods can be categorized into in-place and laboratory tests. The testing program developed for this study is conducted on lab-prepared HMA specimens with a complete set of equipment. Laboratory mechanical tests can be further grouped based on the test mode, such as direct tension, indirect tension, compression, flexural, shear, and torsion. Pavement design using elastic layer theory needs two elastic parameters for each material layer used: Young's modulus (stiffness) and Poisson's ratio. In the NCHRP 9-19 report (2001), many tests had been proposed as a simple performance test, including the dynamic modulus test, the indirect tensile creep compliance test, resilient modulus test, tensile strength test and other test methods. Details of the test methods utilized in this study are discussed in the following sections.

2.4.2 Indirect Diametral Tests in Tension

The indirect diametral test is used extensively by state highway and other agencies for routine tests. The 1986 AASHTO Pavement Design Guide, which recommended the use of resilient modulus to characterize pavement materials, has led to accelerated use of this type of test. This test is usually conducted on cylindrical specimens subjected to a compressive load along two opposite generators resulting in a relatively uniform tensile stress acting perpendicular to and along the diametral plane of the applied load. A splitting failure generally occurs as a result along the diametral plane (Figure 2-15). If a repetitive pulsating load is applied diametrically to the sample, the dynamic load results in dynamic deformations across the horizontal diametral plane. The transducers mounted on each side of the horizontal specimen axis record these deformations. The resilient modulus (M_R) of HMA mixtures can be determined by the dynamic load and deformation. The indirect diametral test is originally specified by ASTM D4123-82 Standard Test Method for Indirect Tension Test for Resilient Modulus of Bituminous Mixtures, which was withdrawn in 2003. The resilient modulus (M_R) has been used in the AASHTO Design Guide (AASHTO 1993) since 1993. The resilient modulus laboratory test procedure is described in AASHTO TP 31. The test is defined as a repetitive 0.1 second haversine load followed by a 0.9 second rest period, continued at 1 Hz intervals. Many empirical relationships have been developed throughout the years relating M_R to other tests like the

California bearing ratio (CBR) and the Marshall stability test (AASHTO 1993), since it has long been considered the defining characteristic for HMA layers.

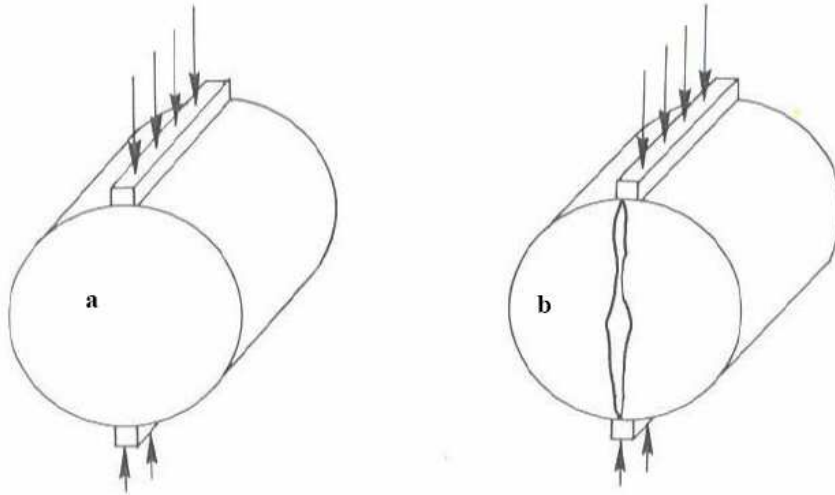


Figure 2-15: Indirect diametral test during loading and at failure

After the specimens were well prepared, they were placed in a controlled temperature cabinet and brought to the specified test temperature. The specimen was placed into the loading apparatus and the loading strips were positioned to be parallel and centered on the vertical diametral plane. The specimen was preconditioned by applying a repeated haversine or other suitable waveform load without impact for a minimum period sufficient to obtain uniform deformation readout. Depending upon the loading frequency and temperatures, a minimum of 50 to 200 load repetitions is typical; however, the minimum for a given situation must be determined so that the resilient deformations are stable. Resilient modulus evaluation will usually include tests at three temperatures, for example, 41, 77, and 104°F (5, 25, and 40°C), at one or more loading frequencies. The horizontal and vertical deformations were continuously monitored during the test.

The required test equipment is a loading device capable of applying a load pulse over a range of frequencies, load durations and load levels. Some form of temperature control system is required. The temperature-control system should be capable of control over a temperature range from 41 to 104°F (5 to 40°C). The measurement and recording system should include sensors for measuring and recording horizontal and vertical deformations. The values of vertical and horizontal deformation can be measured by linear variable differential transducers (LVDTs) or

other suitable devices. LVDTs should be at mid-height opposite each other on the specimen's horizontal diameter. A metal loading strip with a concave surface having a radius of curvature equal to the normal radius of the test specimen is required to apply load to the specimen. The specimens should have a height of at least two inches and a minimum diameter of four inches for aggregate up to one inch maximum size, and a height of at least three inches and a minimum diameter of six inches for aggregate up to 1.5 inches maximum size.

Hondros (1959) derived the stress equations to model the actual test conditions as well as to determine Young's modulus and Poisson's ratio of the material. The theoretical distribution of stresses for a concentrated load is shown in Figure 2-16 and Figure 2-17.

Roque and Buttlar (1992) developed a measurement and analysis system to determine asphalt concrete properties, primarily thermal cracking, using the indirect tensile testing mode, which was incorporated in AASHTO TP9-96, Standard Test Method for Determining the Creep Compliance and Strength of Hot Mix Asphalt (HMA) Using the Indirect Tensile Test Device. They proposed the gauge-point-mounted device to measure horizontal and vertical deformations across a gauge length of 25.4mm (1 inch). Poisson's ratio was also obtained from the horizontal and vertical deformations instead of using assumed values. Correction factors from 3-D finite element analysis were used to account for: (1) the effect of specimen bulging on deformation measurement, and (2) approximation of 2-D plane stress assumption. Roque et al. (1997) made further modifications and improvements on the SHRP IDT system for characterizing relevant asphalt mixture properties. The test procedures and data reduction methodologies were also summarized in Long-Term Pavement Performance (LTPP) Protocol P07 (2001): Test Method for Determining the Creep Compliance, Resilient Modulus and Strength of Asphalt Materials Using the Indirect Tensile Test Device.

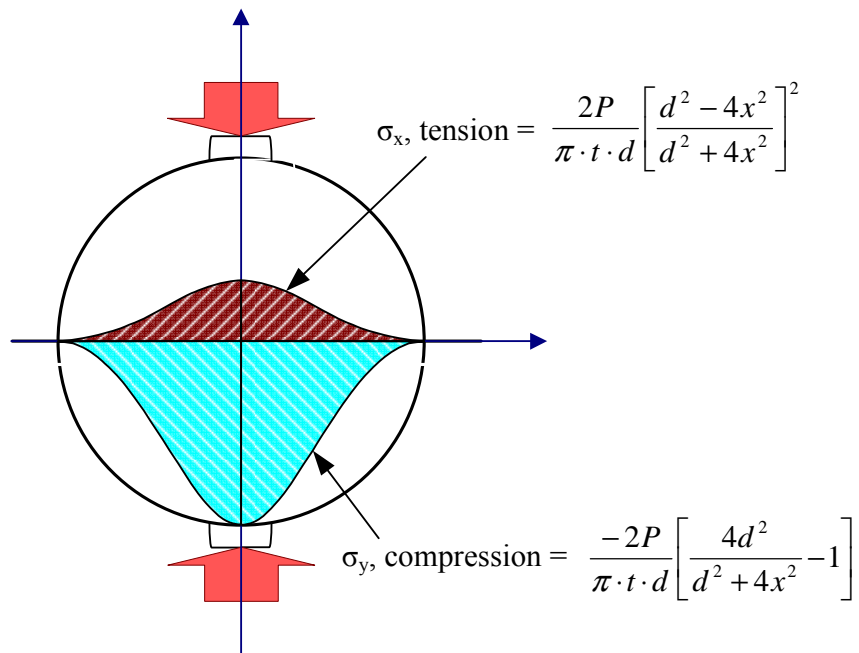


Figure 2-16: Theoretical stress distribution on horizontal diametral plane for indirect tensile test (After Yoder et al. 1975)

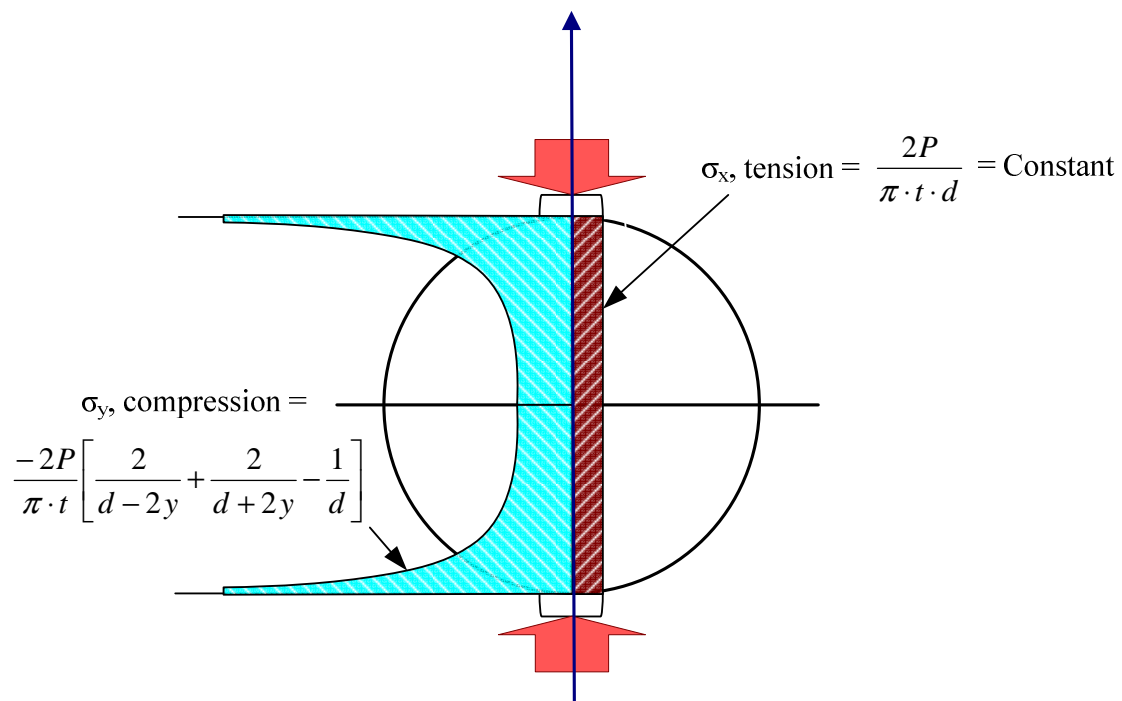


Figure 2-17: Theoretical stress distribution on vertical diametral plane for indirect tensile test (After Yoder et al. 1975)

2.5 HMA Fracture Mechanics Concepts

2.5.1 Background

It is commonly considered necessary to study real cracking growth mechanisms in order to essentially understand the crack damage in HMA. Research conducted by Roque et al. (2002) on top-down cracking of asphalt pavement indicated that the tearing-apart effect from vehicle tires can cause a certain level of tensile stress leading to cracking of the pavement surface and crack propagation. The conventional linear elastic fracture mechanics presume that there are intrinsic flaws in a material. A crack initiates from the flaws and is propagated continuously under a critical loading condition. The crack growth rate of linear elastic materials is assumed to follow Paris's law:

$$\frac{da}{dN} = A(\Delta K)^n \quad (2-15)$$

where a is crack length, N is number of load repetitions, K is stress intensity factor, and A and n are constants.

However, Jacobs (1996) investigated the fracture mechanics for HMA mixtures and pointed out that the non-homogeneity of asphalt concrete could cause the discontinuity of crack propagation in the mixture. It was shown that a crack in asphalt concrete grows discontinuously. Zhang (2000) and Zhang et al. (2001) found that the continuous crack growth assumption cannot characterize the cracking performance of asphalt concrete mixtures observed in the field, which occurs in a stepwise manner rather than a continuous one. They indicated that there is a specific threshold below which the damage is considered to be on a micro scale and healable with a rest period or temperature increase, whereas the damage would be permanent on a macro scale when the threshold is reached or exceeded.

Shen et al. (2005) introduced the plateau value (PV) concept using the ratio of dissipated energy change (RDEC) to show its relationship with damage and failure at normal or low strain levels (70 – 500 micro-strains). Carpenter et al. (2006) applied this RDEC approach to analyze healing and HMA fatigue behavior at normal and low strain levels using the standard four-point bending beam fatigue test procedure specified in AASHTO standards (21): constant strain at 500 micro-strains, $20 \pm 0.5^\circ\text{C}$ temperature, 10Hz frequency with haversine load waveform, etc.

Healing was observed at low strain conditions or long rest period, and hence may increase the fatigue life of HMA material.

2.5.2 HMA Fracture Mechanics Model from IDT

An HMA fracture model for predicting pavement cracking was developed by Zhang et al. (2001) and Roque et al. (2002, 2004). Crack growth laws were identified for asphalt mixtures using IDT. The linear elastic finite element method was used to simulate the IDT specimens at different cracking lengths. They established a relationship between the theoretical crack length and the deformation measured between the vertical gage points. Besides the three types of regular IDT tests (resilient modulus, creep compliance, and tensile strength), another type of fracture test was performed. The specimens for the fracture test have 150 mm diameter and 25 mm thickness with an 8 mm hole in the center. The fracture test was conducted under the same load mode as M_R test but at higher deformation levels in order to determine the crack growth characteristics of the specimen. The test was performed at 10°C. The repeated load was applied until the specimen failed. The crack growth rate parameters for Paris law ($da/dN = A(K)^n$) were determined by the following steps:

- Establish the relationships of cracking length (a) versus horizontal deformation (δ_H) and stress intensity factor (K) using theoretical finite element analysis.
- Establish a relationship between horizontal deformation (δ_H) and loading repetitions (N) from fracture test.
- Incorporate the theoretical calculation into the test results to develop a relationship between cracking length growth rate (da/dN) and stress intensity factor (K).
- Obtain the fracture parameters, A and n , by regression analysis.

The regression models were used to evaluate the mixture cracking resistance. Discrepancies between laboratory tests and field performance were observed. Regression analyses were conducted to determine the relationship between the mixture properties (tensile strength, m -value, fracture energy and resilient modulus) and measured crack growth rates. It was determined that dissipated creep strain energy to failure is not dependent on mode of loading and could be used as a threshold to explain the inconsistency of lab and field observations, as shown in Figure 2-18 (Roque et al. 2002). There are two possible reasons for fracture to occur: 1) a number of

continuous repeated loads can cause damage accumulation due to creep strain energy, and fracture can develop if the DCSE threshold is reached, even when the loading stress is below the tensile strength. It also should be noted that the mixture may never crack if the healing effect makes the induced dissipated energy below the threshold regardless of the load repetitions; 2) fracture may occur if any large single load exceeds the fracture energy (FE) threshold. Case 3 in Figure 2-18 shows that cracking would not occur during a single load application unless the upper FE threshold is exceeded, even when the dissipated energy (DE) is exceeded.

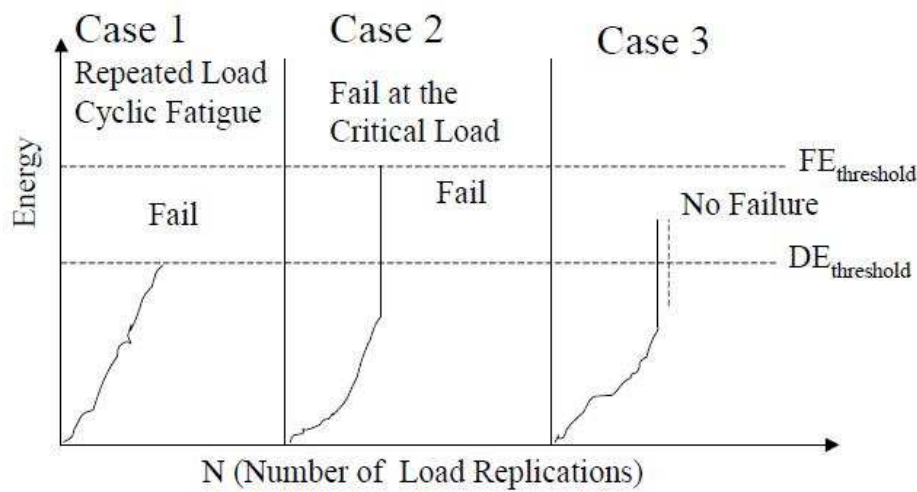


Figure 2-18: Illustration of potential loading condition (Roque et al. 2002)

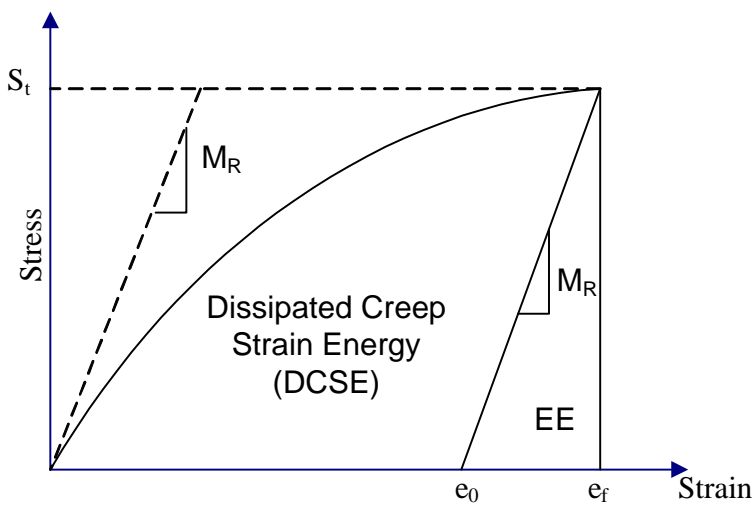


Figure 2-19: Determination of fracture energy and dissipated creep strain energy

The concepts of fracture energy (FE) and dissipated creep strain energy (DCSE) were introduced in the model to account for the pavement structure crack performance. The two energy values are determined using the tensile strength test along with the resilient modulus test. The schematics used to calculate these limits are shown in Figure 2-19. The values are calculated by the following equations:

$$FE = \int_0^{S_t} \sigma \cdot d\varepsilon \quad (2-16)$$

$$\varepsilon_{EE} = \varepsilon_f - \varepsilon_0 = \frac{S_t}{M_R} \quad (2-17)$$

$$EE = \frac{1}{2} \cdot \varepsilon_{EE} \cdot S_t = \frac{(S_t)^2}{2 \cdot M_R} \quad (2-18)$$

$$DCSE = FE - EE \quad (2-19)$$

Where

FE = fracture energy, total energy applied to the specimen till fracture

EE = elastic energy, recoverable energy

DCSE = dissipated creep strain energy absorbed by the specimen prior to fracture

S_t = tensile strength of the mixture

ε_f = failure strain

M_R = resilient modulus of the mixture

It was shown that the dissipated creep strain energy at failure ($DCSE_f$) is the threshold that controls crack propagation, which can be described as a step function consisting of crack initiation ($DCSE$ below the threshold) and crack propagation ($DCSE$ over the threshold). It was also found that micro-damage in HMA can be healed while macro-damage cannot be healed at rest period or temperature increase conditions. $DCSE$ per cycle and number of load repetitions can be further estimated using the following equations:

$$DE_{CreepStrain} / cycle = \frac{1}{20} \sigma_{AVE} (\sigma_{AVE} D_1 m (100)^{m-1}) \quad (2-20)$$

$$N_f = DCSE_f / (DCSE / cycle) \quad (2-21)$$

where σ_{ave} is the average stress near the crack tip, m and D_1 are power law parameters obtained from the creep compliance test, and N_f is the number of cycles to failure.

Villiers (2004) used the HMA Cracking Model along with the IDT sweep of tests to evaluate the sensitivity of Superpave mixtures with regards to cracking performance. The mixtures were tested at 10°C to determine the cracking performance when subjected to the acceptable variances. A statistical evaluation was conducted to examine the variation in the IDT testing parameters. Significant variation was observed for all the IDT parameters which were consistent with research conducted by Roque et al. (2004). It was found that the average values used from the IDT test parameter could be used to distinguish between pavements that exhibited top-down cracking and those that did not.

Roque et al. (2004) showed that cracking performance of HMA is complex and controlled by multiple mixture properties. The energy ratio concept was derived as a fundamental material property using the HMA fracture mechanics model. It is defined as the ratio of dissipated creep strain energy threshold of the mixture to the minimum dissipated creep strain energy required, which can be determined from Superpave IDT including resilient modulus, creep compliance, and tensile strength tests. N_f of 6000 was set as the critical value that distinguishes mixture performance. The equations to calculate the Energy Ratio are presented below:

$$ER = \frac{a \times DCSE_f}{m^{2.98} \cdot D_1} \quad (2-22)$$

$$a = 0.0299 \cdot \sigma^{-3.1} \cdot (6.36 - S_t) + 2.46 \times 10^{-8} \quad (2-23)$$

Where

σ = Tensile stress of the asphalt layer in psi (pavement structure)

S_t = Tensile strength in MPa (IDT tensile strength test)

The other parameters are the same as those defined earlier. The HMA fracture mechanics were implemented to examine all test sections, based on which performance criteria of ER greater than 1 and DCSE greater than 0.75 were defined to evaluate cracking performance. They showed that no single property can be an accurate performance indicator since fracture properties are interrelated as a system. The Energy Ratio appeared to be a suitable parameter for evaluating top-down cracking situations of sections within a pavement system at low in-service temperatures.

Kim (2005) developed an HMA thermal fracture model based on the same principle and failure criteria used in the HMA fracture model introduced above. The Superpave IDT tests were designed at three temperatures (0, 10, and 20°C) which are typical low in-service temperatures in Florida. The performance evaluation of the model showed potential to reliably evaluate the performance of asphalt mixtures subjected to thermally induced damage.

CHAPTER 3

MATERIALS AND EXPERIMENTAL PROGRAM

3.1 General

The method of measuring fracture mechanics properties of HMA in this research study was the indirect diametral tension test (IDT). The test method was reviewed in more detail in Chapter 2. Originally, the IDT resilient modulus test was specified by AASHTO TP31-94 and ASTM D4123-82. This study adopts the SHRP IDT Testing and Analysis System (Roque et al. 1997) to measure the resilient modulus, creep compliance, and tensile strength. A complete dynamic testing system was acquired to perform the temperature-controlled dynamic tests to determine the engineering properties of Florida HMA mixtures. In this study, a Servopac Gyrotory Compactor and an Interlaken Asphalt Test System were used to compact the asphalt mixture and measure the dynamic response of asphalt concrete, respectively.

The experimental program involved two standard mix designs as control mixes. For each control mix, two modified gradations were selected while using the same base asphalt binder (PG 67-22). In addition, each of the two Superpave control mixes was modified using three levels of SBS polymer-modified asphalt binder instead of the original asphalt binder to evaluate SBS polymer effects on fracture mechanics properties of asphalt concrete mixes. Therefore, the overall experimental program involved a total of twelve HMA concrete mixtures. All specimens were prepared at targeted optimum air voids of 4%.

The physical properties of the materials used, including their aggregate properties, aggregate gradation, asphalt binder characteristics, and mixture design series, are presented in detail in this chapter according to the purpose of the studies.

3.2 Mix Designs and Aggregate Gradation Modifications

One Georgia granite mix (SP 04-3034A, TL-D, Ga553), referred to as “F2C,” and one South Florida limestone mix (LD 02-2529A, TL-D, SFL), designated as “F4C,” were selected as the control mixes for the fracture mechanics tests. The two Superpave mix designs are commonly used in Florida and were approved by Florida Department of Transportation (FDOT). They are

both coarse mixes with the gradation curves passing below the Superpave restricted zone, which were selected with the intention of making adjustments to their coarse aggregate proportions to study the effect of gradation on mixtures' fracture mechanics properties.

The nominal maximum aggregate size for both F2C and F4C is 12.5 mm. They are commonly used FDOT gradations and are known to perform well in the field. Both gradation curves of the two control level mixtures go below the restricted zone and then sharply rise upward across the maximum density line at No. 4 sieve size, and continue a certain amount higher than the maximum density line through the coarse sizes. The main purpose of this shape is to assure sufficient air voids content of the asphalt mixture. In order to facilitate study of the coarse aggregate effect on asphalt concrete mixtures, the coarse part (No. 4 sieve size and larger) of each mix design was modified to two different compositions with the fine parts of the mixes kept unchanged. The job mix formulas of the original standard mix designs and associated gradation modifications are summarized in Table A-5 and Table A-6. The corresponding gradation charts for all mix design series (sieve size raised to 0.45 power mm) are presented in Figure 3-1 and Figure 3-2 for illustration. As shown in the charts, the first set of modified gradations, named F2G1 and F4G1, have gradation curves slightly lower than the original mix design in the coarse part, but still above the maximum density line. The second set, denoted as F2G2 and F4G2, have gradation curves further lower than the first modified one, and go below the maximum density line in the coarse part. Figure 3-3 and Figure 3-4 show comparisons of percent retained on top three sieves between control level and modified gradations. The asphalt content levels for mixtures with modified gradation were kept the same as for the original control mixes.

3.3 SBS Polymer-modified Asphalt Binder

The grade of asphalt cement used in mixtures is one important factor that can affect the strength of asphalt concrete and amount of rutting which occurs in the mix. The unmodified asphalt PG 67-22 (AC-30), which is commonly used in Florida, was selected as the base asphalt for both fracture mechanics tests and the dynamic modulus test. The asphalt binder PG67-22 grading report is summarized in Appendix Table A-1. The base asphalt to which varying amounts of polymer were added was the same unmodified PG 67-22 (AC-30). Three levels of

SBS polymer-modified asphalt are produced and used in the SBS effects study. The SBS modified asphalt binder grading reports are summarized in Table A-2 through Table A-4. The base asphalt and the other three levels of polymer-modified asphalt (PMA) are listed as follows:

1. Control level

Base asphalt A (PG 67-22) + Aggregates = Control Mix

Mixtures are referred to as F2C and F4C.

2. Mix plus 3% SBS polymer A

[Base asphalt A + 3% SBS polymer A] = PMA PG 76-22

PMA PG 76-22 + Aggregates = Mix with 3% PMA

Mixtures are referred to as F2P1 and F4P1.

3. Mix plus 4.5% SBS polymer A

[Base asphalt A + 4.5% SBS polymer A] = PMA PG 82-22

PMA PG 82-22 + Aggregates = Mix with 4.5% PMA

Mixtures are referred to as F2P2 and F4P2.

4. Mix plus 6% SBS polymer A

[Base asphalt B (softer) + 6% SBS polymer A] = PMA PG 82-22

PMA PG 82-22 + Aggregates = Mix with 6% PMA

Mixtures are referred to as F2P3 and F4P3.

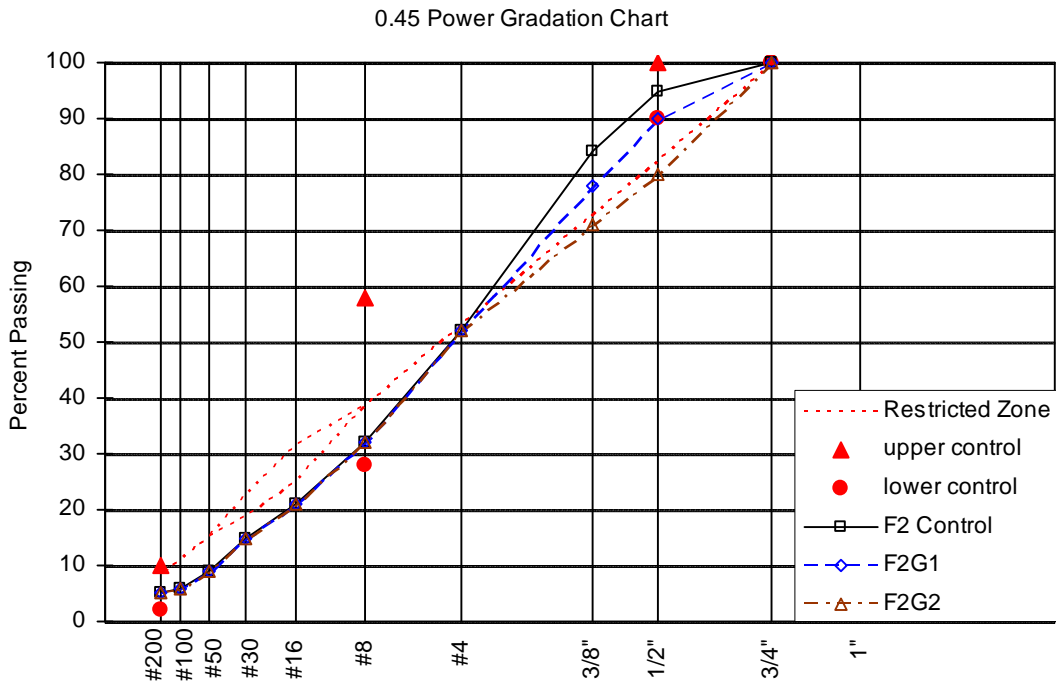


Figure 3-1: Gradation curves for F2 and its trial adjustments

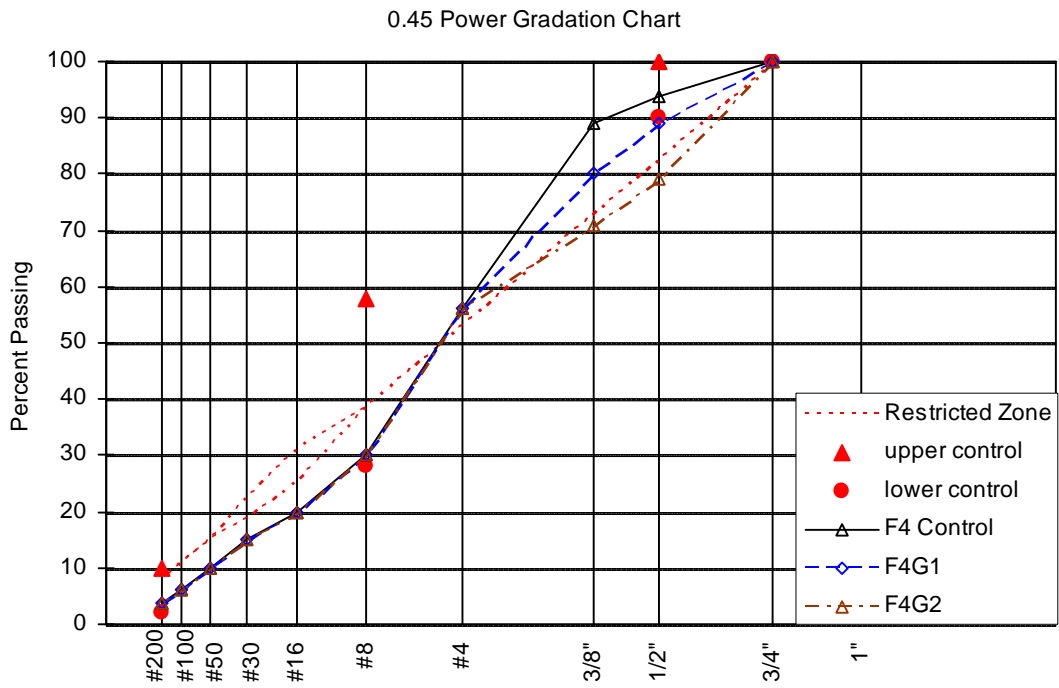


Figure 3-2: Gradation curves for F4 and its trial adjustments

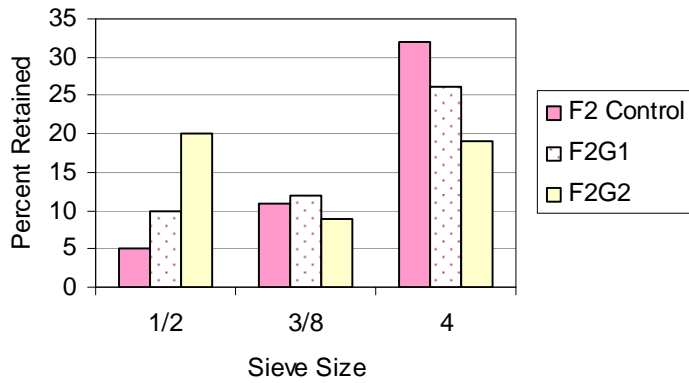


Figure 3-3: Change of percent retained on top 3 sieves for F2 series

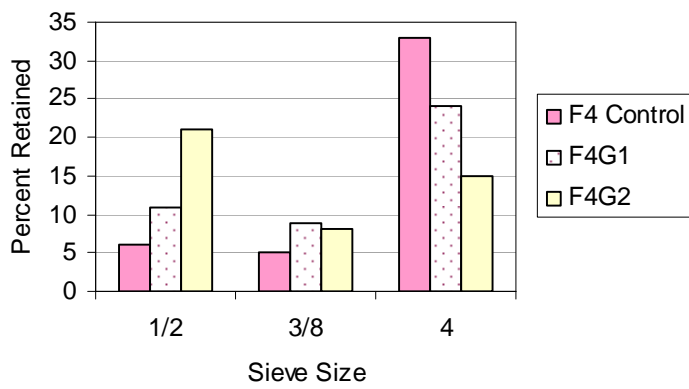


Figure 3-4: Change of percent retained on top 3 sieves for F4 series



Figure 3-5: Cutting of raw specimen

3.5 Specimen Preparation and Volumetric Properties

Raw gyratory specimens with dimensions of 150 mm (5.9 in.) in diameter by 165 mm (6.5 in.) in height were first prepared on the required air void content (4%) using a Servopac Gyratory Compactor for the selected HMA mixtures. The Servopac compaction parameters used for the design were a 1.25° gyratory angle, a 600-kPa ram pressure, and 30 gyrations per minute. The maximum theoretical specific gravity was measured using Rice maximum theoretical specific gravity method specified in AASHTO T 209/ASTM D 2041 standards. In this case, the mixtures were allowed to cool down in the loose state. The sample preparation for the IDT test was based on the findings from the NCHRP Project 1-28A, “Harmonized Test Methods for Laboratory Determination of Resilient Modulus for Flexible Pavement Design.” The mixture design process was verified for the mixture volumetric properties before the production of test specimens. Test specimens were prepared by sawing at least 6 mm off both sides of each gyratory specimen to provide smooth, parallel surfaces for mounting the measurement gauges. The gyratory specimen was then further sawed to the required thickness (two specimens out of each compacted pill, Figure 3-5, referred to as A and B) to produce the final test specimen. This sample preparation procedure was done to make eight test specimens for each HMA mixture. The G_{mb} values were measured for the prepared test specimens to assure that the air voids were within targeted range. Resilient modulus test, creep compliance test, and tensile strength test were performed on these 150 mm (6 in.) in diameter by 63 mm (2.5 in.) thick test specimens. Table 3-1 through Table 3-3 show a summary of the specimens prepared for each mix and the corresponding volumetric properties measured in the lab.

Table 3-1: Number of specimens prepared

Mixes	F2 Control (F2C)			F4 Control (F4C)		
# of Specimens	8			8		
Gradation Modifications	F2G1	F2G2	--	F4G1	F4G2	--
# of Specimens	8	8	--	8	8	--
SBS Polymer Modification	F2P1	F2P2	F2P3	F4P1	F4P2	F4P3
# of Specimens	8	8	8	8	8	8

Table 3-2: Specimens tested for fracture mechanics properties

Gradation Study						
Mix	F2C	F2G1	F2G2	F4C	F4G1	F4G2
Specimen Number	1A, 1B					
	2A, 2B					
	3A, 3B					
	4A, 4B					
SBS Modifier Study						
Mix	F2P1	F2P2	F2P3	F4P1	F4P2	F4P3
Specimen Number	1A, 1B					
	2A, 2B					
	3A, 3B					
	4A, 4B					

Table 3-3: Specific gravities and air voids of the mixtures

Gradation Study						
Mix	F2C	F2G1	F2G2	F4C	F4G1	F4G2
G_{mm}	2.589	2.585	2.585	2.253	2.260	2.260
G_{mb}	2.479	2.487	2.490	2.173	2.179	2.179
VTM (V_a)	4.3	3.8	3.7	3.5	3.6	3.6
SBS Modifier Study						
Mix	F2P1	F2P2	F2P3	F4P1	F4P2	F4P3
G_{mm}	2.573	2.573	2.573	2.253	2.253	2.253
G_{mb}	2.472	2.463	2.479	2.179	2.130	2.187
VTM (V_a)	3.9	4.3	3.7	3.3	5.4	3.0

3.6 Test Procedures

3.6.1 Resilient Modulus Test

After the specimens were prepared, they were placed in a controlled-temperature cabinet and brought to the specified test temperature. The specimens were placed into the loading apparatus; and the loading strips were positioned in a parallel format and centered on the vertical diametral plane (Figure 3-6). Tests were performed at temperatures of -10, 5, 25, and 40°C at 1.0 Hz frequency. Testing began with the lowest temperature and proceeded to the highest temperature. Typical load and deformation outputs that form a resilient modulus test are shown in Figure 3-7.

On the night before testing, extensometers were placed on the test specimen using glue. The specimen was then placed in a controlled temperature cabinet overnight at -10°C to ensure temperature equilibrium. On the morning of testing, the specimen was placed in the environmental chamber at -10°C and allowed to equilibrate for two hours.

To begin testing, the extensometers were zeroed, and a minimal contact load was applied to the specimen. Each stress cycle was made up of a 0.1 second haversine pulse followed by a 0.9 second hold cycle to simulate moving wheel loads. The data acquisition system was set up to record the last six cycles at each frequency with about 400 points per cycle. The raw force and displacement data were manipulated to obtain the resilient modulus for each specimen. After the entire cycle of testing was complete at -10°C, the environmental chamber was set to the next temperature. After two hours of conditioning, the above steps were repeated until the entire sequence of temperatures was completed.

The test was conducted based on the SHRP IDT testing procedures. The resilient modulus is the ratio of the applied stress to the recoverable strain as shown in Equation 3-1. During the test, the load was carefully measured so that the horizontal strain was within 100 and 300 micro-strains. These limits were established based on research conducted by Roque et al. (1997) to accurately evaluate the resilient modulus and Poisson's Ratio of bituminous materials. The upper limit was set to make sure that the horizontal strains were within the linear viscoelastic range and the lower limit was set to obtain sufficient amplitude of strain against system noises.

$$M_R = \sigma_r / \epsilon_r \quad (3-1)$$

The resilient modulus and Poisson's ratio were calculated using the equations developed by Roque et al. (1997) based on a three-dimensional finite element analysis (Equation 3-2 through Equation 3-4).

$$M_R = \frac{P \times GL}{\Delta H \times t \times D \times C_{CMPL}} \quad (3-2)$$

$$C_{CMPL} = 0.6354 \times (X/Y)^{-1} - 0.332 \quad (3-3)$$

$$\nu = -0.1 + 1.480 \times (X/Y)^2 - 0.778 \times (t/D)^2 \times (X/Y)^2 \quad (3-4)$$

Where

M_R = Resilient Modulus P = Maximum Load GL = Gage Length

ΔH = Horizontal Deformation t = Thickness D = Diameter

C_{CMPL} = Non-dimensional Factor ν = Poisson's Ratio

(X/Y) = Ratio of Horizontal to Vertical Deformation



Figure 3-6: Indirect diametral resilient modulus test setup

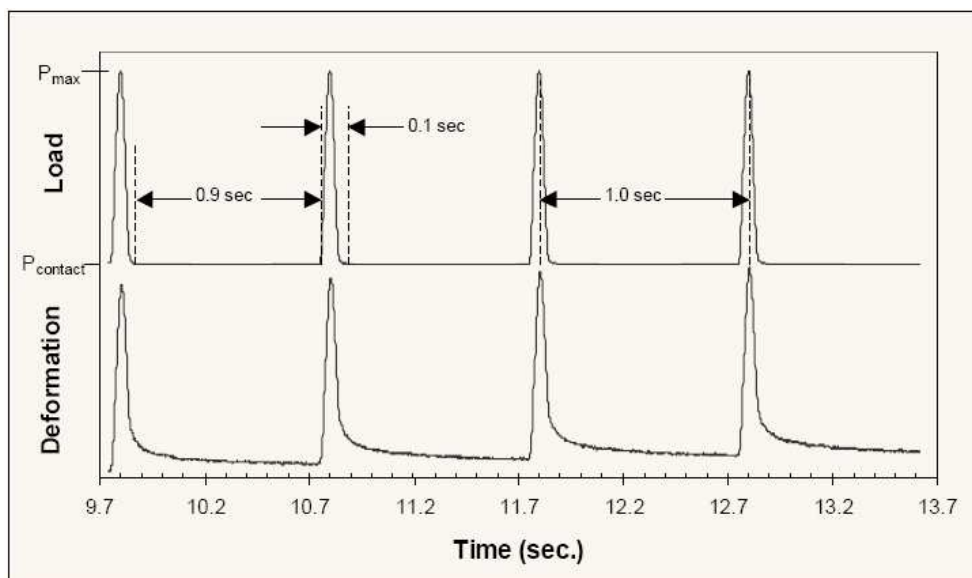


Figure 3-7: Load & deformations in a typical resilient modulus test

3.6.2 Creep Compliance Test

Creep compliance is a function of time-dependent strain (ϵ_t) divided by constraint stress (σ) (Equation 3-5). Once the resilient modulus test was completed, the creep test was conducted by applying a static load on the specimen for 100 seconds. Similar to the M_R test, the horizontal strain was limited from 150 to 300 micro-strains at 100 seconds to avoid excessive permanent deformation of the specimen. The equation used to calculate the creep compliance is presented in Equation 3-6.

$$D(t) = \frac{\epsilon(t)}{\sigma} \quad (3-5)$$

$$D(t) = \frac{\Delta H \times t \times D \times C_{CMPL}}{P \times GL} \quad (3-6)$$

where $D(t)$ is the creep compliance at time t with a unit of $1/\text{GPa}$, other parameters are the same as defined in resilient modulus equations. The specimen set-up and transducers attachment are the same as for the resilient modulus test. Figure 3-8 displays typical load and deformation curves of the creep compliance test.

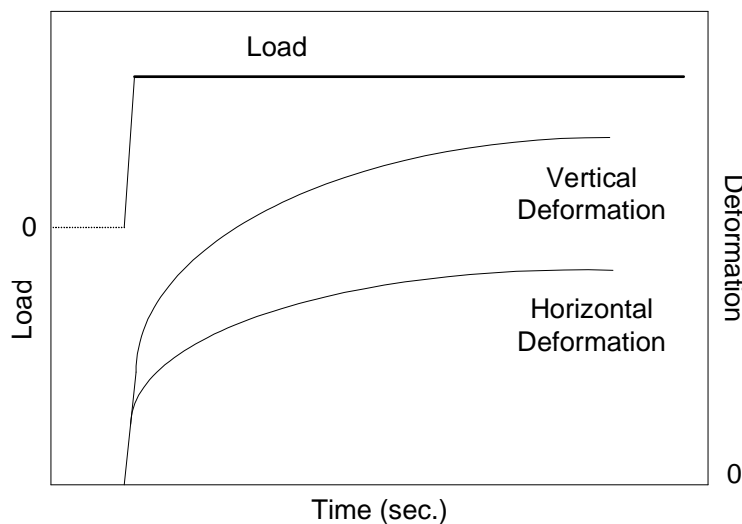


Figure 3-8: Load and deformation curves of creep compliance test

3.6.3 Tensile Strength Test

The strength test is a destructive test. The strength test, along with the M_R test, was used to determine asphalt mixture fracture mechanics properties which included the tensile strength (S_t), fracture energy (FE), dissipated creep strain energy (DCSE), and Failure Strain. The procedures used to calculate these limits are presented in the following equations (Roque et al. 1997):

$$S_t = \frac{2P(C_{SX})}{\pi \cdot t \cdot D} = \frac{2P \cdot (0.948 - 0.01114 \cdot (t/D) - 0.2693 \cdot \nu + 1.436 \cdot (t/D) \cdot \nu)}{\pi \cdot t \cdot D} \quad (3-7)$$

$$FE = \int_0^{S_t} \sigma \cdot d\varepsilon \quad (2-16)$$

$$EE = \frac{1}{2} \cdot \varepsilon_{EE} \cdot S_t = \frac{(S_t)^2}{2 \cdot M_R} \quad (2-18)$$

$$DCSE = FE - EE \quad (2-19)$$

Where C_{SX} is the stress correction factor, t is specimen thickness, D is specimen diameter, ν is Poisson's ratio, and other variables are the same as defined in section 2.5.

The specimen set-up and transducers attachment are the same as for the resilient modulus test. However, the tensile strength test was conducted in a displacement control mode by applying a constant rate of displacement of 12.5 mm/min at -10°C , 25 mm/min at 5°C , and 50 mm/min at 25 and 40°C . Figure 3-9 displays a specimen broken along the diametral direction after the strength test.

3.7 Testing Program

One coarse mix of Georgia granite and one coarse mix of limestone were selected from typical Florida HMA Superpave mixtures as control mixes to study aggregate gradation and SBS polymer-modified binder effects using the SHRP IDT testing and data processing method. Each mix was modified to two gradation levels and three SBS polymer content levels. The Superpave

mixture designs were selected because they are commonly used FDOT gradations and are known to perform well in the field.

The HMA mixtures were compacted in the laboratory and the specimens were prepared for the IDT. A flowchart is shown in Figure 3-10 to illustrate the experimental program for measuring fracture mechanics properties of HMA mixtures. The standard granite (Ga553, 04-3034A) and South Florida limestone (SFL, 02-2529A) mixtures at control level are named F2C and F4C, respectively.

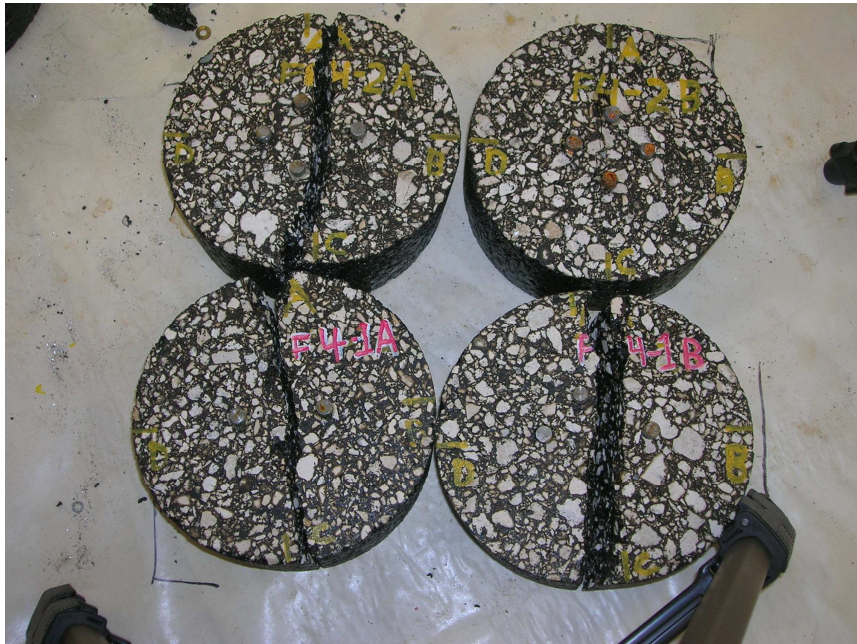


Figure 3-9: Specimen fails after tensile strength test

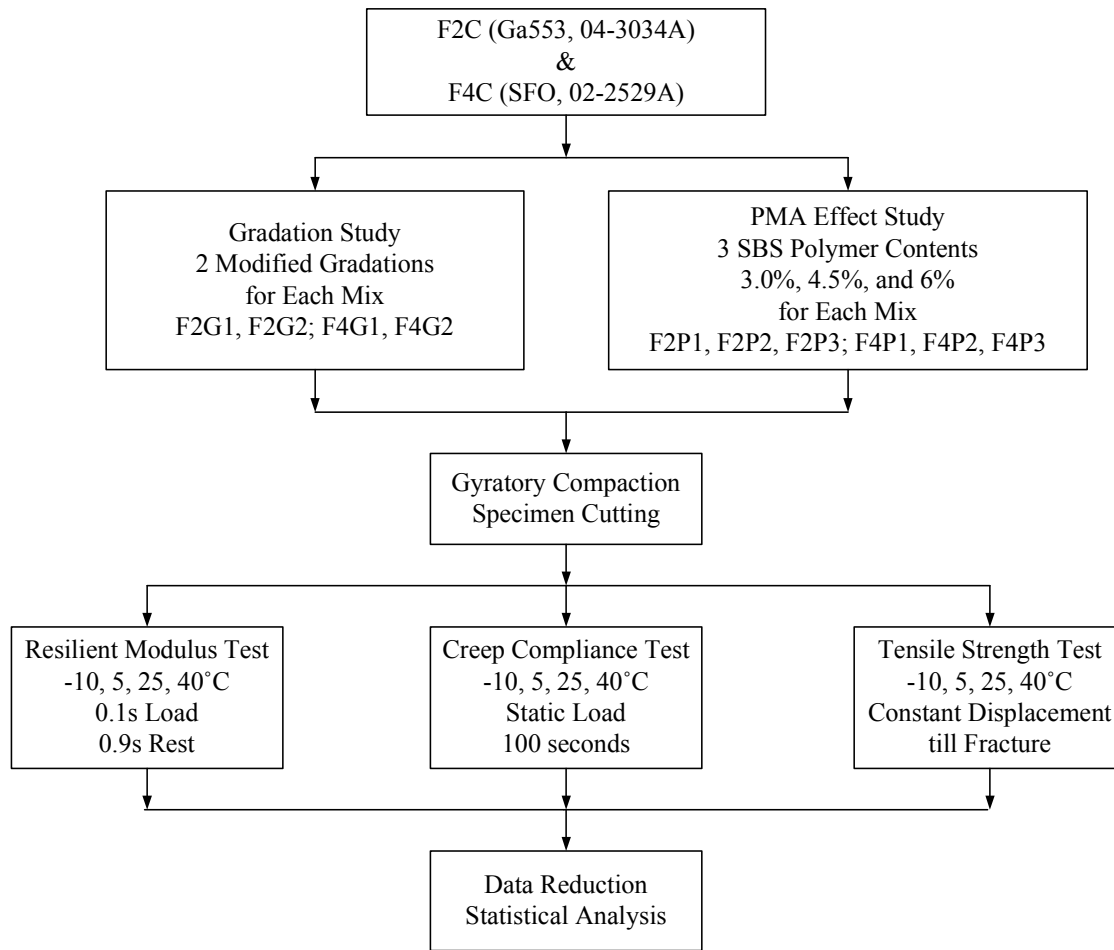


Figure 3-10: Flowchart of the experimental program for measuring fracture mechanics properties of HMA mixtures

CHAPTER 4

FRACTURE MECHANICS PROPERTIES FROM IDT

The laboratory testing program conducted in this study included resilient modulus testing, creep compliance testing, and tensile strength testing. All types of testing were conducted in unconfined conditions. An Interlaken dynamic test system was used for testing all of the sliced specimens to obtain the fracture mechanics properties including resilient modulus (M_R), creep compliance (D_i), fracture energy (FE), and dissipated creep strain energy (DCSE). The data reductions were performed according to the procedures presented by Roque et al. (1997).

4.1 Resilient Modulus Testing Procedures and Results

4.1.1 Test Procedures

After the specimens were prepared, they were placed in a controlled temperature cabinet and brought to the specified test temperature. The specimens were placed into the loading apparatus; the loading strips were positioned in a parallel format and centered on the vertical diametral plane. Tests were performed at temperatures of -10, 5, 25, and 40°C and at 1.0 Hz frequency. Testing began with the lowest temperature and proceeded to the highest. On the night before testing, extensometers were placed on the test specimen using glue. The specimen was then placed in a controlled temperature cabinet overnight at -10°C to ensure temperature equilibrium. On the morning of testing, the specimen was placed in the environmental chamber at -10°C and allowed to equilibrate for two hours.

To begin testing, the extensometers were zeroed, and a minimal contact load was applied to the specimen. Each stress cycle was made up of a 0.1 second haversine pulse followed by a 0.9 second hold cycle to simulate moving wheel loads. The data acquisition system was set up to record the last six cycles at each frequency with about 400 points per cycle. The raw force and displacement data were manipulated to obtain the resilient modulus for each specimen as described in section 3.2. The load was selected to keep the horizontal strain in the linear viscoelastic range which is typically 150 to 350 micro-strains. After the entire cycle of testing was complete at -10°C, the environmental chamber was set to the next temperature. After two

hours of conditioning, the above steps were repeated until completion of the entire sequence of temperatures. Upon completion of the resilient modulus tests, all samples were placed in the environmental chamber for overnight conditioning before creep compliance testing and tensile strength testing.

4.1.2 Resilient Modulus Data Analysis and Results

For the measurement and analysis system used, two vertical and horizontal measurements were obtained for each specimen. Data from five load cycles were recorded after 100 cycles of equilibrium. The maximum load and the maximum deformation were determined for each cycle from the load and deformation curves. Linear regression was performed on the unloading and recovery portion of each deformation wave to determine the instantaneous and total recoverable deformations (Figure 4-1). The trimmed mean deformations and the average load were obtained from the replicate specimens tested. The average total resilient modulus for each mixture was calculated using Equation 3-2 through Equation 3-4. Table 4-1 through Table 4-8 show the resilient modulus test results for all mixtures.

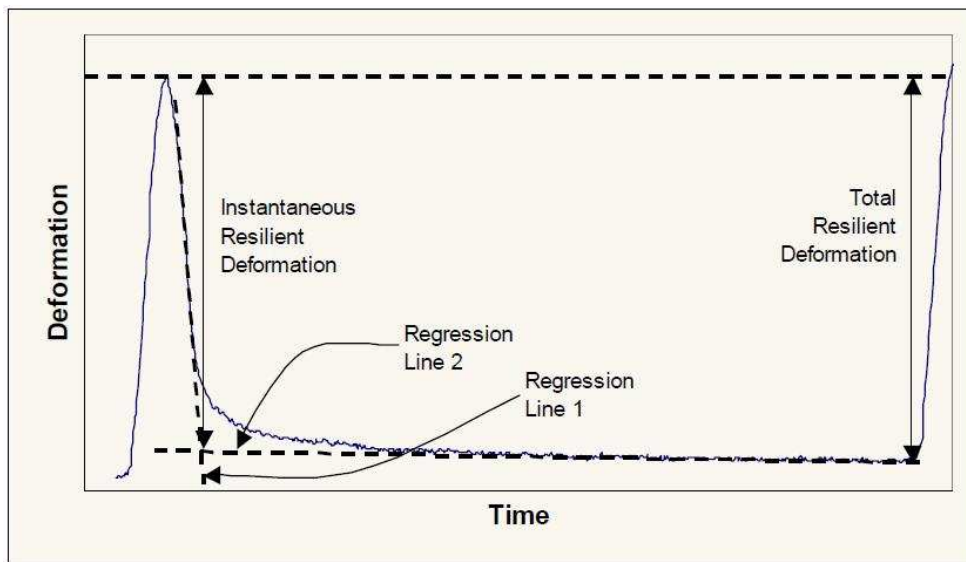


Figure 4-1: Instantaneous and total resilient deformations

Table 4-1: Resilient modulus test results at -10°C (SI units)

Mixtures with Modified Gradations						
	Control		G1		G2	
	F2	F4	F2	F4	F2	F4
PrI	0.35	0.35	0.25	0.32	0.29	0.31
PrT	0.35	0.35	0.25	0.32	0.28	0.31
MrI (GPa)	28.91	20.98	30.08	21.79	29.19	20.55
MrT (GPa)	28.15	20.61	29.62	21.41	28.50	20.26
Mixtures with SBS Polymer-modified Binder						
	P1 (3.0%)		P2 (4.5%)		P3 (6.0%)	
	F2	F4	F2	F4	F2	F4
PrI	0.33	0.28	0.35	0.26	0.31	0.33
PrT	0.33	0.27	0.35	0.26	0.31	0.33
MrI (GPa)	27.10	19.24	24.93	16.42	23.06	14.49
MrT (GPa)	26.61	18.91	24.49	16.14	22.45	14.01

Note: PrI: Poisson's Ratio, instantaneous; PrT: Poisson's Ratio, total;
 MrI: Resilient Modulus, instantaneous; MrT: Resilient Modulus, total.
 1 GPa = 145 ksi 1 ksi = 6.89475 MPa

Table 4-2: Resilient modulus test result at -10°C (English units)

Mixtures with Modified Gradations						
	Control		G1		G2	
	F2	F4	F2	F4	F2	F4
PrI	0.35	0.35	0.25	0.32	0.29	0.31
PrT	0.35	0.35	0.25	0.32	0.28	0.31
MrI (ksi)	4193	3043	4363	3160	4234	2981
MrT (ksi)	4082	2989	4296	3105	4134	2939
Mixtures with SBS Polymer-modified Binder						
	P1 (3.0%)		P2 (4.5%)		P3 (6.0%)	
	F2	F4	F2	F4	F2	F4
PrI	0.33	0.28	0.35	0.26	0.31	0.33
PrT	0.33	0.27	0.35	0.26	0.31	0.33
MrI (ksi)	3931	2790	3616	2382	3345	2102
MrT (ksi)	3860	2743	3552	2340	3256	2032

Table 4-3: Resilient modulus test results at 5°C (SI units)

Mixtures with Modified Gradations						
	Control		G1		G2	
	F2	F4	F2	F4	F2	F4
PrI	0.36	0.31	0.32	0.33	0.36	0.32
PrT	0.36	0.32	0.32	0.33	0.36	0.33
MrI (GPa)	19.22	13.40	18.57	13.31	19.50	11.90
MrT (GPa)	18.25	12.90	17.59	12.81	18.52	11.36
Mixtures with SBS Polymer-modified Binder						
	P1 (3.0%)		P2 (4.5%)		P3 (6.0%)	
	F2	F4	F2	F4	F2	F4
PrI	0.35	0.36	0.35	0.27	0.29	0.39
PrT	0.34	0.36	0.35	0.27	0.29	0.39
MrI (GPa)	19.71	12.49	17.24	10.97	14.80	7.93
MrT (GPa)	18.86	11.98	16.39	10.57	13.57	7.26

Table 4-4: Resilient modulus test result at 5°C (English units)

Mixtures with Modified Gradations						
	Control		G1		G2	
	F2	F4	F2	F4	F2	F4
PrI	0.36	0.31	0.32	0.33	0.36	0.32
PrT	0.36	0.32	0.32	0.33	0.36	0.33
MrI (ksi)	2788	1944	2693	1930	2828	1726
MrT (ksi)	2647	1871	2551	1858	2686	1648
Mixtures with SBS Polymer-modified Binder						
	P1 (3.0%)		P2 (4.5%)		P3 (6.0%)	
	F2	F4	F2	F4	F2	F4
PrI	0.35	0.36	0.35	0.27	0.29	0.39
PrT	0.34	0.36	0.35	0.27	0.29	0.39
MrI (ksi)	2859	1812	2500	1591	2147	1150
MrT (ksi)	2735	1738	2377	1533	1968	1053

Table 4-5: Resilient modulus test results at 25°C (SI units)

Mixtures with Modified Gradations						
	Control		G1		G2	
	F2	F4	F2	F4	F2	F4
PrI	0.43	0.43	0.28	0.34	0.32	0.46
PrT	0.44	0.45	0.31	0.33	0.34	0.44
MrI (GPa)	6.21	4.80	5.58	4.96	5.29	4.90
MrT (GPa)	5.53	4.22	4.92	4.51	4.56	4.36
Mixtures with SBS Polymer-modified Binder						
	P1 (3.0%)		P2 (4.5%)		P3 (6.0%)	
	F2	F4	F2	F4	F2	F4
PrI	0.37	0.37	0.30	0.39	0.28	0.29
PrT	0.37	0.35	0.31	0.39	0.29	0.30
MrI (GPa)	6.15	4.32	4.90	4.53	3.54	2.21
MrT (GPa)	5.24	3.78	4.29	4.04	3.06	1.99

Table 4-6: Resilient modulus test result at 25°C (English units)

Mixtures with Modified Gradations						
	Control		G1		G2	
	F2	F4	F2	F4	F2	F4
PrI	0.43	0.43	0.28	0.34	0.32	0.46
PrT	0.44	0.45	0.31	0.33	0.34	0.44
MrI (ksi)	901	696	810	719	767	711
MrT (ksi)	802	612	713	654	661	633
Mixtures with SBS Polymer-modified Binder						
	P1 (3.0%)		P2 (4.5%)		P3 (6.0%)	
	F2	F4	F2	F4	F2	F4
PrI	0.37	0.37	0.30	0.39	0.28	0.29
PrT	0.37	0.35	0.31	0.39	0.29	0.30
MrI (ksi)	892	627	711	657	513	321
MrT (ksi)	760	548	622	586	444	289

Table 4-7: Resilient modulus test results at 40°C (SI units)

Mixtures with Modified Gradations						
	Control		G1		G2	
	F2	F4	F2	F4	F2	F4
PrI	0.35	0.39	0.32	0.32	0.38	0.36
PrT	0.38	0.36	0.32	0.31	0.33	0.39
MrI (GPa)	1.39	1.48	1.40	1.66	1.65	1.42
MrT (GPa)	1.19	1.03	1.23	1.47	1.45	1.28
Mixtures with SBS Polymer-modified Binder						
	P1 (3.0%)		P2 (4.5%)		P3 (6.0%)	
	F2	F4	F2	F4	F2	F4
PrI	0.41	0.41	0.45	0.36	0.44	0.47
PrT	0.40	0.43	0.46	0.38	0.47	0.41
MrI (GPa)	1.96	1.28	2.09	1.40	1.22	1.25
MrT (GPa)	1.67	1.13	1.93	1.25	1.08	1.10

Table 4-8: Resilient modulus test result at 40°C (English units)

Mixtures with Modified Gradations						
	Control		G1		G2	
	F2	F4	F2	F4	F2	F4
PrI	0.35	0.39	0.32	0.32	0.38	0.36
PrT	0.38	0.36	0.32	0.31	0.33	0.39
MrI (ksi)	202	215	203	241	239	206
MrT (ksi)	173	149	178	213	210	186
Mixtures with SBS Polymer-modified Binder						
	P1 (3.0%)		P2 (4.5%)		P3 (6.0%)	
	F2	F4	F2	F4	F2	F4
PrI	0.41	0.41	0.45	0.36	0.44	0.47
PrT	0.40	0.43	0.46	0.38	0.47	0.41
MrI (ksi)	284	186	303	203	177	181
MrT (ksi)	242	164	280	181	157	160

4.2 Creep Compliance Testing Procedures and Results

4.2.1 Test Procedures

The mounting of LVDTs and the preloading for the creep compliance test were the same as those for the resilient modulus test. A static load was applied on specimen for 100 seconds. The horizontal strains at the 30th second were controlled to be between 100 and 200 micro-strains to ensure the specimen was tested in viscoelastic range. If the range limit was exceeded, the load was immediately removed from the specimen and a minimum of three minutes rest period was allowed for the specimen to recover before reloading at another appropriate level. The data acquisition program records the loads and specimen deformations at a rate of 10 Hz. Matlab scripts were generated to analyze the load and deformation data and to calculate the creep compliance values at points of specified time. All specimens were placed in the environmental chamber for at least one overnight recovery prior to the tensile strength test.

4.2.1 Creep Compliance Data Analysis and Results

For each creep compliance data file collected, the creep test start point and the initial extensometer reading were determined first. Then the deformations for each creep time point were calculated by determining the corresponding extensometer readings. The deformations and axial load were averaged for the replicate specimens tested. The creep compliance for each time point was calculated using Equation 3-6. The creep compliance test results are summarized in Appendix B.

4.3 Tensile Strength Testing Procedures and Results

4.3.1 Test Procedures

The tensile strength test was conducted in a displacement control mode by applying a constant rate of displacement until the specimen failed. It was observed that the specimens were failed too quickly to obtain sufficient data points if the rate of displacement was relatively high at a certain level of temperature. In order to make data records and reduction more accurate, the displacement rate was set as 12.5 mm/min (0.5 in/min) at -10°C, 25 mm/min (1.0 in/min) at 5°C,

50 mm/min (2.0 in/min) at 25°C and 40°C. The horizontal and vertical deformation and the applied load were recorded at a rate of 20 Hz during the test. The dissipated creep strain energy (DCSE) and fracture energy (FE) can be determined from the tensile strength and resilient modulus of the specimen. The schematics used to calculate these limits are described in section 2.5 and are displayed in Figure 4-2 for convenience.

4.3.2 Tensile Strength Data Analysis and Results

Similar to the data reduction procedures for resilient modulus and creep compliance, the load and deformations at each time point were determined first for each tensile strength data file. Specifically, the instant of failure is identified as the time when the difference between the vertical and horizontal deformations reaches a peak ((Y-X) peak). The tensile strength was then calculated using Equation (3-7). The strength of the mixture was obtained by taking the average value of the replicated specimens tested. Stress and strain at each time point were calculated from the start of the load cycle to the instant of specimen failure using the following equations (Roque et al. 1997):

$$\sigma(t) = \frac{2 \cdot \text{Load}}{\pi \cdot t \cdot D} \cdot (0.948 - 0.01114 \cdot (t/D) - 0.2693 \cdot \nu + 1.436 \cdot (t/D) \cdot \nu) \quad (4-1)$$

$$\varepsilon(t) = 1.072 \cdot \frac{\text{Deformation}(t)}{GL} \cdot (1.03 - 0.189 \cdot (t/D) - 0.081 \cdot \nu + 0.089 \cdot (t/D)^2) \quad (4-2)$$

Where, $\sigma(t)$ is stress and ε is strain. Other variables are the same as defined in Section 3.6. The fracture energy is obtained by integrating the area under the stress-strain curve until failure as shown in Figure 4-2 for reference. All fracture mechanics parameters obtained from the tensile strength test were calculated using Equations (2-16) through (2-19) and are presented in Table 4-9 and Table 4-12.

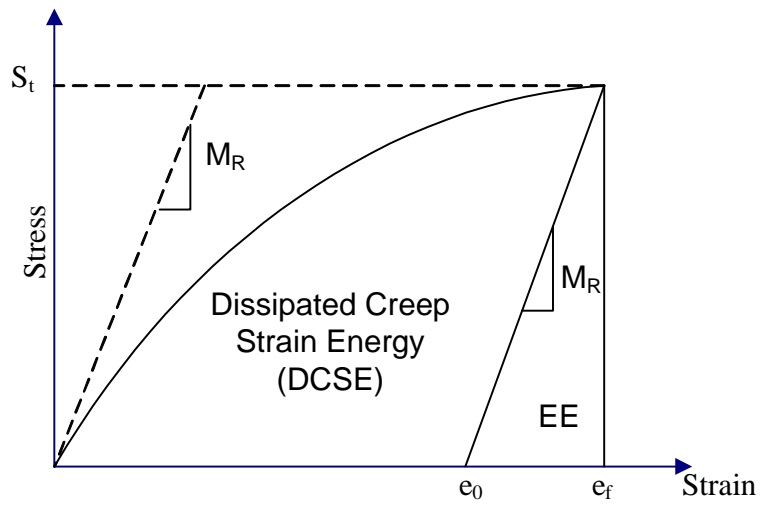


Figure 4-2: Determination of fracture energy and dissipated creep strain energy

Table 4-9: Tensile strength test results for F2 series mixtures (SI units)

F2 Control				
Temperature (°C)	-10	5	25	40
EE (KPa)	0.45	0.27	0.07	0.04
DCSE (KPa)	2.37	5.16	3.37	1.84
FE (KPa)	2.82	5.43	3.44	1.88
TS (MPa)	5.04	3.11	0.90	0.32
FS (10 ³ micro)	0.86	4.35	5.56	10.78
F2G1				
Temperature (°C)	-10	5	25	40
EE (KPa)	0.28	0.30	0.10	0.05
DCSE (KPa)	1.07	4.82	2.79	1.26
FE (KPa)	1.35	5.12	2.89	1.31
TS (MPa)	4.07	3.23	1.00	0.35
FS (10 ³ micro)	0.54	2.04	3.75	5.13
F2G2				
Temperature (°C)	-10	5	25	40
EE (KPa)	0.39	0.28	0.15	0.06
DCSE (KPa)	2.34	4.69	2.46	2.41
FE (KPa)	2.73	4.97	2.61	2.47
TS (MPa)	4.72	3.22	1.15	0.43
FS (10 ³ micro)	0.87	2.00	2.95	7.63
F2P1 (3.0%)				
Temperature (°C)	-10	5	25	40
EE (KPa)	0.30	0.50	0.15	0.06
DCSE (KPa)	1.99	6.93	3.14	1.06
FE (KPa)	2.29	7.43	3.29	1.12
TS (MPa)	3.88	4.33	1.23	0.43
FS (10 ³ micro)	0.77	2.28	3.73	3.55
F2P2 (4.5%)				
Temperature (°C)	-10	5	25	40
EE (KPa)	0.41	0.20	0.46	0.03
DCSE (KPa)	2.58	5.06	4.73	2.37
FE (KPa)	3.00	5.25	5.19	2.40
TS (MPa)	4.44	2.52	1.99	0.34
FS (10 ³ micro)	3.04	2.64	3.30	9.00
F2P3 (6.0%)				
Temperature (°C)	-10	5	25	40
EE (KPa)	0.42	0.19	0.15	0.08
DCSE (KPa)	3.12	7.27	3.76	2.65
FE (KPa)	3.53	7.46	3.91	2.72
TS (MPa)	4.33	2.25	0.96	0.41
FS (10 ³ micro)	1.66	5.90	5.29	9.19

Note

EE: elastic energy

DCSE: dissipated creep strain energy

FE: total fracture energy

TS: tensile strength

FS: failure strain

1 MPa = 145 psi

1 ksi = 6.89475 MPa

1 micro-strain = 10⁻⁶ mm/mm (in./in.)

Table 4-10: Tensile strength test results for F2 series mixtures (English units)

F2 Control				
Temperature (°C)	-10	5	25	40
EE (psi)	0.066	0.040	0.010	0.005
DCSE (psi)	0.343	0.748	0.489	0.268
FE (psi)	0.409	0.787	0.499	0.273
TS (psi)	730.8	450.6	130.1	46.0
FS (10 ³ micro)	0.86	4.35	5.56	10.78
F2G1				
Temperature (°C)	-10	5	25	40
EE (psi)	0.041	0.043	0.015	0.007
DCSE (psi)	0.155	0.699	0.405	0.183
FE (psi)	0.196	0.743	0.419	0.191
TS (psi)	590.0	469.0	144.9	51.3
FS (10 ³ micro)	0.54	2.04	3.75	5.13
F2G2				
Temperature (°C)	-10	5	25	40
EE (psi)	0.057	0.041	0.021	0.009
DCSE (psi)	0.340	0.680	0.357	0.349
FE (psi)	0.397	0.720	0.378	0.358
TS (psi)	684.0	466.6	166.7	62.6
FS (10 ³ micro)	0.87	2.00	2.95	7.63
F2P1 (3.0%)				
Temperature (°C)	-10	5	25	40
EE (psi)	0.043	0.072	0.021	0.008
DCSE (psi)	0.289	1.005	0.455	0.154
FE (psi)	0.332	1.077	0.477	0.162
TS (psi)	562.2	628.4	178.8	62.4
FS (10 ³ micro)	0.77	2.28	3.73	3.55
F2P2 (4.5%)				
Temperature (°C)	-10	5	25	40
EE (psi)	0.060	0.028	0.067	0.004
DCSE (psi)	0.375	0.733	0.686	0.344
FE (psi)	0.434	0.762	0.753	0.348
TS (psi)	644.1	365.4	288.8	49.4
FS (10 ³ micro)	3.04	2.64	3.30	9.00
F2P3 (6.0%)				
Temperature (°C)	-10	5	25	40
EE (psi)	0.060	0.027	0.022	0.011
DCSE (psi)	0.452	1.054	0.545	0.384
FE (psi)	0.512	1.081	0.567	0.395
TS (psi)	627.2	326.9	139.2	59.2
FS (10 ³ micro)	1.66	5.90	5.29	9.19

Note

EE: elastic energy

DCSE: dissipated creep strain energy

FE: total fracture energy

TS: tensile strength

FS: failure strain

1 MPa = 145 psi

1 ksi = 6.89475 MPa

1 micro-strain = 10⁻⁶ mm/mm (in./in.)

Table 4-11: Tensile strength test results for F4 series mixtures (SI units)

F4 Control				
Temperature (°C)	-10	5	25	40
EE (KPa)	0.41	0.49	0.11	0.07
DCSE (KPa)	1.69	4.57	3.86	1.91
FE (KPa)	2.11	5.06	3.98	1.98
TS (MPa)	4.10	3.57	0.98	0.37
FS (10 ³ micro)	0.86	1.95	9.85	6.36
F4G1				
Temperature (°C)	-10	5	25	40
EE (KPa)	0.25	0.40	0.09	0.04
DCSE (KPa)	2.25	4.21	2.01	1.52
FE (KPa)	2.51	4.61	2.10	1.56
TS (MPa)	3.30	3.21	0.88	0.36
FS (10 ³ micro)	1.12	1.84	3.13	5.56
F4G2				
Temperature (°C)	-10	5	25	40
EE (KPa)	0.36	0.45	0.07	0.04
DCSE (KPa)	1.92	4.72	2.80	1.90
FE (KPa)	2.28	5.18	2.87	1.94
TS (MPa)	3.81	3.21	0.77	0.30
FS (10 ³ micro)	0.93	2.16	4.66	8.52
F4P1 (3.0%)				
Temperature (°C)	-10	5	25	40
EE (KPa)	0.52	0.48	0.10	0.10
DCSE (KPa)	2.44	5.76	4.18	3.68
FE (KPa)	2.96	6.24	4.31	3.79
TS (MPa)	4.42	3.38	0.85	0.48
FS (10 ³ micro)	1.09	2.50	6.25	10.24
F4P2 (4.5%)				
Temperature (°C)	-10	5	25	40
EE (KPa)	0.67	0.47	0.15	0.06
DCSE (KPa)	1.85	5.83	3.20	3.00
FE (KPa)	2.52	6.29	3.35	3.06
TS (MPa)	4.62	3.14	1.09	0.38
FS (10 ³ micro)	0.89	2.62	4.08	11.00
F4P3 (6.0%)				
Temperature (°C)	-10	5	25	40
EE (KPa)	0.68	0.31	0.13	0.13
DCSE (KPa)	8.09	6.38	4.80	5.62
FE (KPa)	8.77	6.69	4.92	5.75
TS (MPa)	4.36	2.12	0.71	0.54
FS (10 ³ micro)	3.10	4.24	11.10	13.70

Note

EE: elastic energy

DCSE: dissipated creep strain energy

FE: total fracture energy

TS: tensile strength

FS: failure strain

1 MPa = 145 psi

1 ksi = 6.89475 MPa

1 micro-strain = 10⁻⁶ mm/mm (in./in.)

Table 4-12: Tensile strength test results for F4 series mixtures (English units)

F4 Control				
Temperature (°C)	-10	5	25	40
EE (psi)	0.060	0.072	0.017	0.010
DCSE (psi)	0.246	0.662	0.560	0.277
FE (psi)	0.305	0.734	0.577	0.286
TS (psi)	593.9	517.5	141.4	54.1
FS (10 ³ micro)	0.86	1.95	9.85	6.36
F4G1				
Temperature (°C)	-10	5	25	40
EE (psi)	0.037	0.059	0.012	0.006
DCSE (psi)	0.327	0.610	0.292	0.221
FE (psi)	0.364	0.668	0.304	0.227
TS (psi)	478.3	465.8	127.5	51.6
FS (10 ³ micro)	1.12	1.84	3.13	5.56
F4G2				
Temperature (°C)	-10	5	25	40
EE (psi)	0.052	0.066	0.010	0.005
DCSE (psi)	0.279	0.685	0.407	0.276
FE (psi)	0.330	0.750	0.416	0.281
TS (psi)	552.3	465.3	111.2	43.8
FS (10 ³ micro)	0.93	2.16	4.66	8.52
F4P1 (3.0%)				
Temperature (°C)	-10	5	25	40
EE (psi)	0.075	0.069	0.015	0.015
DCSE (psi)	0.354	0.836	0.607	0.534
FE (psi)	0.429	0.905	0.625	0.549
TS (psi)	640.8	490.1	123.6	69.4
FS (10 ³ micro)	1.09	2.50	6.25	10.24
F4P2 (4.5%)				
Temperature (°C)	-10	5	25	40
EE (psi)	0.097	0.067	0.021	0.008
DCSE (psi)	0.268	0.845	0.464	0.436
FE (psi)	0.365	0.912	0.486	0.444
TS (psi)	670.4	454.7	158.2	54.5
FS (10 ³ micro)	0.89	2.62	4.08	11.00
F4P3 (6.0%)				
Temperature (°C)	-10	5	25	40
EE (psi)	0.098	0.045	0.018	0.019
DCSE (psi)	1.173	0.925	0.695	0.814
FE (psi)	1.272	0.970	0.714	0.834
TS (psi)	632.4	307.2	103.2	78.7
FS (10 ³ micro)	3.10	4.24	11.10	13.70

Note

EE: elastic energy

DCSE: dissipated creep strain energy

FE: total fracture energy

TS: tensile strength

FS: failure strain

1 MPa = 145 psi

1 ksi = 6.89475 MPa

1 micro-strain = 10⁻⁶ mm/mm (in./in.)

CHAPTER 5

EVALUATION OF FRACTURE MECHANICS PROPERTIES

In this chapter the effect of gradation modification and the effect of SBS polymer-modified asphalt binders are further evaluated with respect to the fracture mechanics properties presented in Chapter 4. The evaluation of each factor will be focused on the following parameters obtained from the sweep of IDT tests: resilient modulus, creep compliance, tensile strength, fracture energy, and dissipated creep strain energy. A brief summary of analyses and discussions will be given at the end of this chapter.

5.1 Aggregate Gradation Effects

5.1.1 Evaluation of Gradation Curves for Modified Gradation Mixtures

The power law model developed by Ruth et al. (2002) was used to fit the gradation curve for each mixture. As described in section 4.3, coarse portions of the control mixtures (percent passing 1/2 in. and 3/8 in. sieves) were modified, and the fine portions were maintained. Therefore, power law constant and exponent (a_{ca} , n_{ca}) for only coarse aggregate were calculated by regression for the mixtures. The format of the power law equation is

$$P_{ca} = a_{ca} \cdot (d)^{n_{ca}} \quad (5-1)$$

Where, P_{ca} is the percent of material by weight passing a given sieve having opening of width d . The break sieve size to distinguish coarse and fine aggregate is defined by the primary control sieve (PCS) based on the Bailey method:

$$PCS = NMPS \times 0.22 \quad (5-2)$$

where PCS is the primary control sieve for the overall blend which defines the break between coarse and fine aggregate, and NMPS is the nominal maximum particle size for the overall blend as defined in Superpave mix design, which is one sieve larger than the first sieve that retains more than 10%. The NMPS for F2 control and F4 control are both 12.5 mm in this study. The break sieve size should be $12.5 \times 0.22 = 2.75$ mm, which corresponds to the No. 8 sieve.

However, since the percent passing No. 4 and smaller sieves are all the same for control and modified gradations, the parameters used for the power law regression are No. 4 and higher sieve sizes. The regression coefficients are also shown in Figure 5-1 and Figure 5-2. For each series, granite or limestone, the regression parameters (a_{ca} and n_{ca}) decreased by a small amount as the coarse size aggregate increased. As expected, the fitted curves are in the same order as their real gradation curves. Table 5-1 summarizes the regression coefficients for the control mixes and those with modified gradations. According to Birgisson et al. (2004), a high n_{ca} implies a low dynamic modulus at high temperature of 40°C when controlling for n_{fa} . The fine portions of the control gradations were maintained in this study, and the mixtures with modified gradations obtained a lower n_{ca} . This implies that the modified gradations would have higher dynamic moduli than control mixes at high temperature levels which are favorable characteristics for HMA performance.

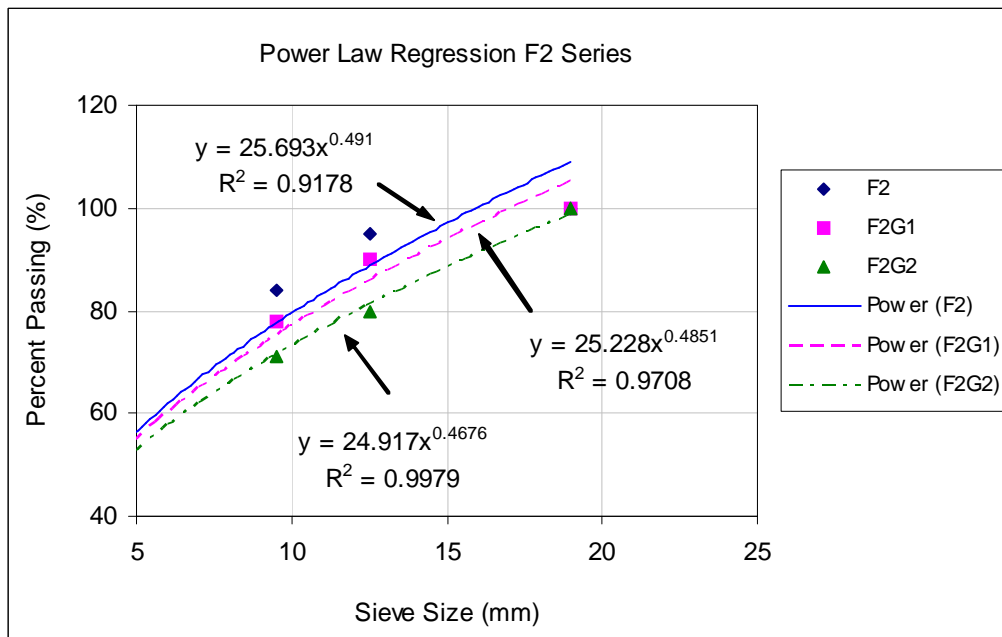


Figure 5-1: Power law regression for F2 gradation series

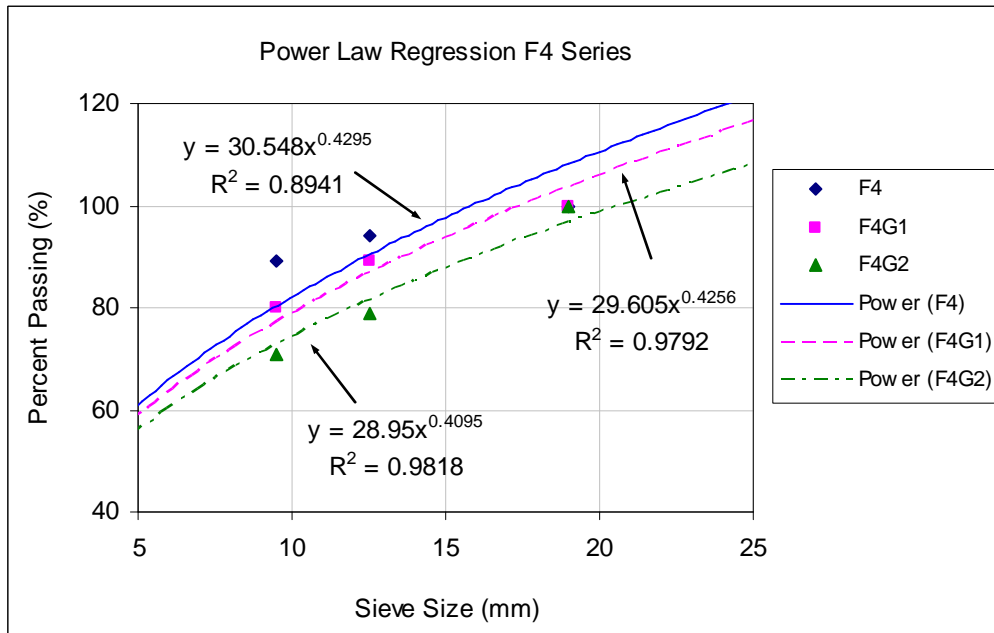


Figure 5-2: Power law regression for F4 gradation series

Table 5-1: Power law regression coefficients for modified gradation mixes

Mixture	F2	F2G1	F2G2	F4	F4G1	F4G2
a_{ca}	25.693	25.228	24.917	30.548	29.605	28.95
n_{ca}	0.491	0.4851	0.4676	0.4295	0.4256	0.4095
R^2	0.9178	0.9708	0.9979	0.8941	0.9792	0.9818

5.1.2 Evaluation of Resilient Modulus for Modified Gradation Mixtures

Figure 5-3 and Figure 5-4 show the resilient modulus comparisons at various temperature levels. Using the resilient modulus values at control level in abscissa and the values at modified gradation in ordinate, a trend line can be plotted to present the relationship of resilient modulus between control and modified gradation mixes, as shown in Figure 5-5. The linear regression coefficient ranges from 0.96 to 1.03. The correlation coefficients (R^2) are all higher than 0.99, which indicates the linear relationship is very strong. From these results, it can be concluded that no significant difference in resilient modulus was present between the control mix design and the mixes with modified gradations. The increase of 1/2 in. coarse aggregate with range of 5% to 15% appeared to have minimum influence on mixtures' resilient modulus.

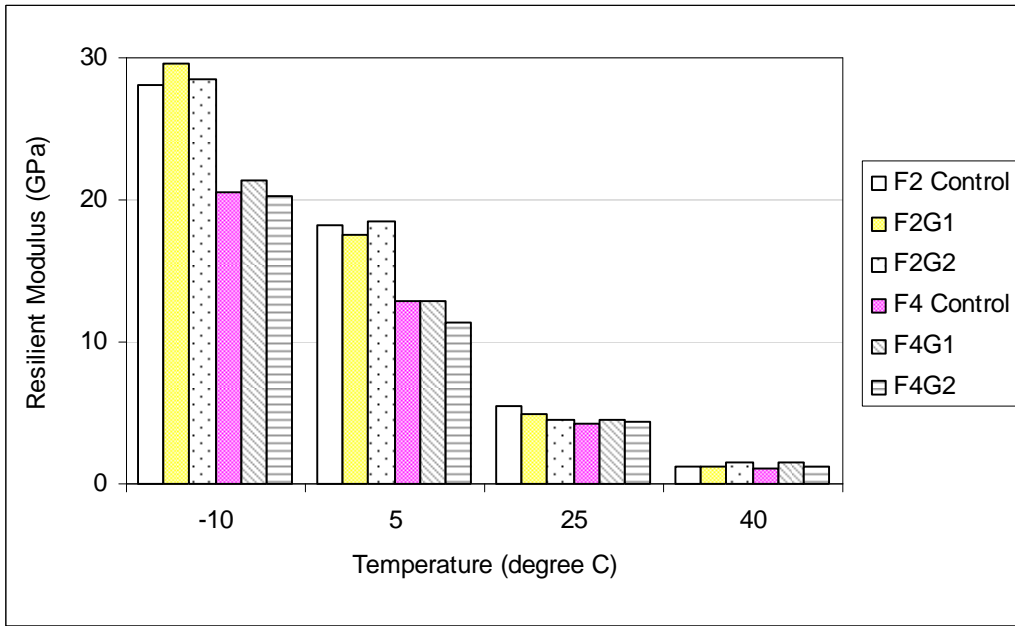


Figure 5-3: Resilient modulus for mixtures with modified gradations (GPa)

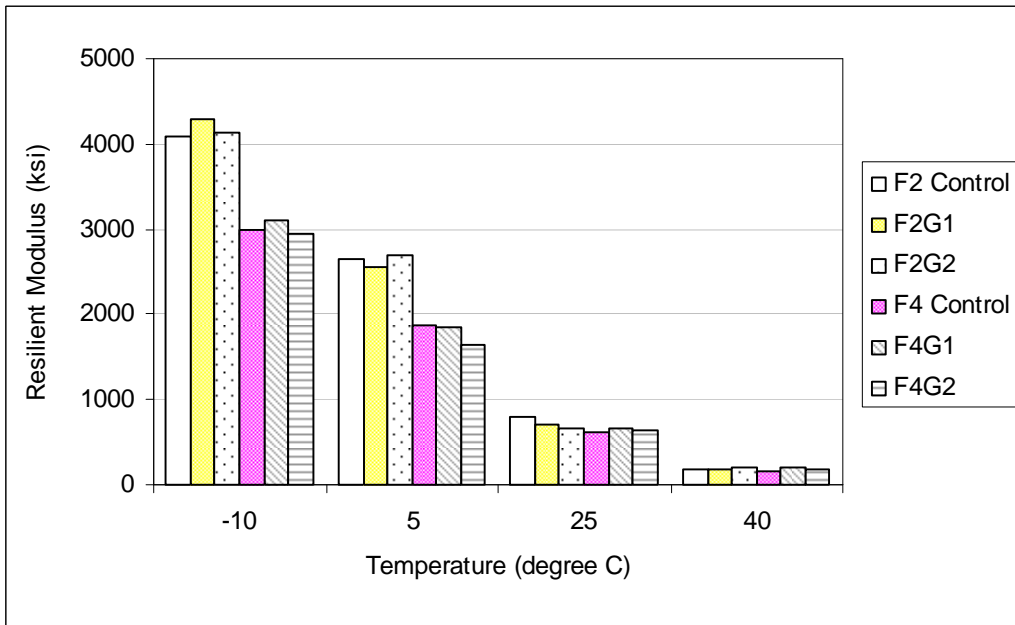


Figure 5-4: Resilient modulus for mixtures with modified gradations (ksi)

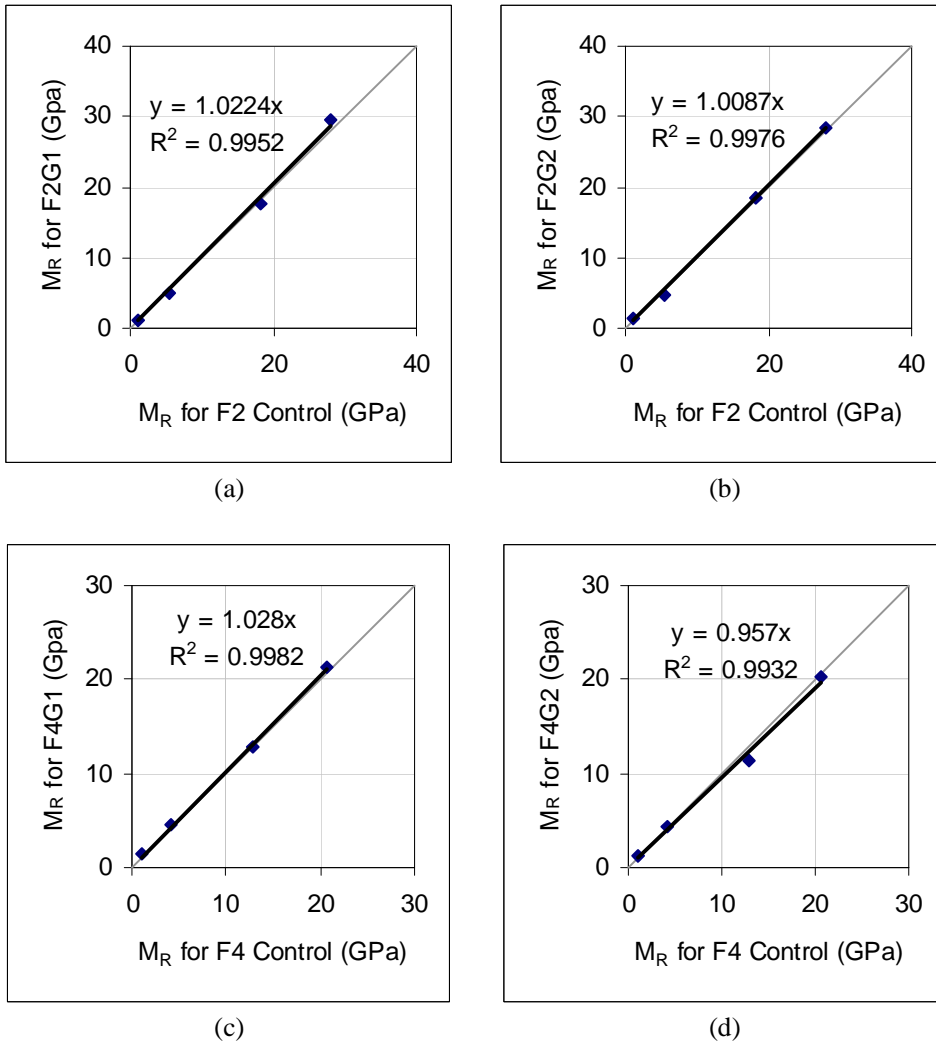


Figure 5-5: Comparison of resilient modulus between control and modified gradations

5.1.3 Evaluation of Creep Compliance for Modified Gradation Mixtures

The creep compliance test results were analyzed using the power law relationship presented by Roque et al. (1997):

$$D(t) = D_0 + D_1 t^m \quad (5-3)$$

It was showed that the parameters obtained from this model are fairly accurate indicators for the viscous response and rutting performance of HMA mixtures. Kim et al. (2005) recommended

a fixed D_0 value (0.0483 1/GPa , or $3.33 \times 10^{-7} \text{ psi}$) to obtain more consistent D_1 and m values for the tests conducted at 0, 10 and 20°C. Master curve construction for creep compliance curves in this study included D_0 in the parametric analysis since the lowest testing temperature of -10°C was used as the reference temperature. Table 5-2, Figure 5-6 and Figure 5-7 show the regression coefficients D_1 and m for all mixes at control level and modified gradations. The comparisons of creep compliance master curves for F2 and F4 gradation series are shown in Figure 5-8 and Figure 5-9, respectively. The creep compliance curves within each aggregate type are very similar to each other, with the exception of the control level granite mixture (F2 Control), which is a little less compliant at high temperature (40°C) than the other two mixes that were blended with higher portions of coarse aggregate. This implies that the increase of 5% to 15% of 1/2 in. aggregate did not make a significant difference in the creep compliance properties for the HMA tested.

Table 5-2: Power model regression coefficients for modified gradation tests

	F2C	F2G1	F2G2	F4C	F4G1	F4G2
D_1 (1/GPa)	0.012	0.007	0.009	0.013	0.007	0.010
m	0.360	0.410	0.398	0.369	0.404	0.370

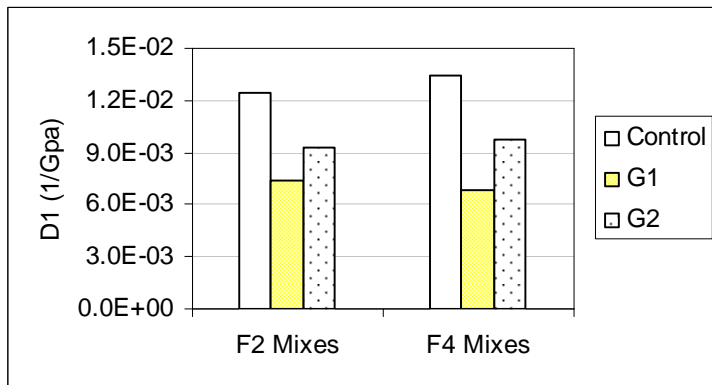


Figure 5-6: Power model parameter D_1 for modified gradations ($1/\text{GPa} = 6.89 \times 10^{-6}/\text{psi}$)

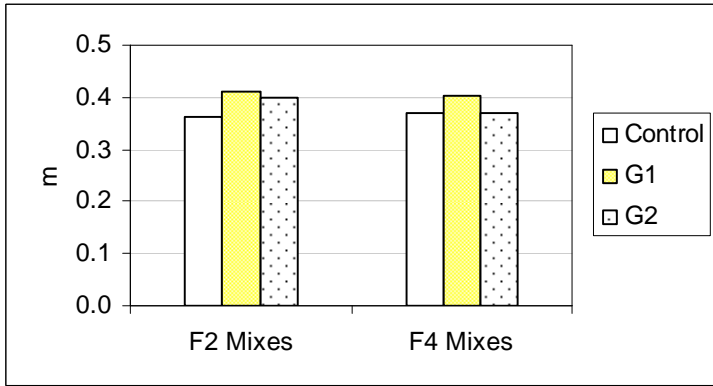


Figure 5-7: Power model parameter m for modified gradations

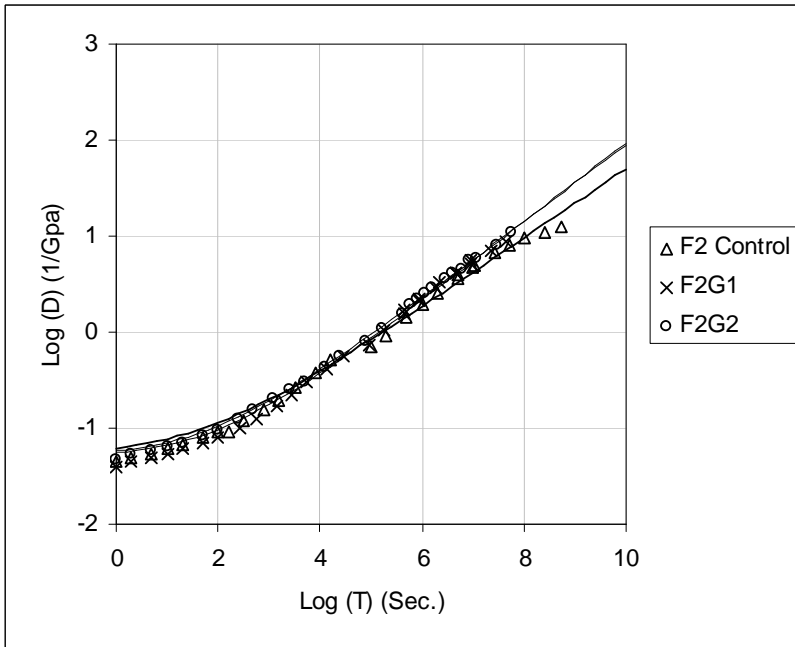


Figure 5-8: Comparison of creep compliance for granite gradation series ($1/\text{GPa} = 6.89 \times 10^{-6}/\text{psi}$)

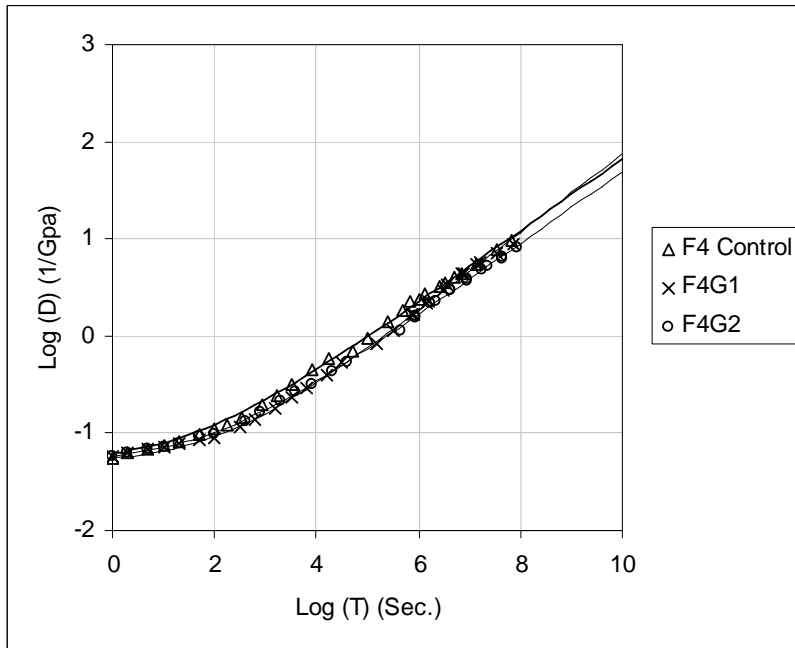


Figure 5-9: Comparison of creep compliance for limestone gradation series (1/GPa = 6.89×10^{-6} /psi)

5.1.4 Evaluation of Tensile Strength and Fracture Energy for Modified Gradation Mixtures

The indirect tensile strength (TS) of control mixtures and the modified gradation mixtures is presented in Figure 5-10 and Figure 5-11. The tensile strength clearly shows the expected trends that the strength value decreases as the temperature increases. A comparison of strength values between control and modified gradation mixtures is shown in Figure 5-12. At mid to high service temperatures (25 and 40°C), the tensile strength values for all mixtures are similar and the differences appear to be negligible. However, at low service temperatures (-10 and 5°C), the tensile strength of mixtures with modified gradations are clearly lower than that of control level mixtures. This tends to indicate that increasing the coarse aggregate in the standard control mixture has an adverse effect on the tensile strength property of the HMA at low temperatures.

Figure 5-13 through Figure 5-16 show the test results of fracture energy (FE) and dissipated creep strain energy (DCSE), respectively, for all mixtures of modified gradation. It is observed that fracture energy values are lower at both low (-10°C) and high (40°C) temperatures than at mid-level temperatures (5 and 25°C). The reason for this trend is that the fracture energy is

calculated as the area under the stress-strain curve of the tensile strength test. At low testing temperatures, the tensile strength of HMA is large but the failure strain is very small. At high temperatures, in contrast, the tensile strength of HMA is the lowest but the failure strain reaches the highest due to the ductile effect of asphalt binder. At some mid-level temperatures, the integration of stress and strain curve attains a peak value. The trend of dissipated energy (DCSE) is essentially the same as for the fracture energy. Comparisons of fracture energy and DCSE between control mixtures and modified gradations are presented in Figure 5-17 and Figure 5-18, respectively. The distributions of the points in the two figures are very similar. A majority of the point falls close to or under the equality line which means that the fracture energy values (or DCSE values) of modified gradations are less than those of the control mixes.

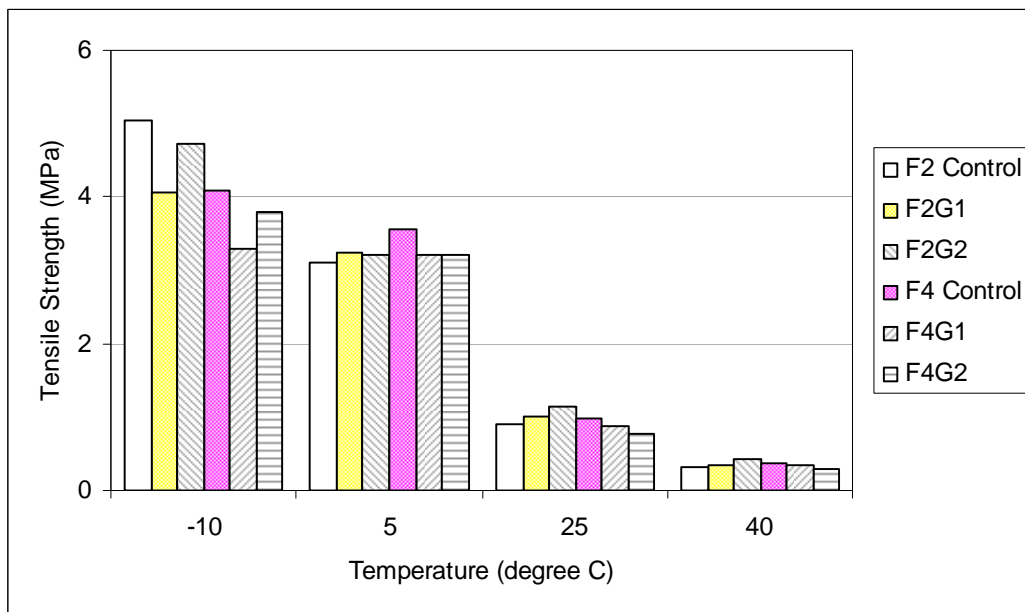


Figure 5-10: Tensile strength for control and modified gradation mixes (MPa)

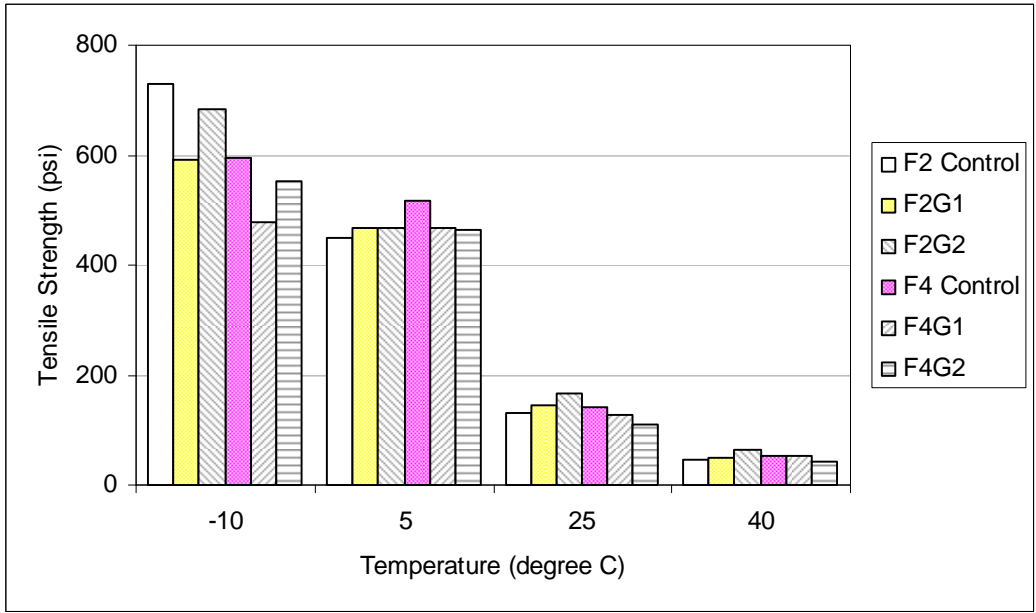


Figure 5-11: Tensile strength for control and modified gradation mixes (psi)

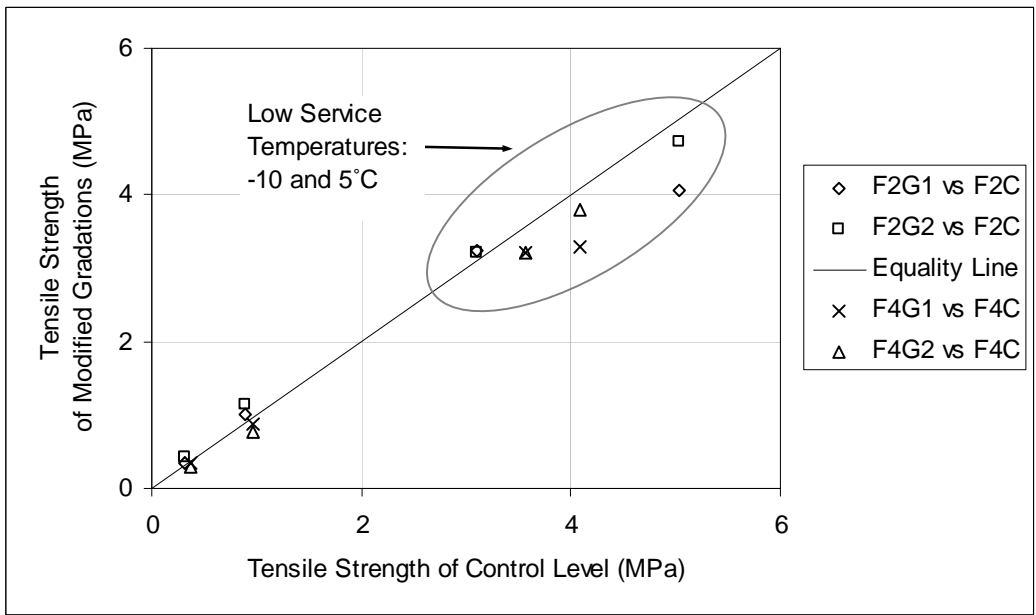


Figure 5-12: Comparison of TS between control and modified gradation mixes

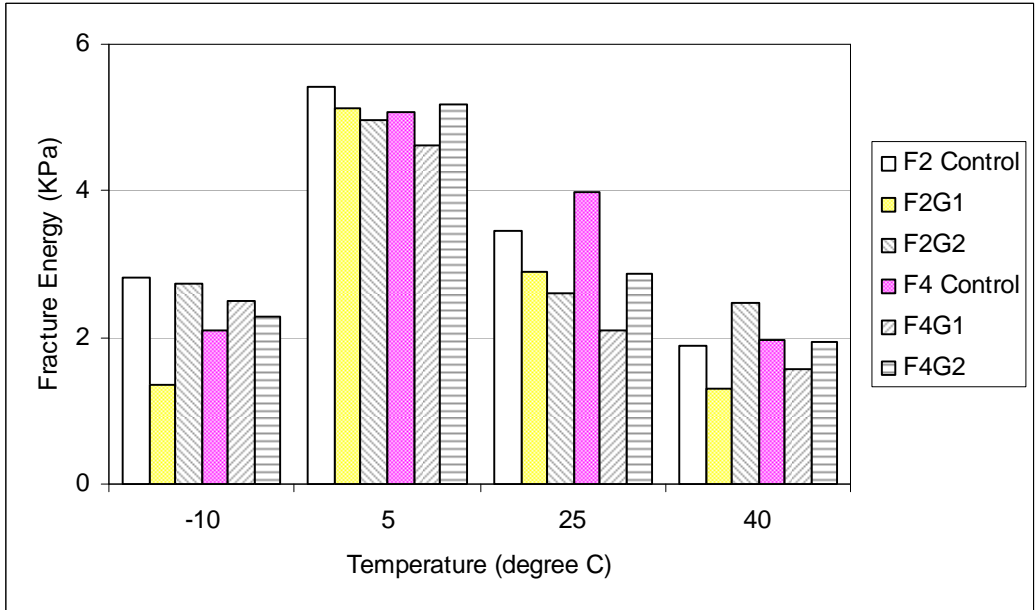


Figure 5-13: Fracture energy for modified gradation mixes (KPa)

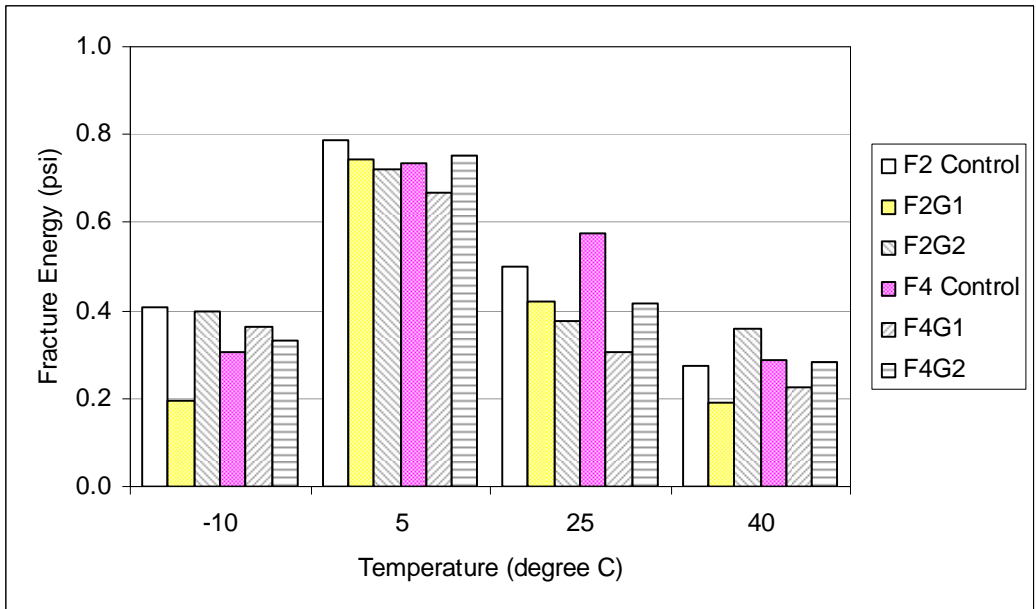


Figure 5-14: Fracture energy for modified gradation mixes (psi)

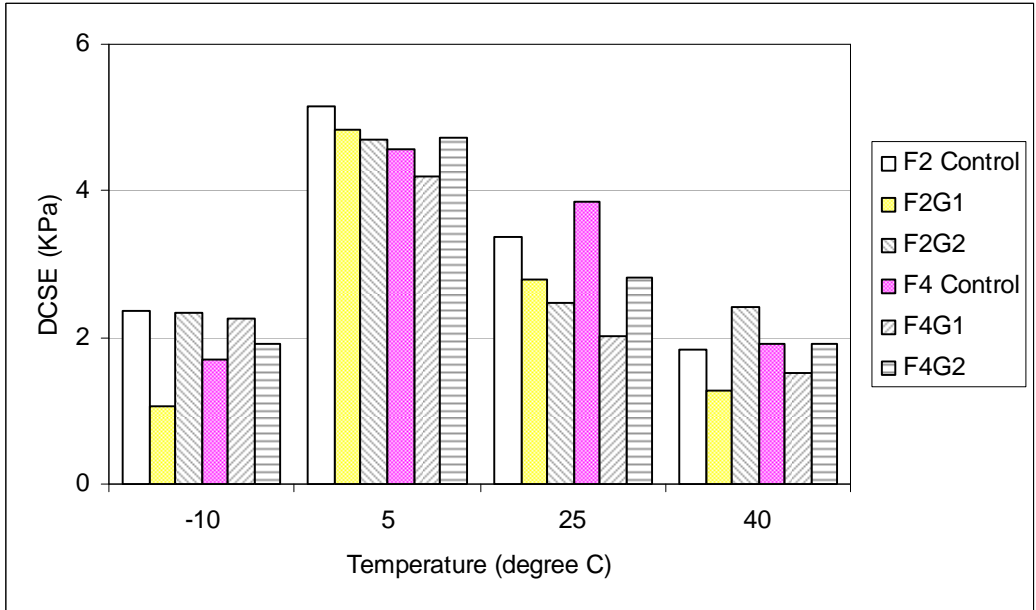


Figure 5-15: DCSE for modified gradation mixes (KPa)

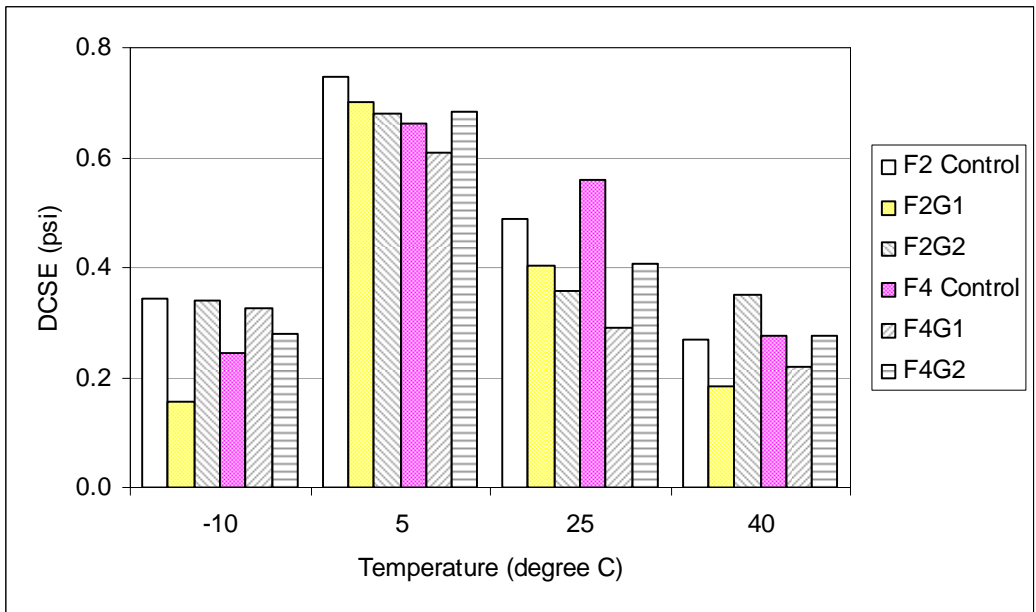


Figure 5-16: DCSE for modified gradation mixes (psi)

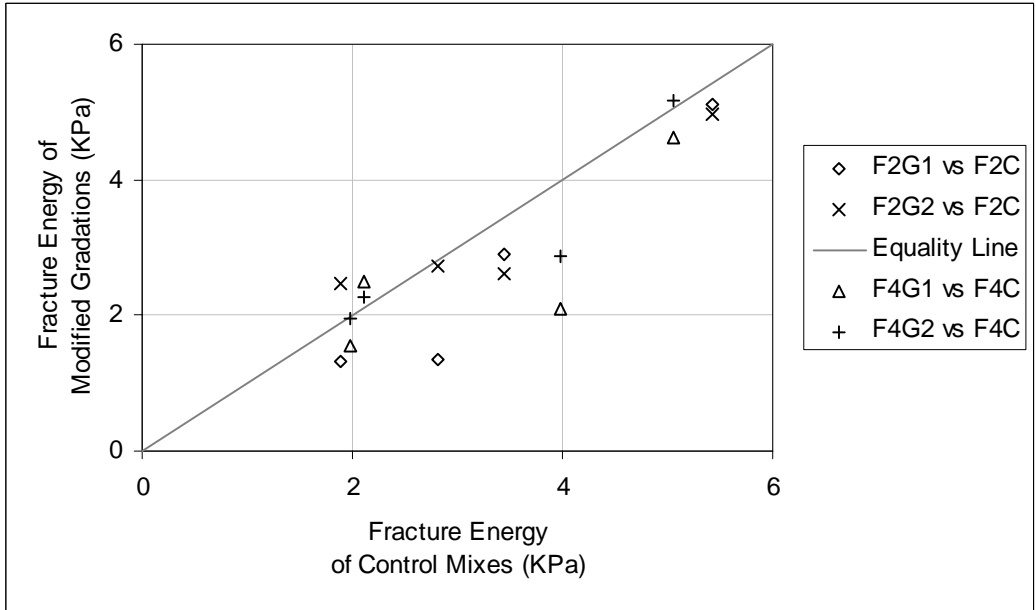


Figure 5-17: Comparison of fracture energy for modified gradation mixtures

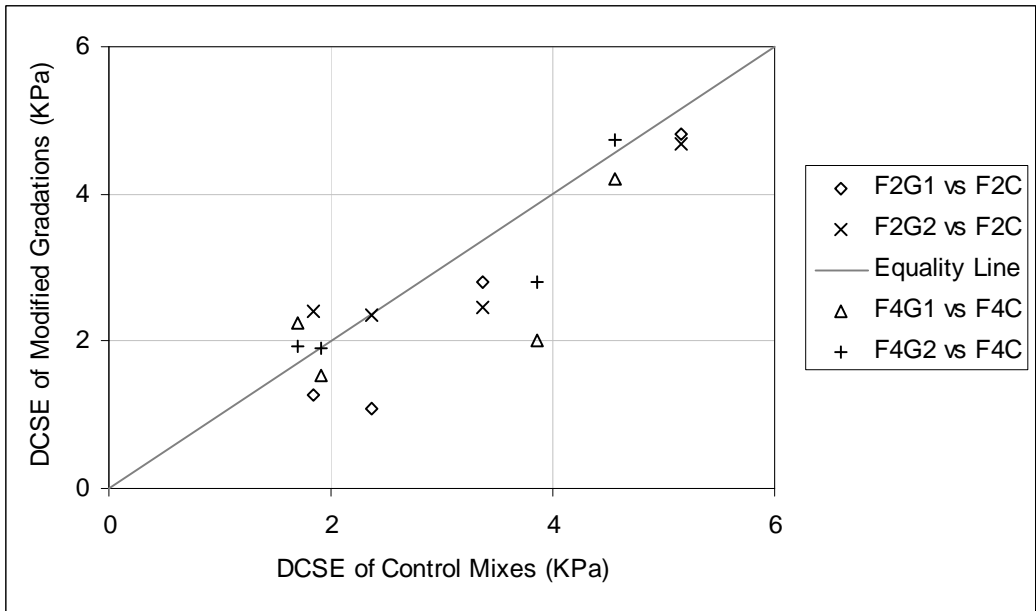


Figure 5-18: Comparison of DCSE for modified gradation mixtures

5.2 SBS Polymer-modified Binder Effects

5.2.1 Evaluation of Resilient Modulus for SBS Polymer-modified Mixtures

Similar to the comparison of resilient modulus between control level and modified gradation mixtures presented in the last section, Figure 5-19 through Figure 5-22 show comparisons of resilient modulus values at various temperature levels for the SBS polymer-modified asphalt mixes of F2 and F4 series, respectively. It can clearly be seen that at low to mid-range temperature levels (-10, 5, and 25°C), the resilient modulus values of PMA mixtures are less than those of control mixtures; and that an increment of SBS polymer content lowers the resilient modulus magnitude. The only exception is that the M_R of F2P1 at 5°C is a little higher than F2 control. On the other hand, at a high testing temperature (40°C), the resilient modulus values of PMA mixtures do not show any clear trend. In general the PMA mixtures tend to keep the same stiffness levels as the mixtures with base asphalt, and an optimum SBS content may exist within the 3% to 6% range depending on the practical mixing and distribution conditions of SBS polymer, base bitumen, and aggregate, which appears to be consistent with the findings presented by Chen et al. (2002, 2003) for SBS modified asphalt binders.

Trend lines are developed in Figure 5-23 for each PMA mixture versus the control mixture. As shown in the figures, the linear regression coefficient decreases as the content of SBS polymer modifier increases, and all correlation coefficient (R^2) values are greater than 0.97. The linear regression indicates an obvious trend that increasing SBS polymer content makes the resilient modulus of HMA lower at low and mid-level temperatures. Based on the above evaluations, the M_R results show that SBS modifiers make HMA softer at mid to low service temperatures and tend to maintain the stiffness levels at the higher testing temperature (40°C). These are favorable attributes for the improvement of the HMA performance issues of low temperature thermal cracking and high temperature rutting.

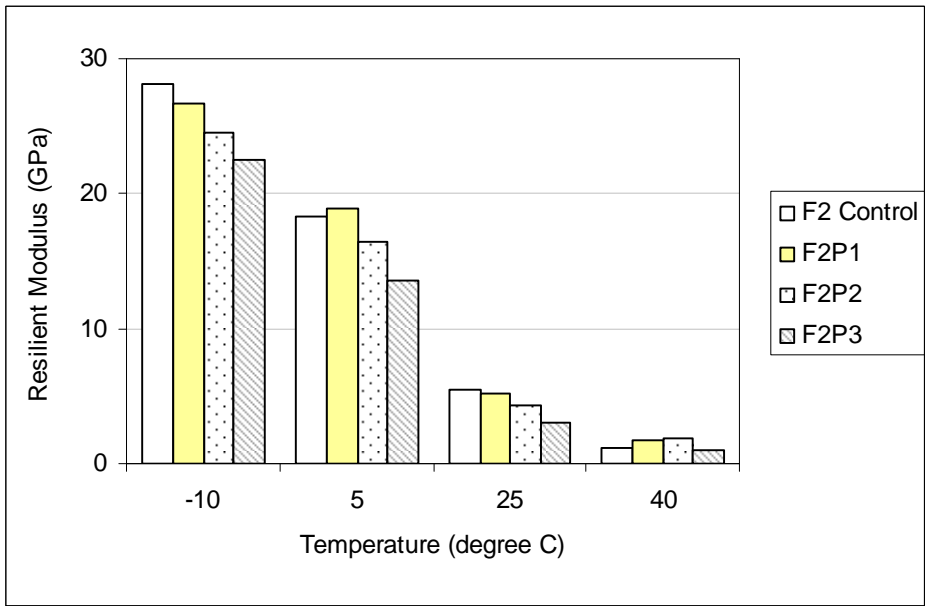


Figure 5-19: Comparison of resilient modulus for F2 SBS PMA mixes (GPa)

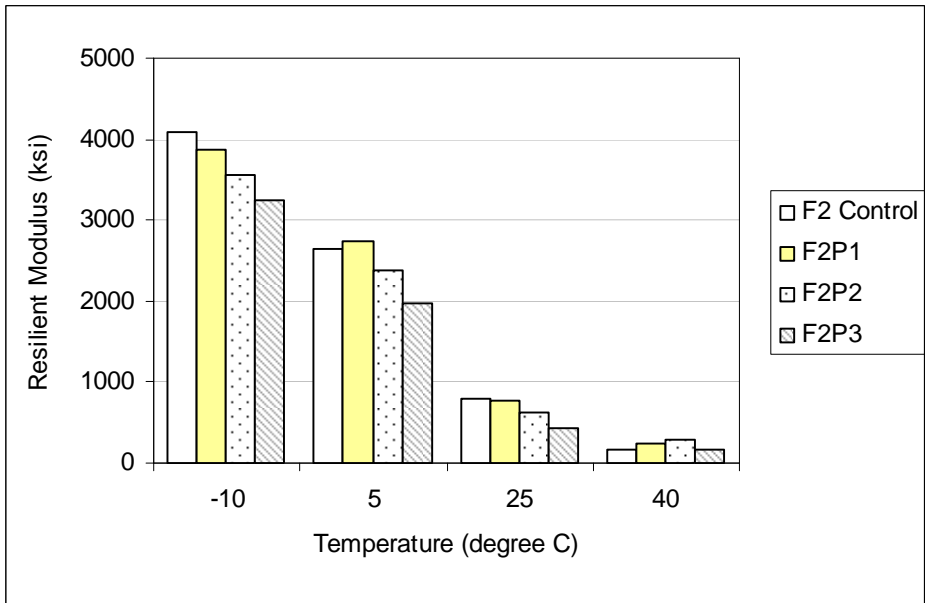


Figure 5-20: Comparison of resilient modulus for F2 SBS PMA mixes (ksi)

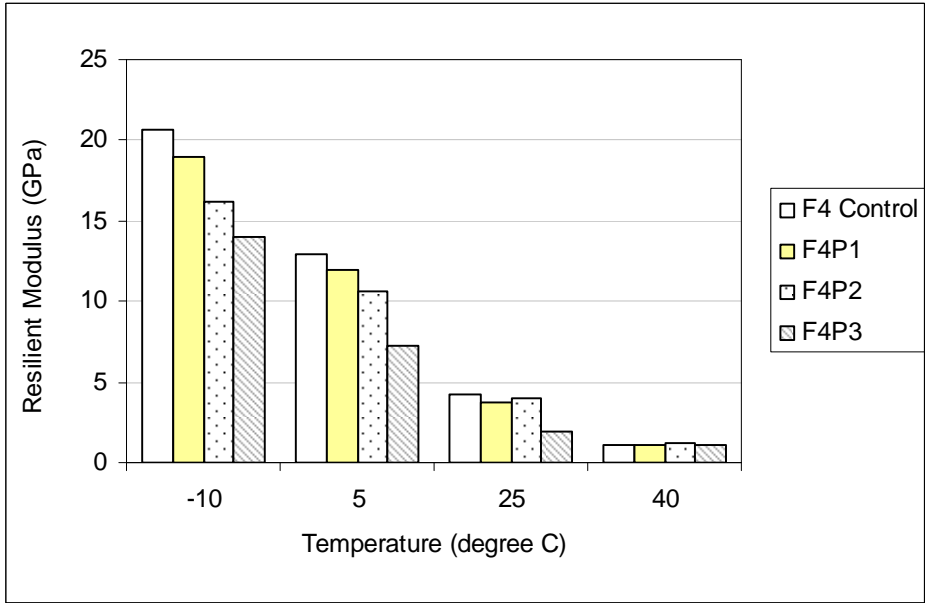


Figure 5-21: Comparison of resilient modulus for F4 SBS PMA mixes (GPa)

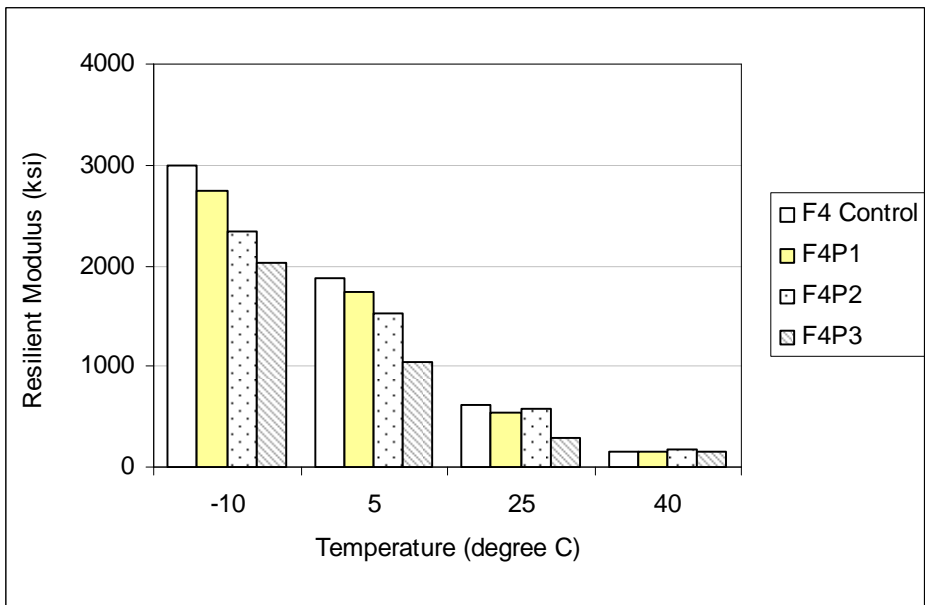
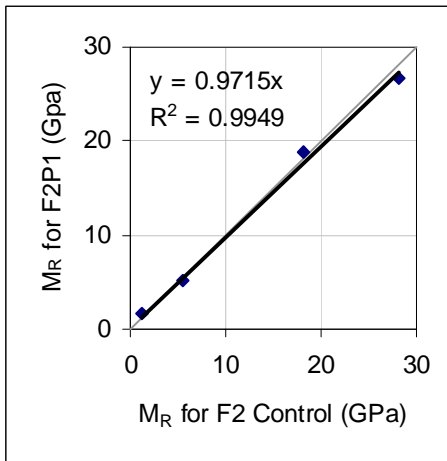
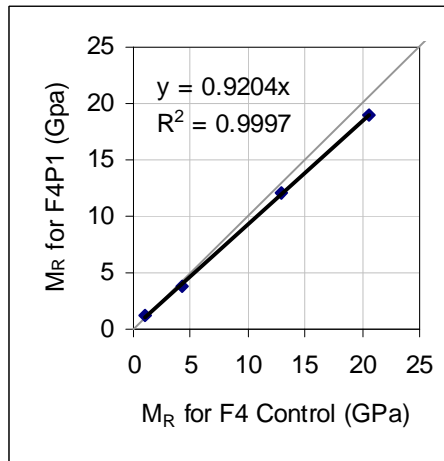


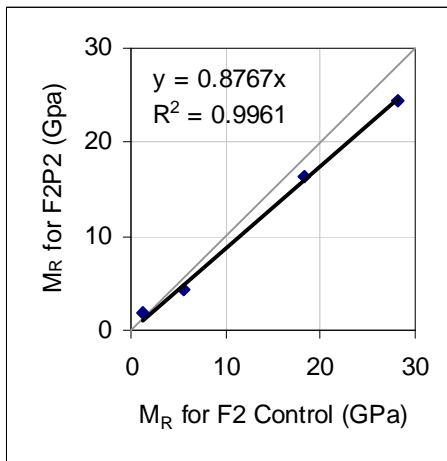
Figure 5-22: Comparison of resilient modulus for F4 SBS PMA mixes (ksi)



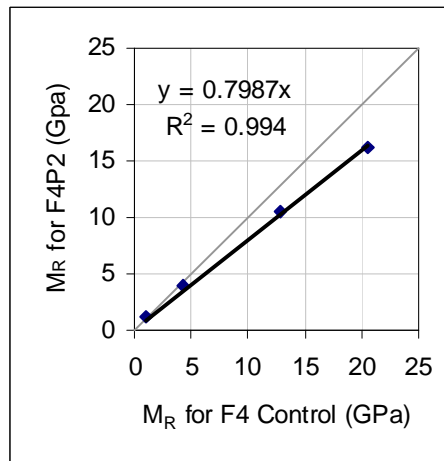
(a)



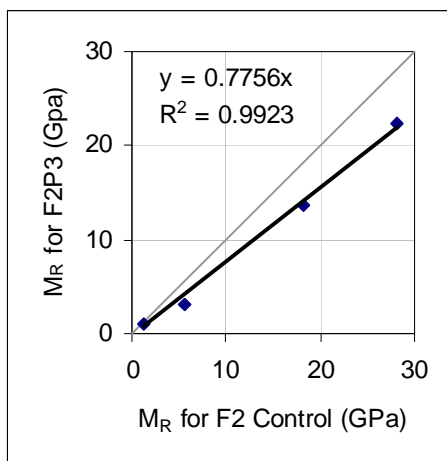
(b)



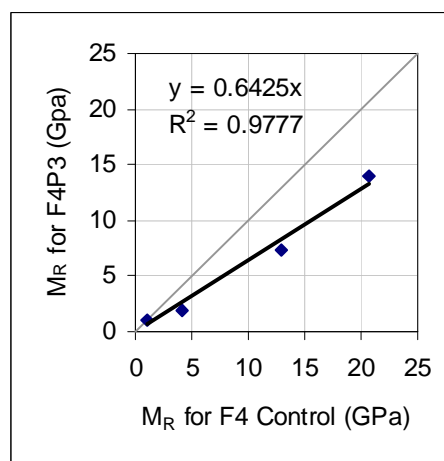
(c)



(d)



(e)



(f)

Figure 5-23: Comparison of M_R between control and PMA mixtures

5.2.2 Evaluation of Creep Compliance for SBS Polymer-modified Mixtures

Table 5-3, Figure 5-24 and Figure 5-25 show the regression coefficients D_1 and m from creep compliance test results for all mixes with SBS polymer-modified binders. The creep compliance master curves are developed and shown in Figure 5-26 and Figure 5-27 for the F2 and F4 series, respectively. As demonstrated in the figures, at low reduced time of about 0 to $10^{4.4}$ seconds, the PMA mixtures are all more compliant than the control mixes. This means the polymer modifier makes the HMA more ductile at low temperatures which would be beneficial to the reduction of thermal cracking. At higher reduced time, the master curves come across each other and the PMA mixture master curves tend to go under the control ones, indicating that the PMA mixes are stiffer and more resistant to rutting at high temperatures. The temperature effect for creep compliance of PMA mixtures can be also observed clearly from the direct testing results plotted in Figure 5-28 through Figure 5-35. At -10°C , all the CP values of PMA mixtures are higher than those of control mixes. On the other hand, at 40°C , the points all drop below the equality line except that F4P2 is a little higher than the F4 control. These observations further verify the SBS polymer effect discussed in the resilient modulus results. At mid-level temperatures (5°C and 25°C), the specimens did not have significant difference in creep compliance. In addition, the linear regression indicates that at a specific temperature level for each mix series, an increment of SBS polymer content usually results in higher creep compliance values. The two exceptions are that the creep compliance of F2P1 is a little higher than that of F2P2 at 5°C , and the creep compliance of F4P2 is higher than that of F4P3 at 40°C .

Table 5-3: Power model regression coefficients for PMA mixture tests

	F2P1	F2P2	F2P3	F4P1	F4P2	F4P3
D_1 (1/GPa)	0.011	0.014	0.034	0.016	0.015	0.017
m	0.413	0.365	0.279	0.353	0.365	0.318

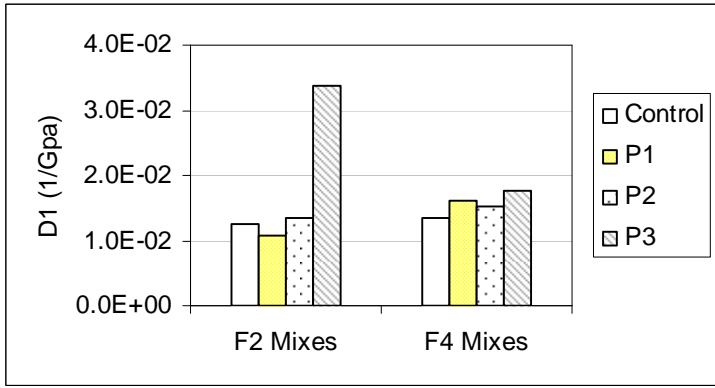


Figure 5-24: Power model parameter D_1 for mixes with SBS PMA ($1/\text{GPa} = 6.89 \times 10^{-6}/\text{psi}$)

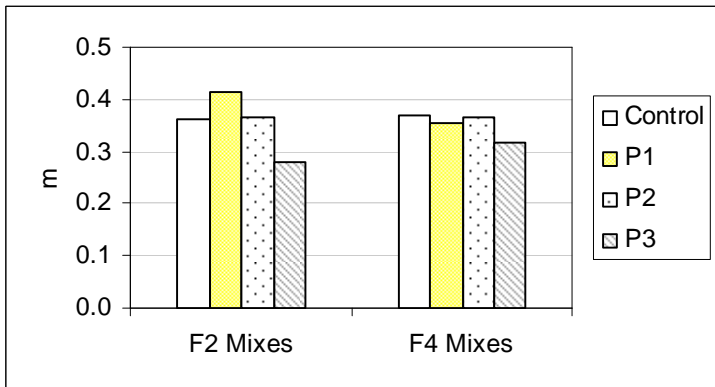


Figure 5-25: Power model parameter m for mixes with SBS PMA

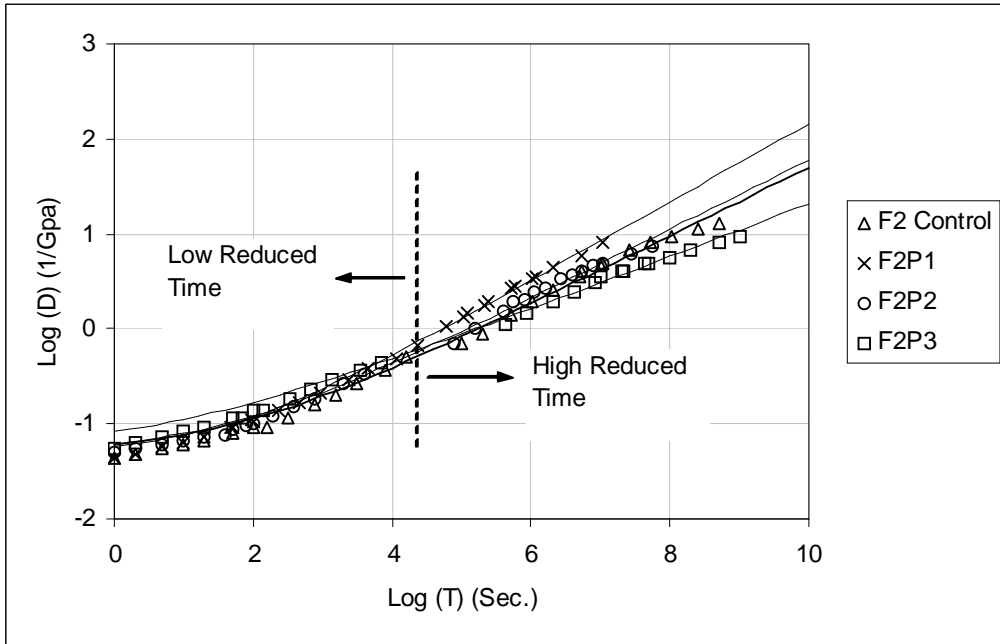


Figure 5-26: Creep compliance master curves for granite PMA mixtures ($1/\text{GPa} = 6.89 \times 10^{-6}/\text{psi}$)

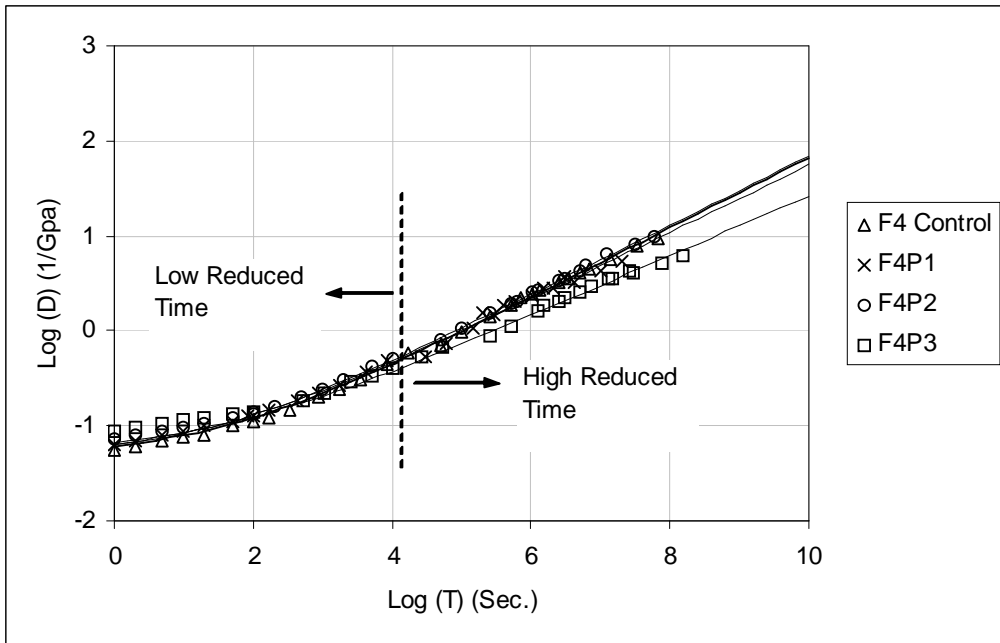


Figure 5-27: Creep compliance master curves for limestone PMA mixtures ($1/\text{GPa} = 6.89 \times 10^{-6}/\text{psi}$)

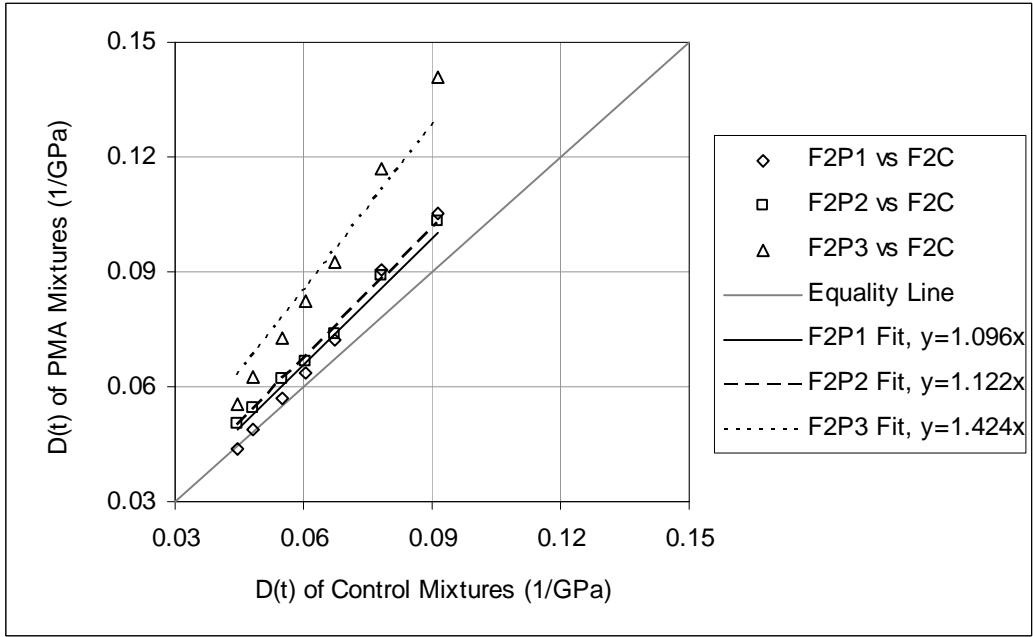


Figure 5-28: Comparison of creep compliance at -10°C for F2 series

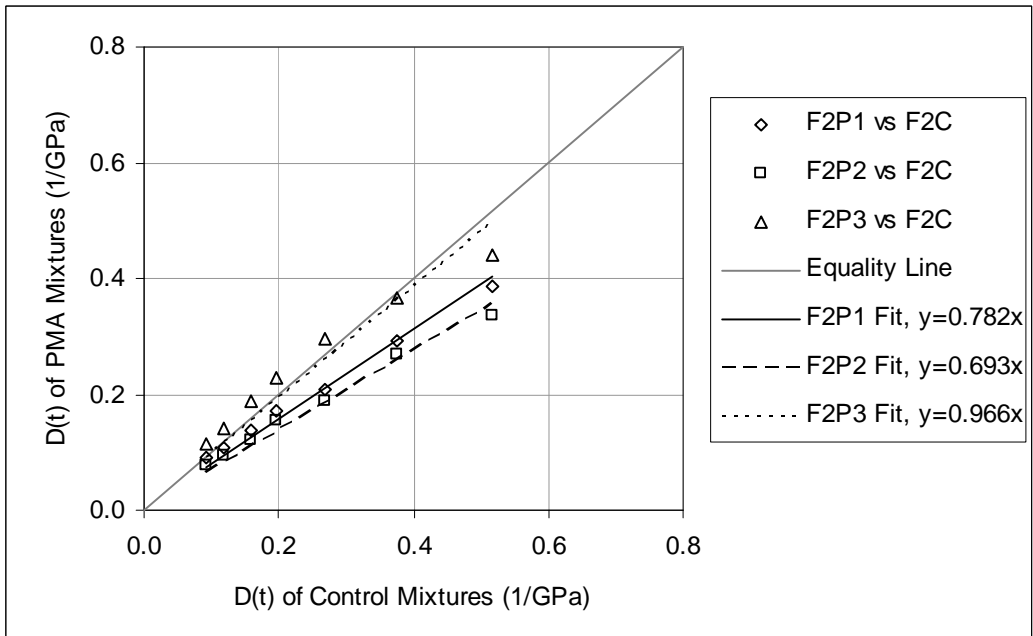


Figure 5-29: Comparison of creep compliance at 5°C for F2 series

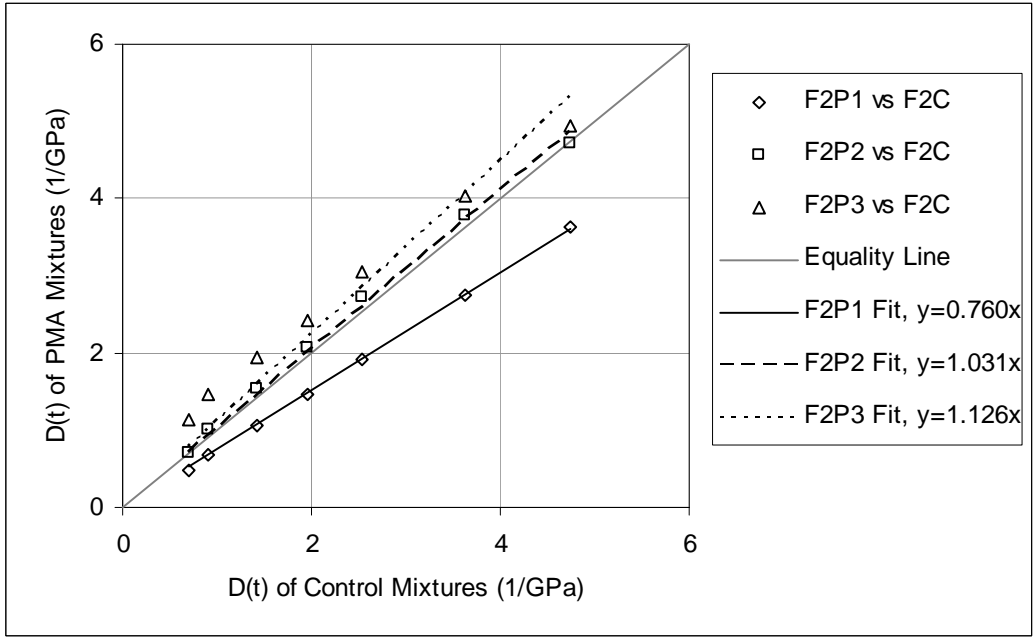


Figure 5-30: Comparison of creep compliance at 25°C for F2 series

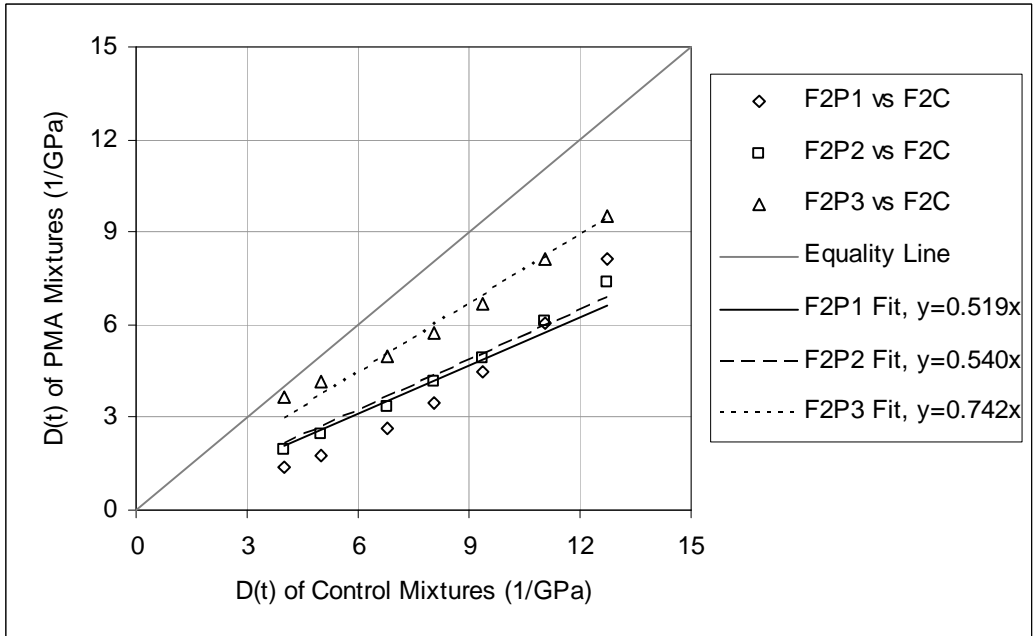


Figure 5-31: Comparison of creep compliance at 40°C for F2 series

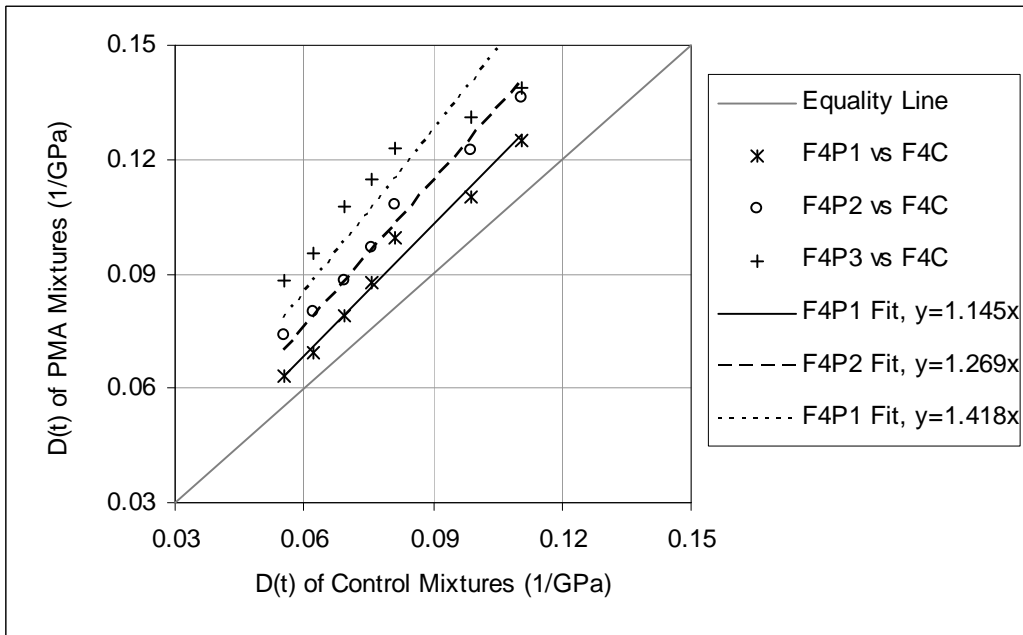


Figure 5-32: Comparison of creep compliance at -10°C for F4 series

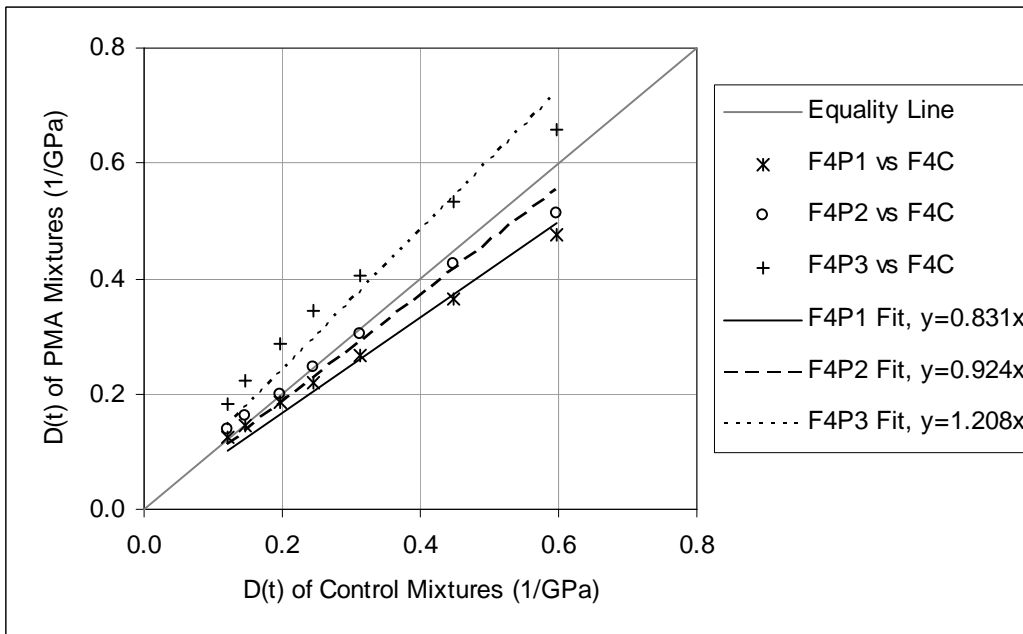


Figure 5-33: Comparison of creep compliance at 5°C for F4 series

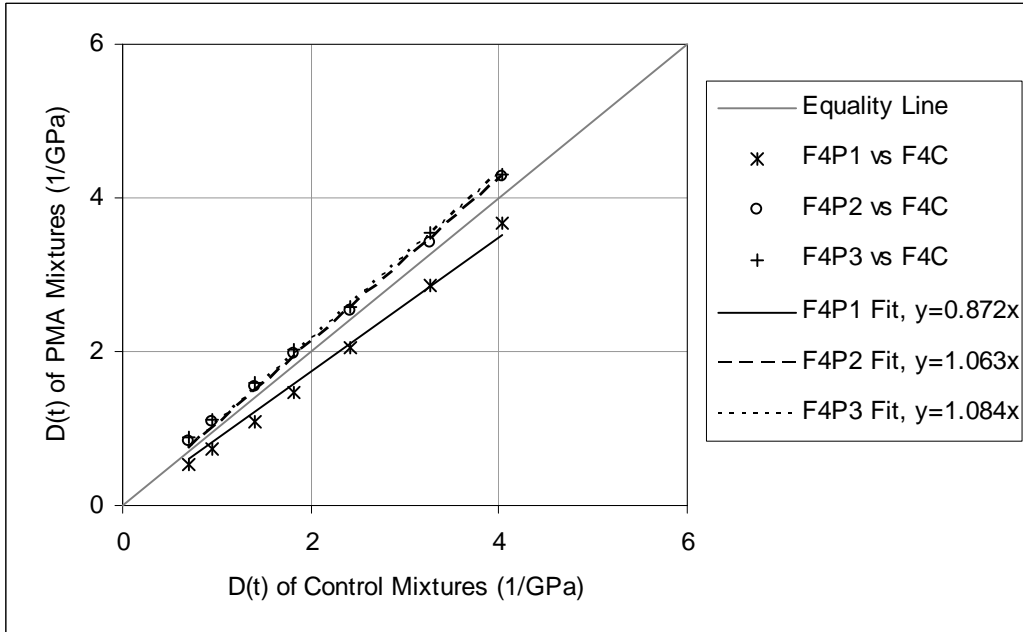


Figure 5-34: Comparison of creep compliance at 25°C for F4 series

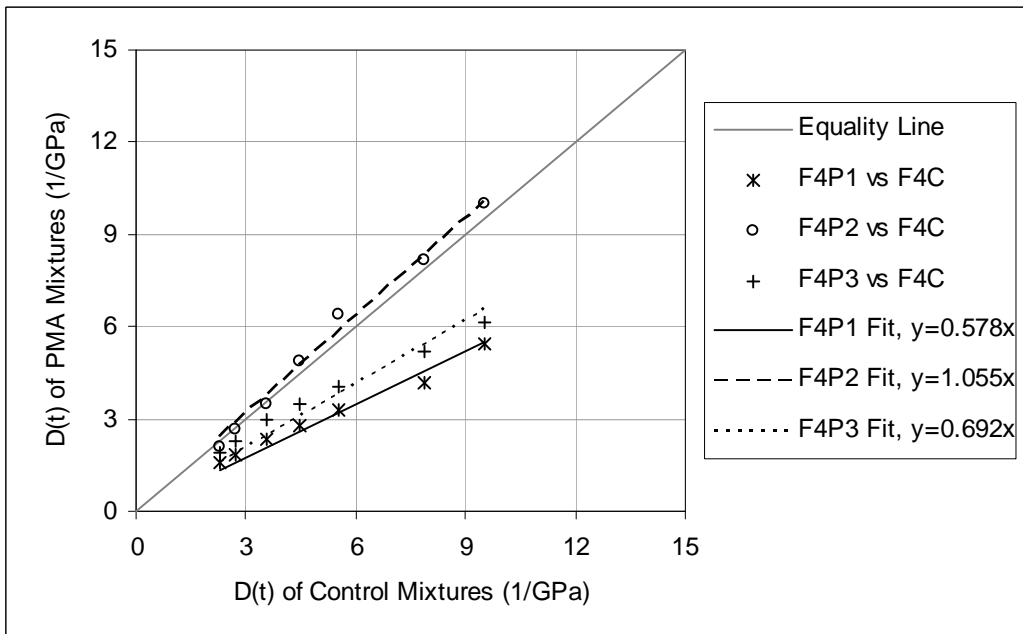


Figure 5-35: Comparison of creep compliance at 40°C for F4 series

5.2.3 Evaluation of Tensile Strength and Fracture Energy for SBS Polymer-modified Mixtures

Figure 5-36 through Figure 5-39 show the test results of Tensile Strength (TS) for control mixtures and polymer-modified asphalt mixtures. The comparison of tensile strength between control and PMA mixtures is presented in Figure 5-40. The SBS polymer did not seem to critically affect the HMA tensile strength.

Figure 5-41 through Figure 5-48 show the test results of fracture energy (FE) and dissipated creep strain energy (DCSE) for control mixtures and PMA mixtures. As discussed in modified gradation mixes, the trend of dissipated energy (DCSE) is the same as for the fracture energy, since the elastic energy part of HMA mixture is essentially determined by tensile strength and resilient modulus, which did not differ noticeably, and for a specific HMA specimen, the magnitude of the elastic energy observed (0-0.7 KPa) is usually much lower than the magnitude of the total fracture energy (1-9 KPa). Comparisons of fracture energy and DCSE values are displayed in Figure 5-49 and Figure 5-50. Most of the points fall above the equality line indicating that SBS polymer tends to increase the fracture energy or DCSE and hence improve the fatigue cracking performance of HMA mixtures. However, no specific relationship was observed between the fracture energy parameters and the SBS polymer content.

At mid to high temperatures (25°C and 40°C), the PMA mixtures exhibit complicated behavior on failure strains which did not show any clear trend, probably due to the enhanced viscous effect of the polymer-modified binder, which make the mixture properties more dependent on the overall particle distributions of the SBS polymer, the asphalt, and the aggregate. At low testing temperatures (-10°C and 5°C), it is found that the failure strain of PMA mixtures tends to increase with an increase of SBS polymer content, as shown in Figure 5-51. This phenomenon is in agreement with the findings reported by Kennedy et al. (1992).

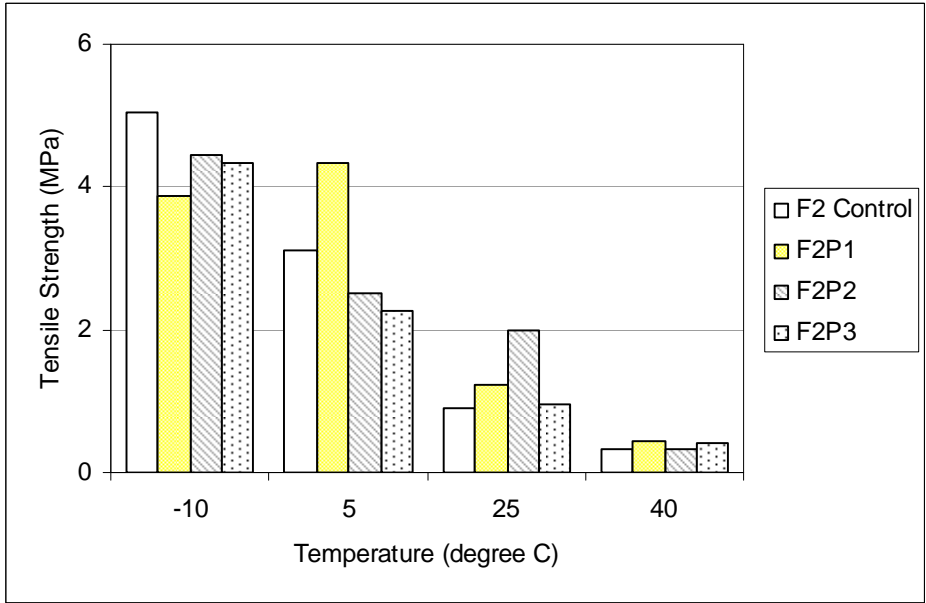


Figure 5-36: Tensile strength for granite PMA mixes (MPa)

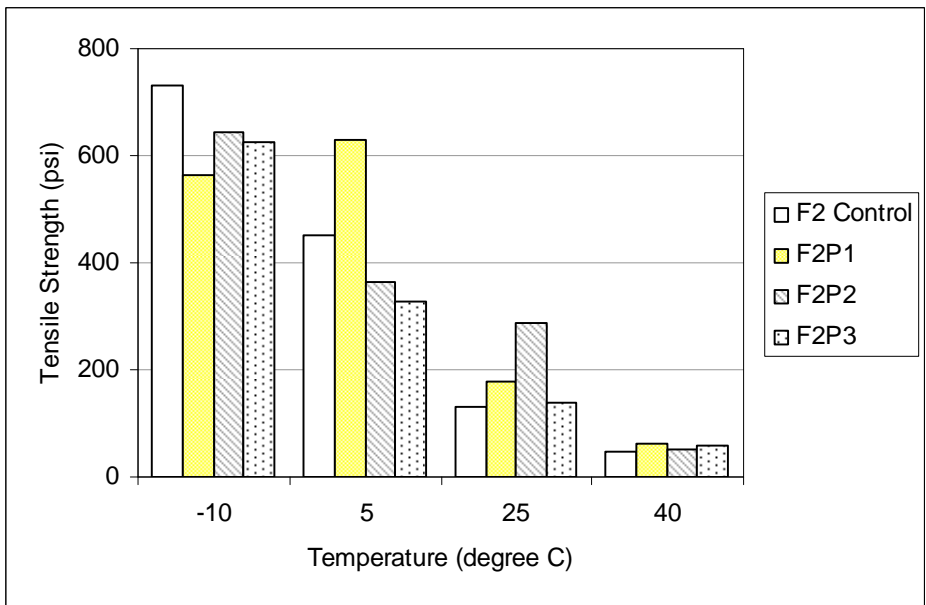


Figure 5-37: Tensile strength for granite PMA mixes (psi)

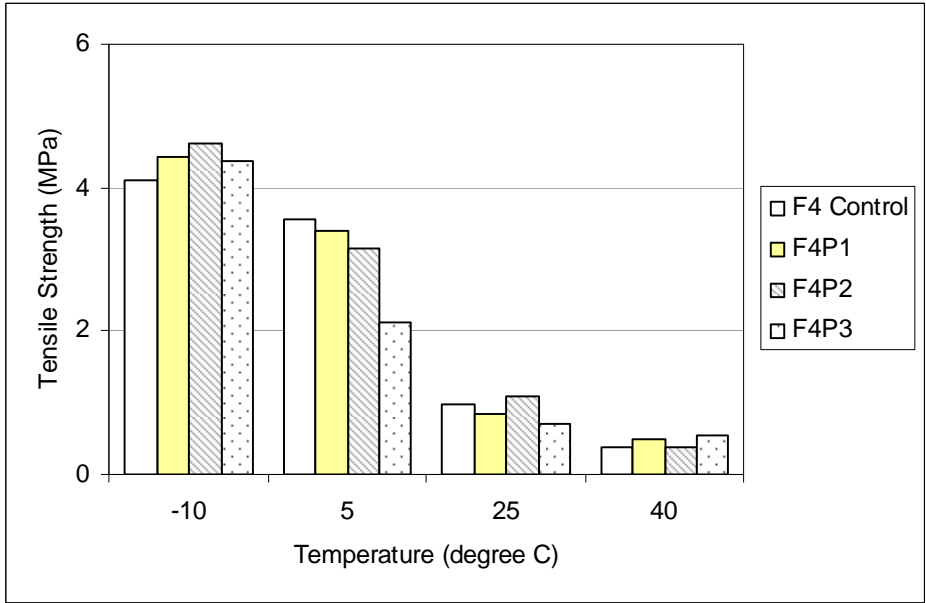


Figure 5-38: Tensile strength for limestone PMA mixes (MPa)

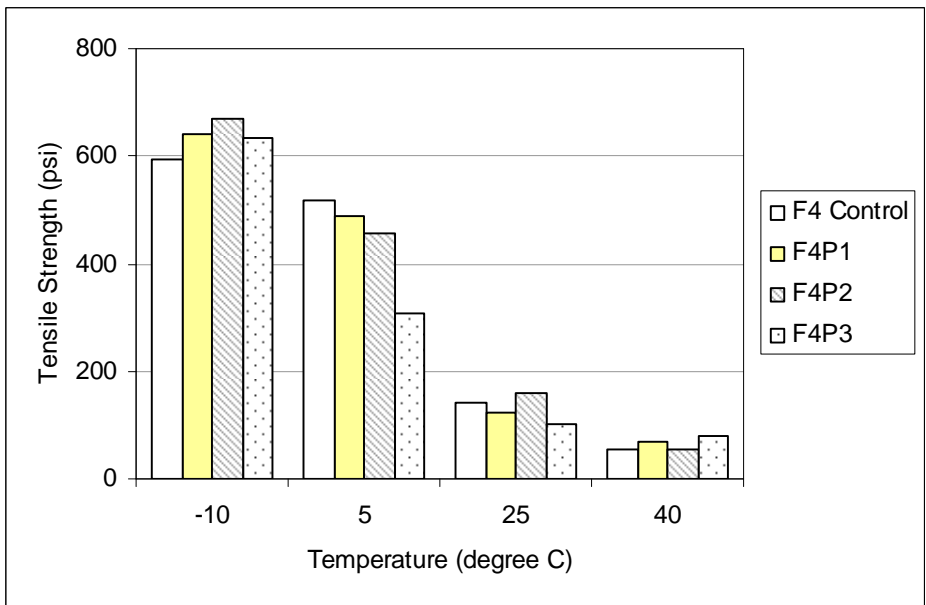


Figure 5-39: Tensile strength for limestone PMA mixes (psi)

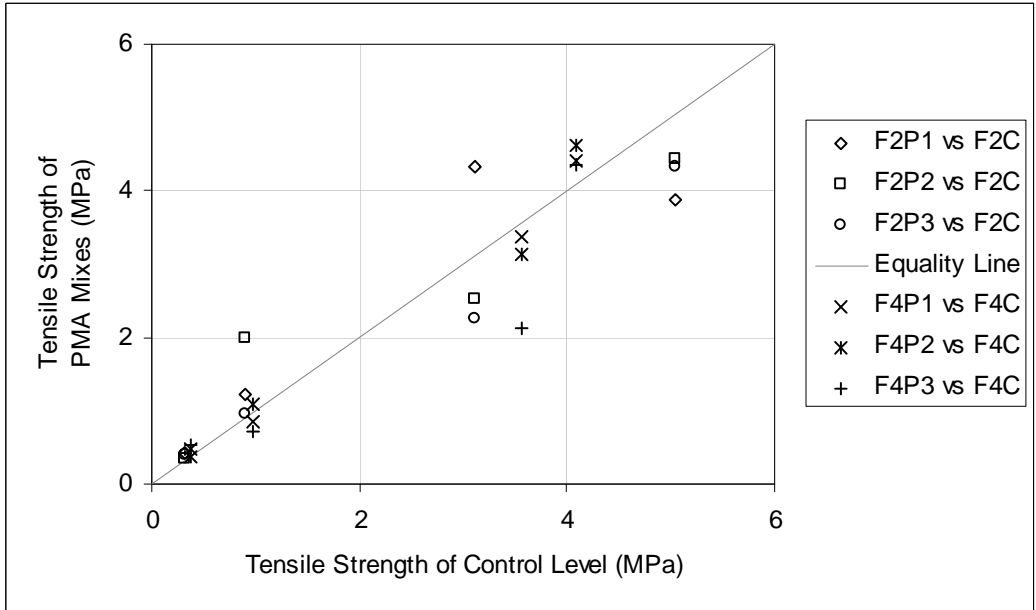


Figure 5-40: Comparison of tensile strength between control and PMA mixes

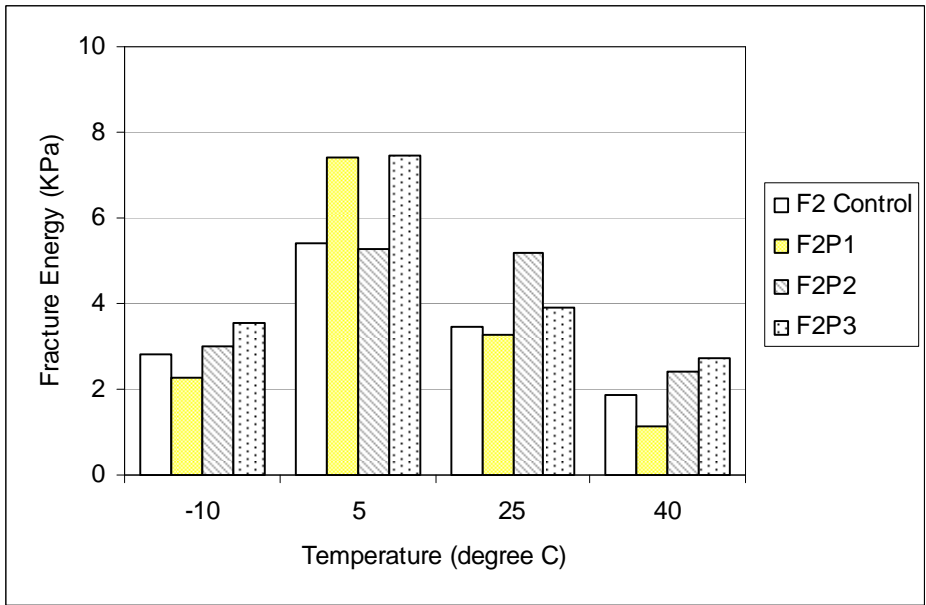


Figure 5-41: Fracture energy for granite PMA mixes (KPa)

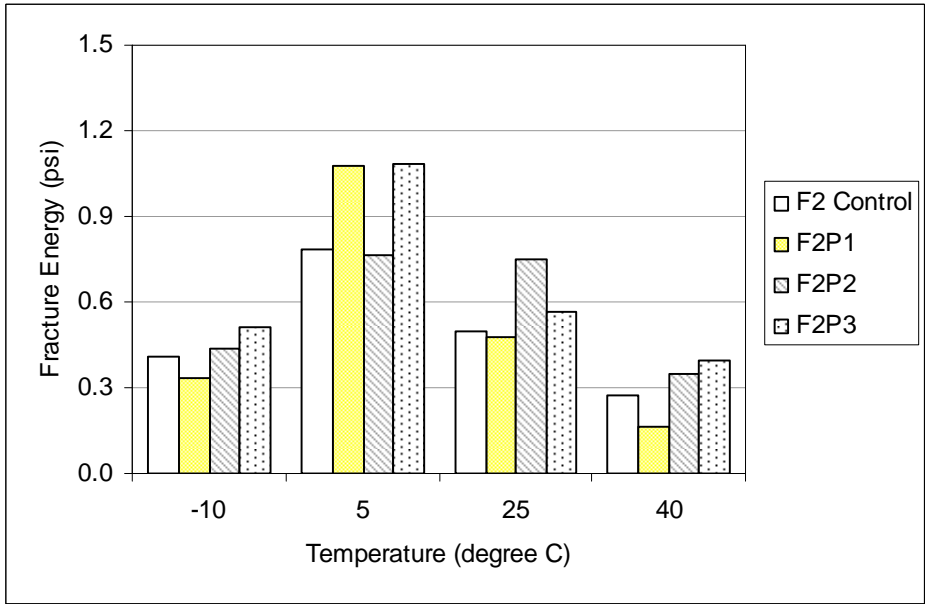


Figure 5-42: Fracture energy for granite PMA mixes (psi)

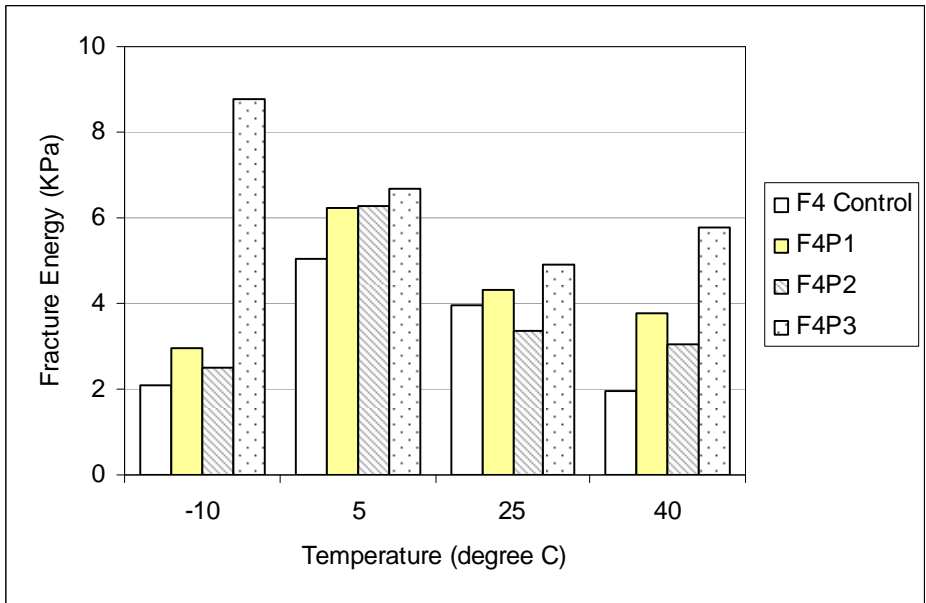


Figure 5-43: Fracture energy for limestone PMA mixes (KPa)

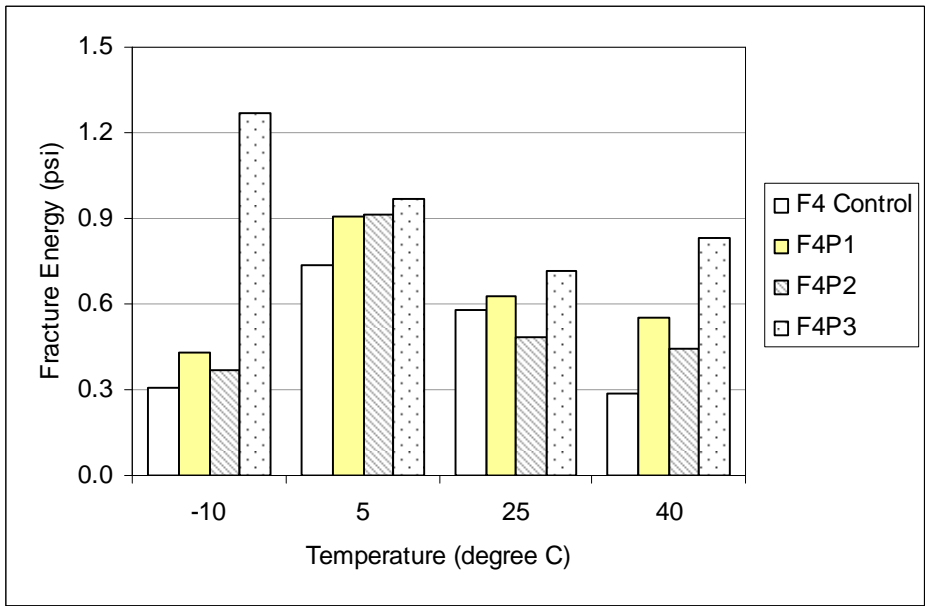


Figure 5-44: Fracture energy for limestone PMA mixes (psi)

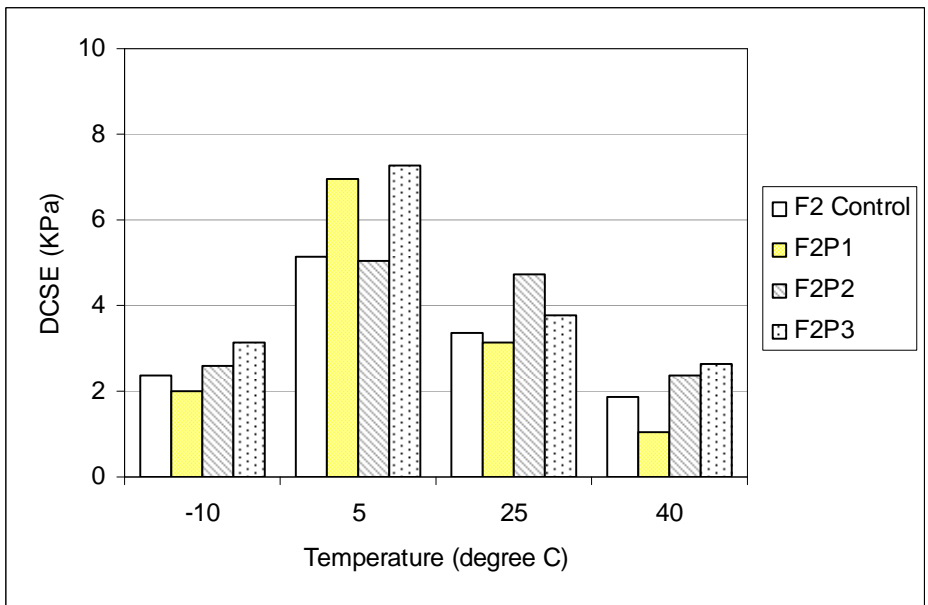


Figure 5-45: DCSE for granite PMA mixes (KPa)

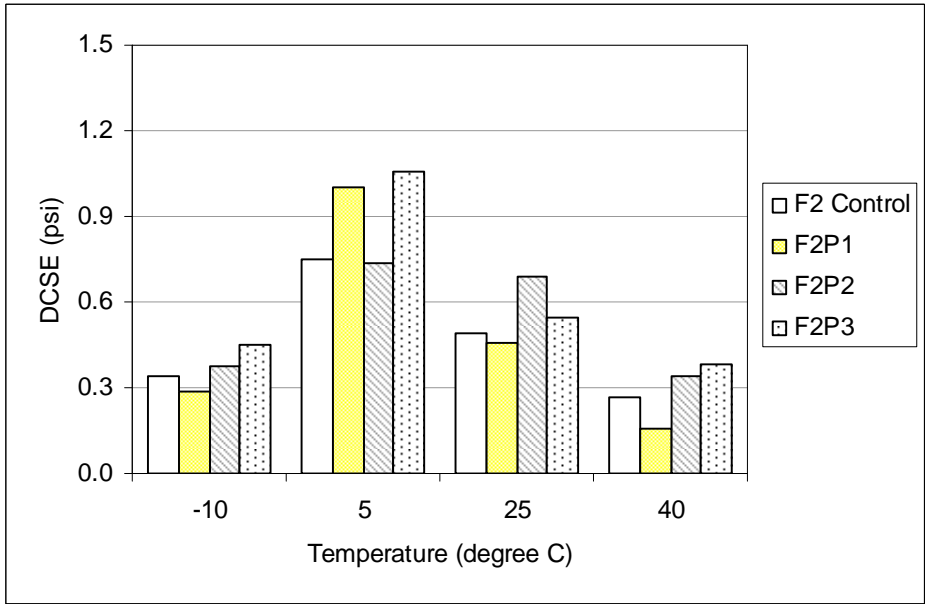


Figure 5-46: DCSE for granite PMA mixes (psi)

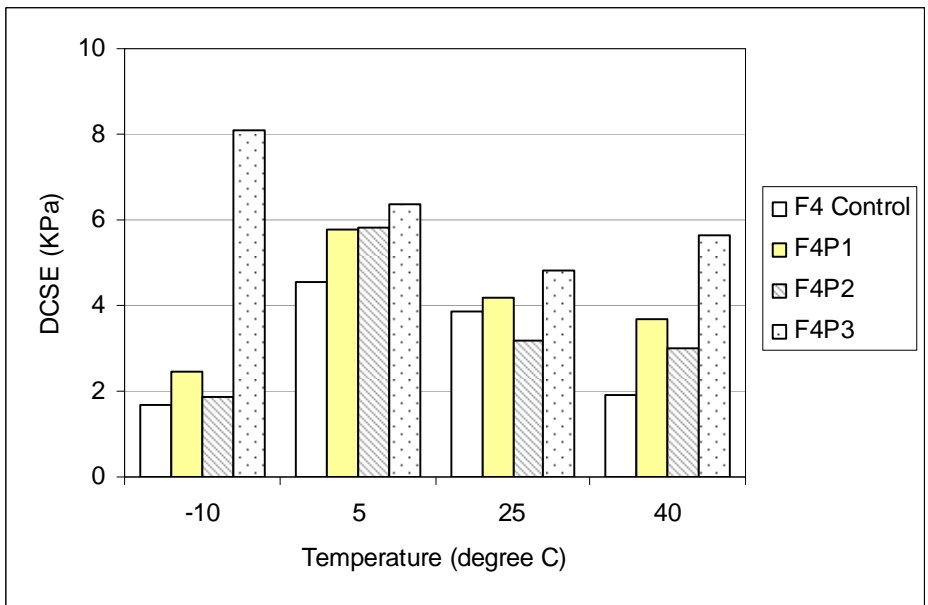


Figure 5-47: DCSE for limestone PMA mixes (KPa)

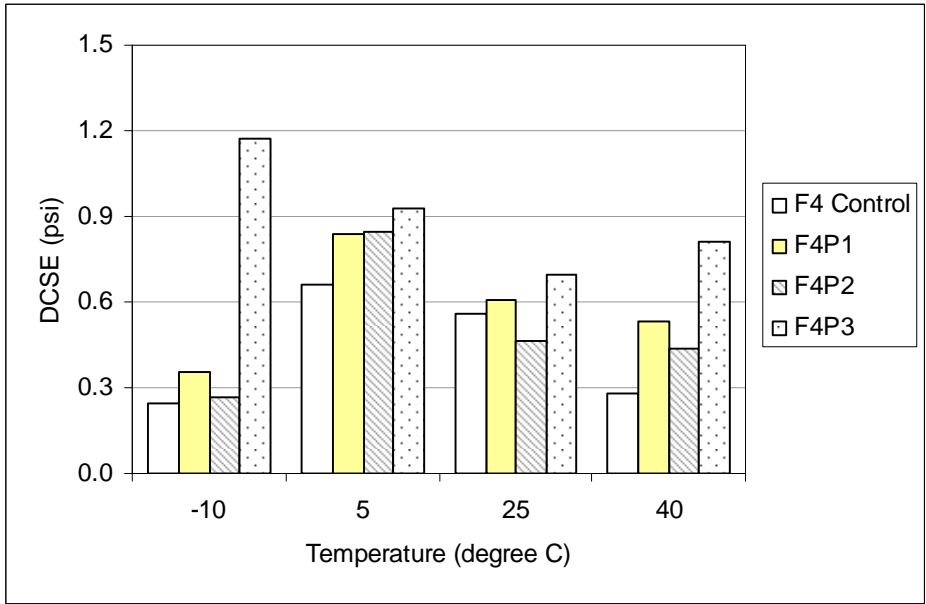


Figure 5-48: DCSE for limestone PMA mixes (psi)

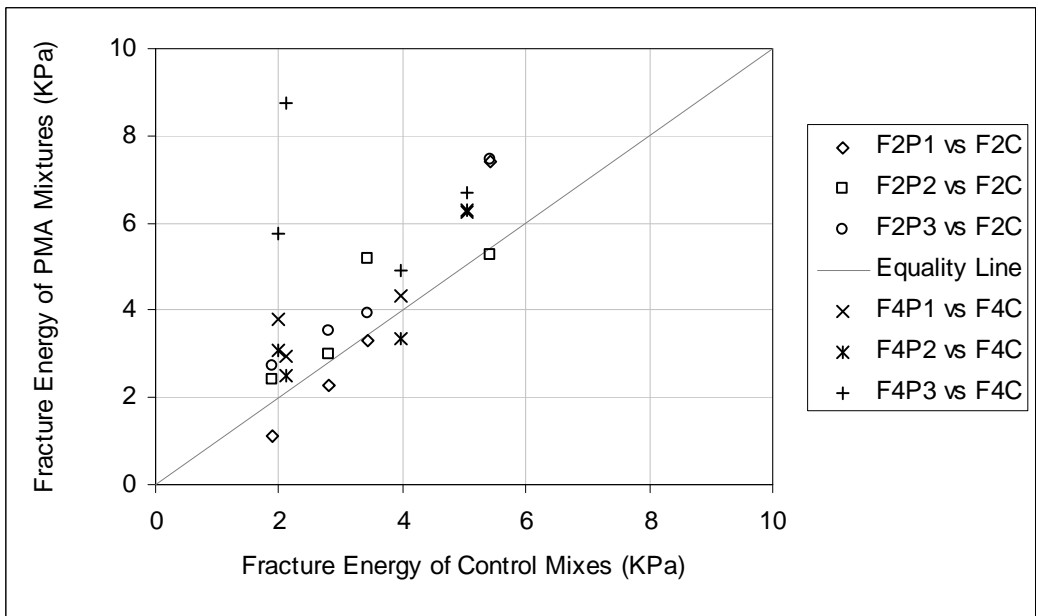


Figure 5-49: Comparison of fracture energy between control and PMA mixes

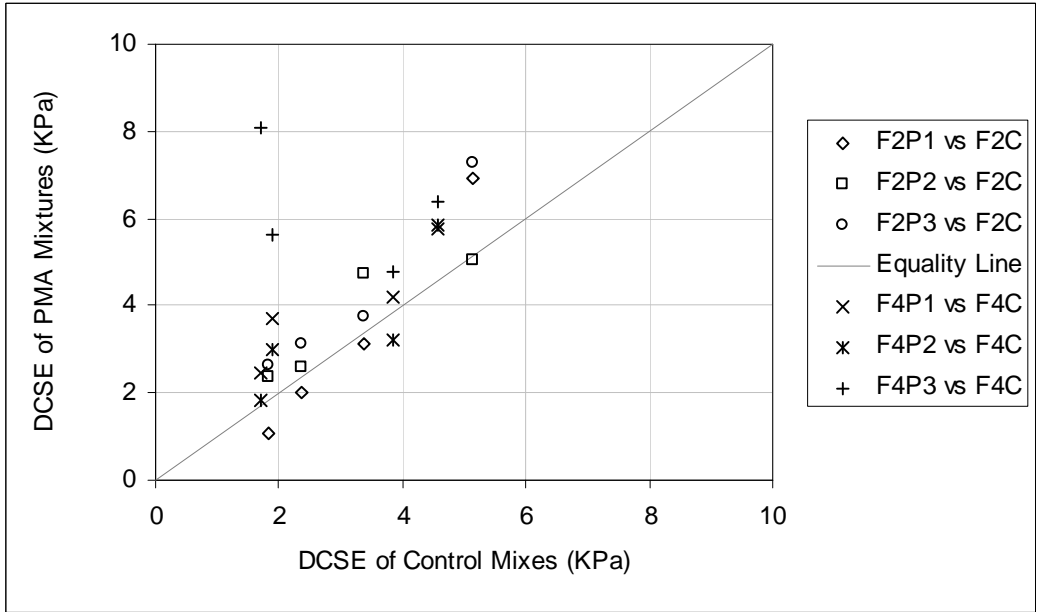


Figure 5-50: Comparison of fracture energy between control and PMA mixes

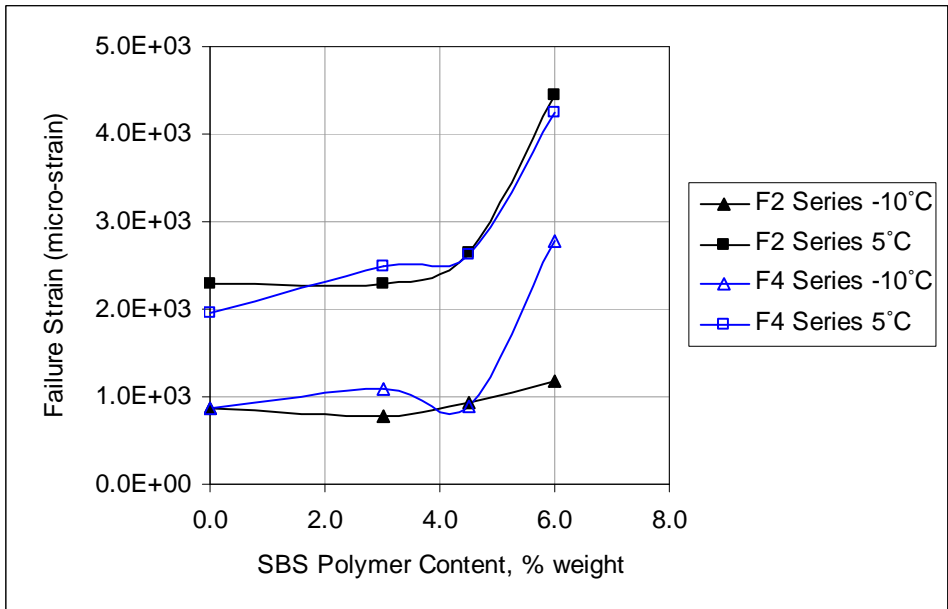


Figure 5-51: Relationship between the observed failure strain and SBS polymer content

5.3 Effect of Aggregate Type

Another important factor that influences the HMA engineering properties is aggregate type. As introduced in the preceding chapter, two major aggregate types, granite and limestone, were used in this HMA fracture mechanics study. For control mixes (F2C and F4C), the mix designs with two different types of aggregate have the same nominal maximum aggregate size (1/2 in. or 12.5 mm), the same control limit points, the same restricted zone, and hence very similar gradation curves (Figure 5-52). For the modified gradation mixes, the adjustment of aggregate amount for each gradation level (G1 or G2) at each sieve size is also close, and this makes the adjusted shapes of gradation curves for the two different types of aggregate appear to be similar. For the mixtures with SBS polymer-modified asphalt binder, the polymer content is identical at each level (3.0%, 4.5%, and 6.0%). All these analogues provided a basis for evaluating the differences of fracture mechanics properties between the two types of aggregate. It is commonly known that limestone aggregate is usually softer than granite aggregate. Figure 5-53 shows a comparison of resilient modulus between granite and limestone mixtures. All points fall below the line of equality, which confirms that the granite mixtures are stiffer than limestone mixtures. In particular, the difference of resilient modulus values between the two types of aggregate at mid to low temperature levels (-10°C and 5°C) is much more remarkable than that at elevated testing temperatures (25°C and 40°C). From this point of view, the limestone mixtures would appear more ductile under low service temperature conditions and, as a result, be capable of improving the performance of thermal cracking of pavement structures.

The comparisons of creep compliance between granite and limestone mixtures at each testing temperature are shown in Figure 5-54 through Figure 5-57. The result is not as simple as that the limestone would be always more compliant than granite. At low temperatures (-10°C and 5°C), the creep compliance values of limestone mixtures are all higher than those of granite mixtures. At 25°C, the data points are distributed closely along the line of equality. When the temperature goes up to 40°C, most of the data points go under the line of equality, which means that the limestone specimens become less compliant than the granite specimens. These characteristics exhibited by limestone mixtures are advantageous to pavement structures in improving the performance of thermal cracking at low service temperature and the rutting

resistance at high service temperatures. This effect, in creep aspect of view, is analogous to that of SBS polymer-modified asphalt binders.

It was expected that the granite mixtures have higher tensile strength values than limestone mixtures because generally the granite material exhibits a higher hardness nature than the limestone material. Figure 5-58 shows the comparison of tensile strength between granite and limestone mixtures. The strength values of the two aggregate types are generally in the same magnitude. The zero interception linear trend line indicates that the limestone mixtures have less tensile strength than the granite mixtures by a small amount. The comparison of fracture energy between granite and limestone mixtures is displayed in Figure 5-59. The plot shows a poor correlation of fracture energy between granite and limestone mixtures. The reason for this poor correlation may be due to the fact that the fracture energy result depends on a few other basic variables including tensile strength, failure strain, and the dynamic stress-strain behavior of each specific mixture.

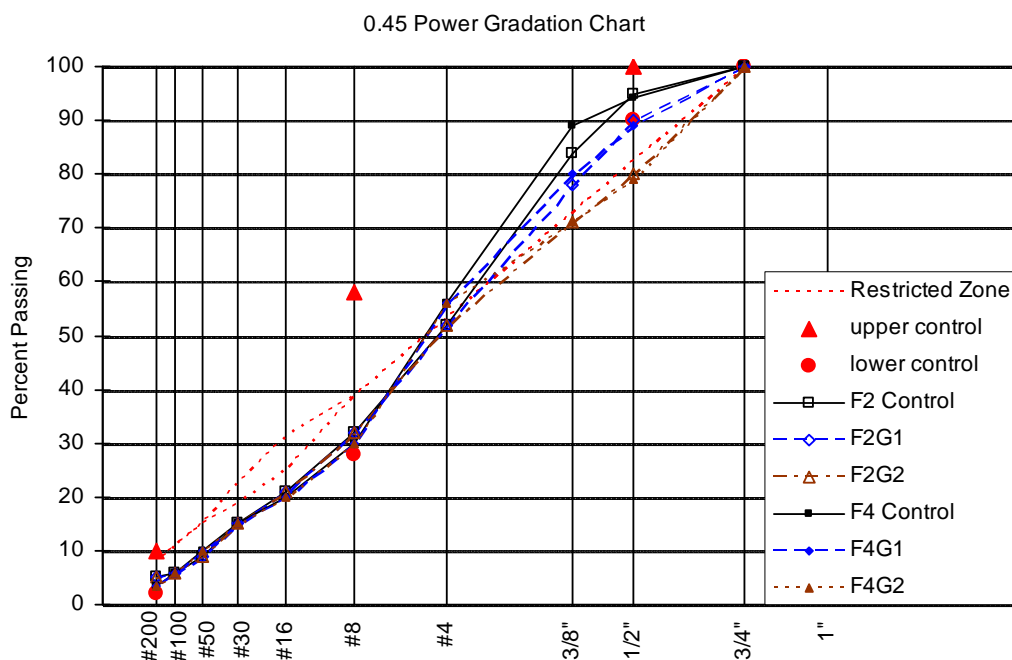


Figure 5-52: Gradation curves for control mixes and the modified gradation mixes

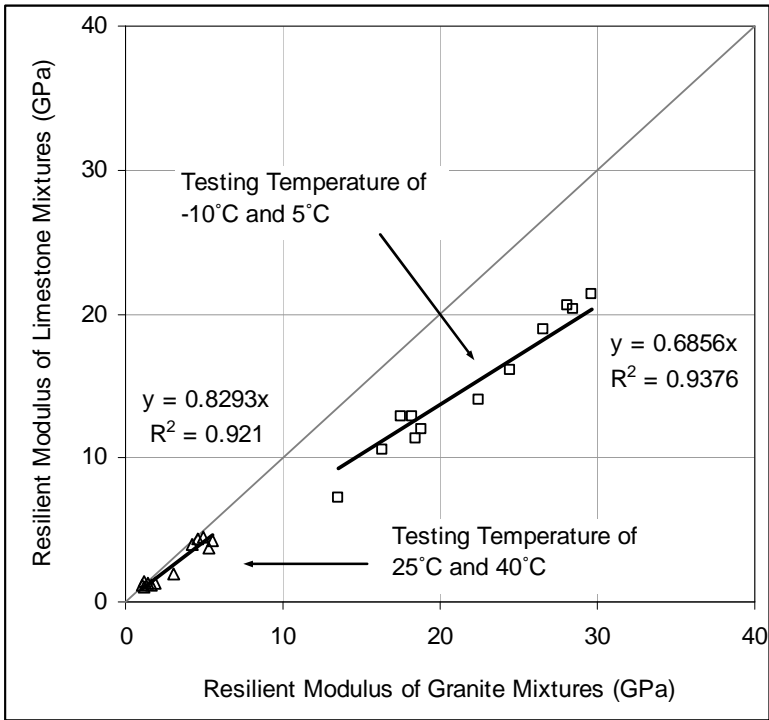


Figure 5-53: Comparison of resilient modulus for granite and limestone mixtures

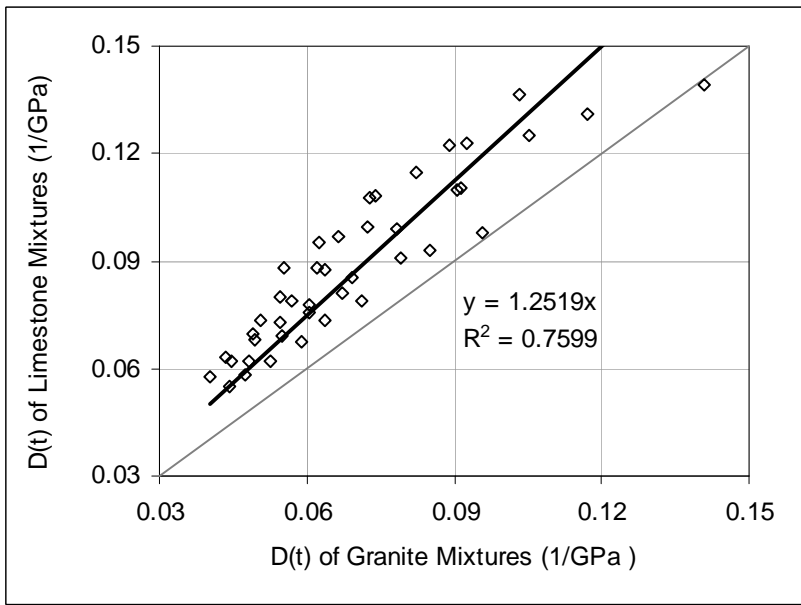


Figure 5-54: Comparison of CP between granite and limestone mixes at -10°C

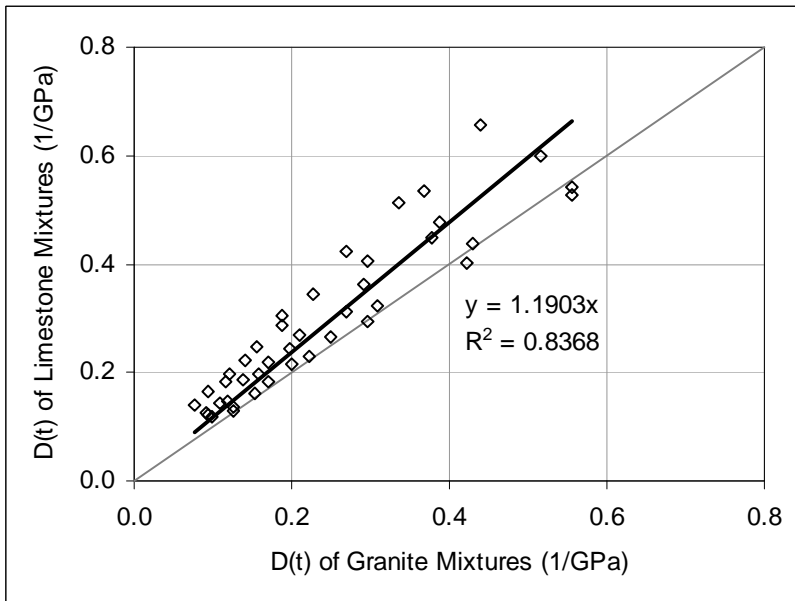


Figure 5-55: Comparison of CP between granite and limestone mixes at 5°C

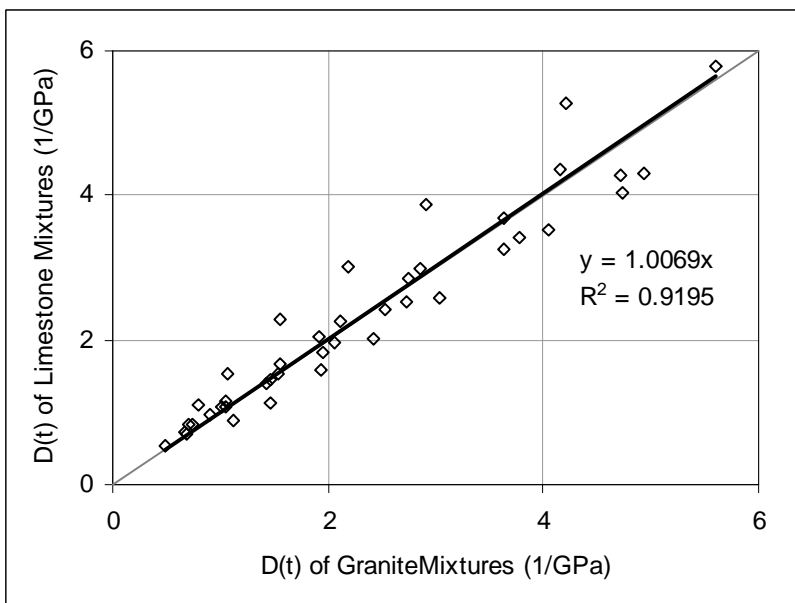


Figure 5-56: Comparison of CP between granite and limestone mixes at 25°C

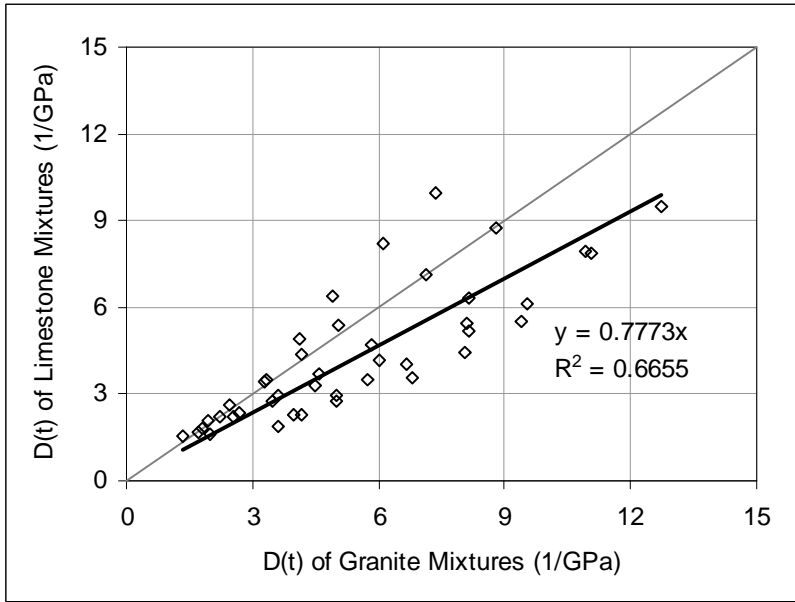


Figure 5-57: Comparison of CP between granite and limestone mixes at 40°C

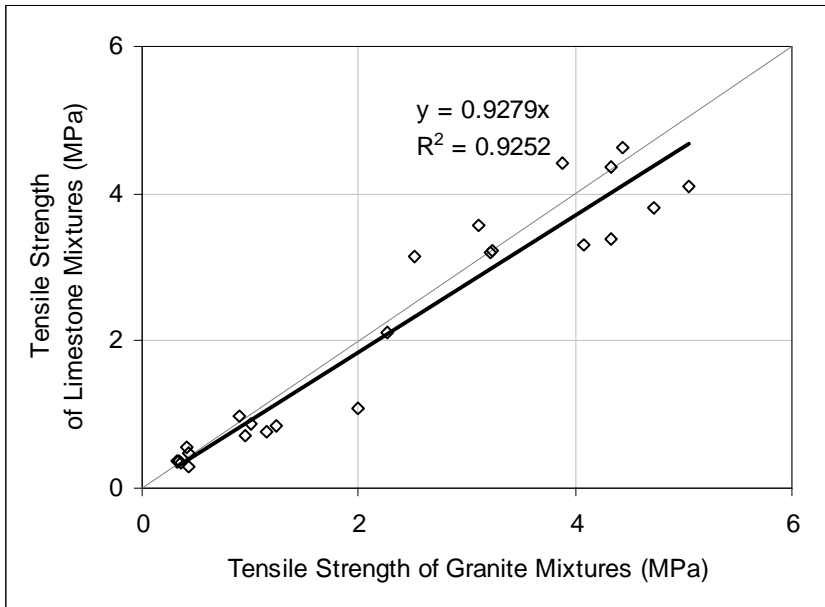


Figure 5-58: Comparison of tensile strength between granite and limestone mixes

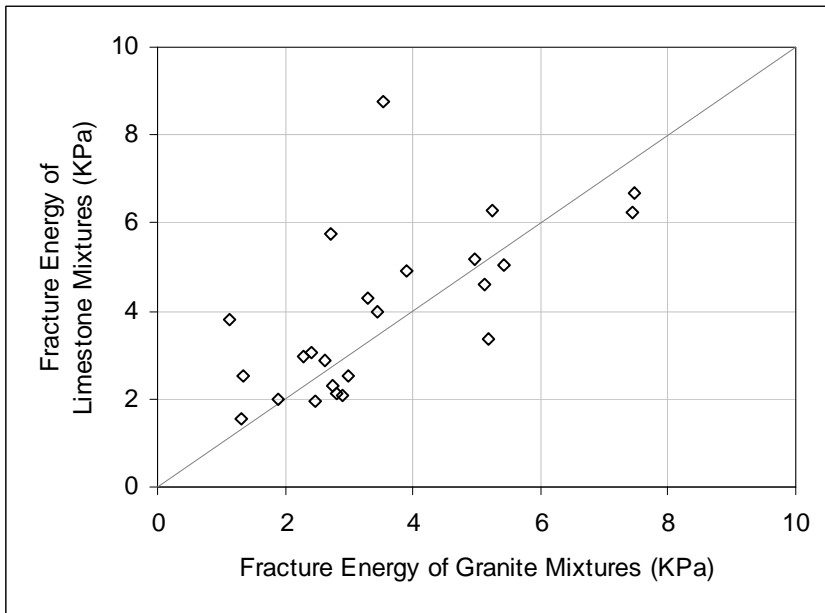


Figure 5-59: Comparison of fracture energy between granite and limestone mixes

5.4 Summary of Analysis and Findings from Fracture Mechanics Tests

In gradation modifications, the amount of aggregate retaining on coarse sieves was increased. However, the power law regression curves for each mix design series turned out to be close to each other. The effect of gradation adjustment by increasing the 12.5 mm (1/2 in.) coarse aggregate with a range of 5% to 15% appeared to be negligible on mixtures' resilient modulus. Similarly, the proposed gradation modifications did not make a significant difference in the creep compliance properties for the HMA tested in this study. But, the tensile strength test results indicated that the increase of coarse aggregate downgraded the HMA tensile strength property at low temperature levels. In general, the binder effect should be relatively important at low temperature levels and the aggregate would play a major role at high temperature levels. In this study, since the coarse aggregate gradation is the only variable when performing comparison based on the assumptions of the testing program, the results imply that the effect of coarse aggregate gradation also plays an important role to the tensile strength of HMA at low temperature levels. In addition, it was found that most of the fracture energy values of modified gradations were lower than those of control mixtures. Overall, the increase of coarse aggregate

amount in this study had negligible or slightly adverse effect on HMA fracture mechanics properties.

The SBS polymer-modified asphalt binder was found to be beneficial to HMA fracture mechanics properties in a few aspects. First of all, the SBS polymer improved the stiffness behavior of asphalt mixtures. The SBS polymer-modified binder made the PMA mixtures less stiff than control mixes with unmodified asphalt binder at low-to-mid range temperature levels (-10°C and 5°C). The resilient modulus values of PMA mixtures decreased with an increase of SBS polymer content throughout the concentration range tested. At the testing temperature of 40°C, the PMA mixtures appeared to maintain the stiffness levels. The increment of SBS polymer dosage did not result in a consistent effect on resilient modulus of the mixtures. However, it should be noted that when the SBS polymer concentration increased from 3.0% to 6.0%, the resilient modulus values of PMA mixtures fluctuated around in small amounts. It appeared to imply that an optimum SBS content existed within the 3.0% to 6.0% range which would make the HMA stiffest at the high testing temperature. These observations were analogous with the results reported by many other research studies (Collins et al. 1991; Shih 1996; Chen et al. 2002, 2003) on polymer-modified binders and PMA mixtures. The analysis on resilient modulus results based on this study indicated that when SBS polymer is used in the HMA, although increasing the SBS polymer content will always improve pavement low temperature performance, limiting the concentration within an optimal range is especially important at high service temperatures.

Secondly, the SBS polymer helped the HMA obtain an upgraded creep performance. The PMA mixtures were more compliant than the control mixes with unmodified asphalt binders at the low temperature level (-10°C). On the other hand, the PMA mixtures became less compliant than the control mixes at the high testing temperature (40°C). At a specific temperature level, a higher SBS polymer concentration generally resulted in higher creep compliance values. At some mid-range temperature levels, the PMA mixtures showed similar creep property to the control mixes. These effects should lead to improved resistance to rutting and thermal cracking of HMA mixtures, and provided a good verification to similar findings drawn by the past research studies (Lalwani et al. 1982; Carpenter et al. 1987; Pradhan 1993). Thirdly, the SBS polymer modifier improved the asphalt mixture fracture properties. The indirect tensile strength test showed that the SBS polymer did not make significant change of HMA tensile strength as Jones et al. (1998)

observed at low temperature levels (around 0°C). However, the SBS polymer generally increased the fracture energy and the creep strain energy which are indicators of mixtures' resistance to fatigue cracking. At low temperatures (-10°C and 5°C), the failure strain of PMA mixtures tended to increase with an increase of SBS polymer content. These performances provided further justification to the benefits of using polymer-modified binder documented by other researchers in the past (Kennedy et al. 1992; King et al. 1993).

Comparison between the two different types of aggregate showed that the limestone mixtures were less stiff than the granite mixtures for all specimens tested in this study. The difference of resilient modulus values between the two types of aggregate was more noticeable at low temperature levels (-10°C and 5°C). In addition, the limestone mixtures were more compliant than granite mixtures at low temperatures. As the temperature increased, the limestone mixtures showed a similar creep property as the granite mixtures at 25°C, and then turned to be less compliant than the granite at high temperature (40°C). These characteristics exhibited by limestone mixtures are advantageous to pavement structures in improving the performance of thermal cracking at low service temperature and the rutting resistance at high service temperatures.

CHAPTER 6

SUMMARY AND CONCLUSIONS

6.1 Summary

The primary objectives of this study were to evaluate engineering properties of Florida HMA mixtures by changing the coarse aggregate gradation limits or SBS polymer-modified binder percentage. The specific goals of the study were to evaluate the coarse aggregate gradation effect by adjusting the coarse part of the mix designs and to evaluate the styrene-butadiene-styrene (SBS) polymer-modified asphalt binder effect utilizing the fracture mechanics tests in indirect diametral tension (IDT) testing mode. To achieve the objectives and goals, a complete dynamic testing system was established to perform the temperature controlled dynamic tests. A laboratory experimental program was developed to evaluate two standard control mixes including four modified mixes with coarse aggregate gradation adjustments and six modified mixes with SBS polymer-modified binder.

The two control mix designs included one granite material (F2C) and one limestone material (F4C). The coarse part of the gradation was adjusted to evaluate the effect of gradation coarse side limits specified in the Superpave mix design criteria. The two control mixtures were further modified by using SBS polymer-modified binder at different concentrations instead of the base asphalt to study the polymer binder effect on fracture mechanics properties of the mixtures.

The sweep of IDT tests included the resilient modulus test, the creep compliance test, and the tensile strength test to characterize the fracture mechanics properties of the asphalt mixtures. The tests were conducted at four temperature levels (-10, 5, 25, and 40°C) covering a typical range of asphalt concrete pavement service temperatures. The creep compliance master curves and the fracture mechanics parameters were analyzed using the fracture energy model developed by Roque et al. (2004). The analysis indicated that the modification of coarse part of the gradation of the mix designs did not influence the fracture properties noticeably. However, the increasing amounts of SBS polymer modifier improved the creep parameters as well as the stiffness characteristics at both low and high temperatures.

6.2 Findings and Conclusions

Based on the test results and analyses of this study, the findings and conclusions may be drawn for the effects of gradation, SBS polymer modifier, and aggregate type as follows:

6.2.1 Gradation Effect

1. The increase in percent of ½ in. coarse aggregate from 5% to 15% had minimal or negligible influence on the resilient modulus values of the mixtures and did not make a significant difference on the creep compliance properties for the tested HMA mixtures.
2. At low test temperatures (-10°C and 5°C), the tensile strength values of mixtures with modified gradations were less than that of control level mixtures, which indicated that increasing the amount of coarse aggregate in the standard control mixture had an adverse effect on the tensile strength property of the HMA at low temperatures. At mid-to-high test temperatures, the differences were negligible.
3. The fracture energy and dissipated creep strain energy values of modified gradations were slightly less than those of the control mixes, which meant that the mixtures with modified gradations would probably have less resistance to fatigue cracking than the control mixtures.

Based on the above findings, it appeared that the aggregate gradation percentage of maximum nominal size should not exceed 10% to 20% range since mixtures with modified gradations showed similar or slightly downgraded fracture mechanics characteristics.

6.2.2 SBS Polymer Modifier Effect

The test results showed that the SBS polymer modifier would improve the HMA properties in the following aspects:

1. The SBS polymer modifier made the HMA mixture softer at mid-to-low test temperatures and maintained the stiffness level at high temperatures, which are favorable attributes for the improvement of HMA performance in terms of low temperature thermal cracking and high temperature rutting.

2. The creep compliance test results showed that the SBS polymer modifier made the HMA mixtures more ductile at low temperatures which would be beneficial for the reduction of thermal cracking. At high temperatures, the PMA mixtures were stiffer and thus more resistant to rutting.
3. The SBS polymer did not critically affect the HMA tensile strength. However, it tended to increase the fracture energy limit, and hence, would improve the fatigue cracking performance of HMA mixtures.
4. The failure strain of PMA mixtures tended to increase with an increase of SBS polymer content at low testing temperatures (-10°C and 5°C), which is a desired attribute to improve the low temperature cracking of HMA pavement.

These findings are in agreement with the theoretical suppositions and other practical studies. Furthermore, the effect of SBS concentration for PMA mixtures appears to be related with the findings for SBS modified asphalt binders reported by other researchers. An optimum SBS content may exist between 3.0% and 6.0% range depending on the actual conditions of mixture production. Excessive amount of polymer content might improve the stiffness, creep, and failure strain behavior at low temperatures; however, its effect on the PMA resilient modulus property at high temperatures is not always favorable, which was probably due to a combined performance of mixing and distribution of SBS polymer modifier, base asphalt binder, and aggregate.

6.2.3 Effect of Aggregate Type

The limestone mixtures were less stiff than the granite mixtures, especially in low temperatures. In addition, the limestone mixtures showed favorable behavior in creep performance compared with the granite materials at all testing temperatures. These properties implied that limestone materials are much more ductile than granite under low service temperature conditions and hence presents an advantage for the cracking performance of HMA. At high temperatures, limestone materials have the potential to increase rutting resistance while maintaining the stiffness of pavement structures. It should be noted that these findings were observed in the laboratory for the two specific types of aggregate commonly used in Florida.

6.3 Recommendations

Based on the conclusions and limitations of this research study, the recommendations are made as follows:

1. The effect of aggregate gradation should be further evaluated by studying more commonly used HMA mixtures. The dynamic complex modulus of the HMA mixtures may also be adopted as an additional indicator for evaluation. The gradation adjustment for fine aggregate could also be taken into consideration with a desire to reduce the mix design cost while maintaining the quality of HMA mechanical properties.

2. A broad range of mixtures could be tested to evaluate the effect of SBS polymer modifier and to obtain a more confident range of optimal concentration. These optimal concentrations should be determined to be worth cost based on increased performance.

3. The relationship between fracture energy and temperature should be further evaluated by studying the engineering properties at wider range of temperature levels.

APPENDIX A LABORATORY ANALYSIS REPORTS

Table A-1: Lab analysis report for 0.0% polymer base asphalt (Graded as PG67-22)

Report Date:	10/1/08	Bituminous Tech. Lab No:	374208
Terminal:	Mariani Asphalt Co.	Address:	500 North 19 th St. Tampa, FL 33605
Sample:	0.0% Polymer	Date Tested:	9/10/08 – 9/11/08
Test	Test Method	Specification	Test Results
Original Binder			
Absolute Viscosity, Poise	T202		3290 Poise
Solubility, % soluble	T44	99.0% minimum	99.98%
Spot Test		Negative	Negative
Flash Point, °C	T48	230°C minimum	316°C+
Smoke Point, °C			260°C
Softening Point, °F			125°F
Rotational Viscosity, Pa.s, @135°C	T316	3.0 maximum	0.5 Pa.s
Dynamic Shear, kPa (G*/sinδ, 10 rad/sec)	T315	1.0 minimum at 64°C 1.0 minimum at 67°C 1.0 minimum at 76°C	1.97 kPa 1.32 kPa 0.9617 kPa
RTFOT Residue			
Mass Change, %	T240	1.0 maximum	+0.028%
Dynamic Shear, kPa (G*/sinδ, 10 rad/sec)	T315	2.2 minimum at 64°C 2.2 minimum at 67°C 2.2 minimum at 76°C	3.42 kPa 2.64 kPa 1.659 kPa
R28, PAV @100°C Residue			
Dynamic Shear, kPa (G*/sinδ, 10 rad/sec)	T315	5000 maximum at 25°C 5000 maximum at 22°C	4070 kPa 5840 kPa
Creep Stiffness, S, @60 sec.	T314	300 maximum at -12°C 300 maximum at -18°C	213 479
Creep Stiffness, m-value, @60 sec.	T314	0.3 minimum at -12°C 0.3 minimum at -18°C	0.321 0.248

Table A-2: Lab analysis report for 3.0% polymer asphalt (Graded as PG76-22)

Report Date:	10/1/08	Bituminous Tech. Lab No:	374108
Terminal:	Mariani Asphalt Co.	Address:	500 North 19 th St. Tampa, FL 33605
Sample:	3.0% Polymer	Date Tested:	9/10/08 – 9/11/08
Test	Test Method	Specification	Test Results
Original Binder			
Absolute Viscosity, Poise	T202		19583 Poise
Solubility, % soluble	T44	99.0% minimum	99.83%
Spot Test		Negative	Negative
Flash Point, °C	T48	230°C minimum	316°C+
Smoke Point, °C			260°C
Softening Point, °F			145°F
Rotational Viscosity, Pa.s, @135°C	T316	3.0 maximum	1.57 Pa.s
Dynamic Shear, kPa (G*/sinδ, 10 rad/sec)	T315	1.0 minimum at 76°C 1.0 minimum at 82°C	1.359 kPa 0.9178 kPa
RTFOT Residue			
Mass Change, %	T240	1.0 maximum	-0.026%
Dynamic Shear, kPa (G*/sinδ, 10 rad/sec)	T315	2.2 minimum at 76°C 2.2 minimum at 82°C	2.37 kPa 1.38 kPa
R28, PAV @100°C Residue			
Dynamic Shear, kPa (G*/sinδ, 10 rad/sec)	T315	5000 maximum at 31°C 5000 maximum at 28°C 5000 maximum at 25°C 5000 maximum at 22°C 5000 maximum at 19°C	1880 kPa 2330 kPa 3450 kPa 4870 kPa 6100 kPa
Creep Stiffness, S, @60 sec.	T314	300 maximum at -12°C 300 maximum at -18°C	176 371
Creep Stiffness, m-value, @60 sec.	T314	0.3 minimum at -12°C 0.3 minimum at -18°C	0.329 0.266

Table A-3: Lab analysis report for 4.5% polymer asphalt (Graded as PG82-22)

Report Date:	10/1/08	Bituminous Tech. Lab No:	374008
Terminal:	Mariani Asphalt Co.	Address:	500 North 19 th St. Tampa, FL 33605
Sample:	4.5% Polymer	Date Tested:	9/16/08 – 9/19/08
Test	Test Method	Specification	Test Results
Original Binder			
Absolute Viscosity, Poise	T202		Too viscous
Solubility, % soluble	T44	99.0% minimum	99.49%
Spot Test		Negative	Negative
Flash Point, °C	T48	230°C minimum	316°C+
Smoke Point, °C			288°C
Softening Point, °F			197.5°F
Rotational Viscosity, Pa.s, @135°C	T316	3.0 maximum	7.40 Pa.s
Dynamic Shear, kPa (G*/sinδ, 10 rad/sec)	T315	1.0 minimum at 76°C 1.0 minimum at 82°C 1.0 minimum at 88°C 1.0 minimum at 94°C 1.0 minimum at 100°C	3.47 kPa 2.40 kPa 1.70 kPa 1.26 kPa 0.3799 kPa
RTFOT Residue			
Mass Change, %	T240	1.0 maximum	-0.030%
Dynamic Shear, kPa (G*/sinδ, 10 rad/sec)	T315	2.2 minimum at 76°C 2.2 minimum at 82°C 2.2 minimum at 88°C	4.45 kPa 2.82 kPa 1.78 kPa
R28, PAV @100°C Residue			
Dynamic Shear, kPa (G*/sinδ, 10 rad/sec)	T315	5000 maximum at 31°C 5000 maximum at 25°C 5000 maximum at 19°C 5000 maximum at 16°C 5000 maximum at 13°C	969 kPa 1860 kPa 3530 kPa 4780 kPa NA
Creep Stiffness, S, @60 sec.	T314	300 maximum at -12°C 300 maximum at -18°C	87.7 368
Creep Stiffness, m-value, @60 sec.	T314	0.3 minimum at -12°C 0.3 minimum at -18°C	0.371 0.262

Table A-4: Lab analysis report for 6.0% polymer asphalt (Graded as PG82-28)

Report Date:	10/1/08	Bituminous Tech. Lab No:	373908
Terminal:	Mariani Asphalt Co.	Address:	500 North 19 th St. Tampa, FL 33605
Sample:	6.0% Polymer	Date Tested:	9/16/08 – 9/19/08
Test	Test Method	Specification	Test Results
Original Binder			
Absolute Viscosity, Poise	T202		Too viscous
Solubility, % soluble	T44	99.0% minimum	99.89%
Spot Test		Negative	Negative
Flash Point, °C	T48	230°C minimum	316°C+
Smoke Point, °C			280°C
Softening Point, °F			204°F
Rotational Viscosity, Pa.s, @135°C	T316	3.0 maximum	5.75 Pa.s
Dynamic Shear, kPa (G*/sinδ, 10 rad/sec)	T315	1.0 minimum at 76°C 1.0 minimum at 82°C 1.0 minimum at 88°C 1.0 minimum at 94°C 1.0 minimum at 100°C	3.32 kPa 2.17 kPa 1.47 kPa 1.05 kPa 0.8748 kPa
RTFOT Residue			
Mass Change, %	T240	1.0 maximum	-0.030%
Dynamic Shear, kPa (G*/sinδ, 10 rad/sec)	T315	2.2 minimum at 76°C 2.2 minimum at 82°C 2.2 minimum at 88°C 2.2 minimum at 94°C	6.94 kPa 4.52 kPa 2.95 kPa 1.91 kPa
R28, PAV @100°C Residue			
Dynamic Shear, kPa (G*/sinδ, 10 rad/sec)	T315	5000 maximum at 31°C 5000 maximum at 25°C 5000 maximum at 19°C 5000 maximum at 16°C	947 kPa 1960 kPa 3840 kPa 5340 kPa
Creep Stiffness, S, @60 sec.	T314	300 maximum at -12°C 300 maximum at -18°C 300 maximum at -24°C	105 231 380
Creep Stiffness, m-value, @60 sec.	T314	0.3 minimum at -12°C 0.3 minimum at -18°C 0.3 minimum at -24°C	0.369 0.314 0.250

Table A-5: Gradations for F2C and its adjustments

Sieve	Size (um)	F2C	F2G1	Adjustment	F2G2	Adjustment
1	25000					
3/4	19000	100	100	0	100	0
1/2	12500	95	90	-5	80	-15
3/8	9500	84	78	-6	71	-13
4	4750	52	52	0	52	0
8	2360	32	32	0	32	0
16	1180	21	21	0	21	0
30	600	15	15	0	15	0
50	300	9	9	0	9	0
100	150	6	6	0	6	0
200	75	5.2	5.2	0	5.2	0

Table A-6: Gradations for F4C and its adjustments

Sieve	Size (um)	F4C	F4G1	Adjustment	F4G2	Adjustment
1	25000					
3/4	19000	100	100	0	100	0
1/2	12500	94	89	-5	79	-15
3/8	9500	89	80	-9	71	-18
4	4750	56	56	0	56	0
8	2360	30	30	0	30	0
16	1180	20	20	0	20	0
30	600	15	15	0	15	0
50	300	10	10	0	10	0
100	150	6	6	0	6	0
200	75	3.6	3.6	0	3.6	0

APPENDIX B CREEP COMPLIANCE TEST RESULTS

Table B-1: Creep compliance test results at -10°C (1/GPa)

Mixtures for Gradation Effects						
	Control		G1		G2	
Time (sec.)	F2	F4	F2	F4	F2	F4
1	0.044	0.055	0.040	0.058	0.048	0.058
2	0.048	0.062	0.045	0.062	0.053	0.062
5	0.055	0.069	0.049	0.068	0.059	0.068
10	0.061	0.076	0.055	0.073	0.064	0.073
20	0.067	0.081	0.061	0.078	0.071	0.079
50	0.078	0.099	0.069	0.086	0.085	0.093
100	0.091	0.111	0.079	0.091	0.096	0.098
Pr	0.382	0.347	0.299	0.322	0.296	0.352
Mixtures with SBS Polymer-modified Binder						
	P1 (3.0%)		P2 (4.5%)		P3 (6.0%)	
Time (sec.)	F2	F4	F2	F4	F2	F4
1	0.044	0.069	0.076	0.077	0.054	0.091
2	0.049	0.076	0.087	0.084	0.060	0.101
5	0.057	0.087	0.104	0.093	0.069	0.116
10	0.064	0.098	0.116	0.104	0.078	0.128
20	0.072	0.109	0.123	0.118	0.088	0.145
50	0.091	0.126	0.156	0.134	0.109	0.178
100	0.105	0.149	0.184	0.151	0.130	0.196
Pr	0.387	0.378	0.380	0.377	0.356	0.296

Table B-2: Creep compliance test results at -10°C (1/psi)

Mixtures for Gradation Effects						
	Control		G1		G2	
Time (sec.)	F2	F4	F2	F4	F2	F4
1	3.06E-07	3.81E-07	2.77E-07	3.97E-07	3.28E-07	4.01E-07
2	3.32E-07	4.28E-07	3.08E-07	4.30E-07	3.63E-07	4.27E-07
5	3.78E-07	4.78E-07	3.41E-07	4.67E-07	4.07E-07	4.67E-07
10	4.18E-07	5.23E-07	3.76E-07	5.01E-07	4.38E-07	5.05E-07
20	4.63E-07	5.60E-07	4.18E-07	5.38E-07	4.92E-07	5.43E-07
50	5.41E-07	6.81E-07	4.78E-07	5.90E-07	5.85E-07	6.42E-07
100	6.30E-07	7.62E-07	5.45E-07	6.27E-07	6.61E-07	6.76E-07
Pr	0.382	0.347	0.299	0.322	0.296	0.352
Mixtures with SBS Polymer-modified Binder						
	P1 (3.0%)		P2 (4.5%)		P3 (6.0%)	
Time (sec.)	F2	F4	F2	F4	F2	F4
1	3.01E-07	4.36E-07	3.47E-07	5.08E-07	3.81E-07	6.09E-07
2	3.38E-07	4.78E-07	3.75E-07	5.51E-07	4.30E-07	6.58E-07
5	3.91E-07	5.45E-07	4.27E-07	6.08E-07	5.02E-07	7.42E-07
10	4.39E-07	6.04E-07	4.59E-07	6.69E-07	5.67E-07	7.91E-07
20	4.98E-07	6.85E-07	5.09E-07	7.44E-07	6.37E-07	8.47E-07
50	6.24E-07	7.59E-07	6.13E-07	8.45E-07	8.07E-07	9.05E-07
100	7.27E-07	8.63E-07	7.12E-07	9.39E-07	9.70E-07	9.58E-07
Pr	0.387	0.378	0.380	0.377	0.356	0.296

Note: 1/GPa = 6.89×10^{-6} /psi 1/psi = 0.145×10^6 /GPa

Table B-3: Creep compliance test results at 5°C (1/GPa)

Mixtures for Gradation Effects						
Time (sec.)	Control		G1		G2	
	F2	F4	F2	F4	F2	F4
1	0.093	0.120	0.099	0.117	0.125	0.131
2	0.117	0.148	0.127	0.138	0.152	0.163
5	0.158	0.198	0.172	0.183	0.200	0.216
10	0.198	0.246	0.221	0.230	0.249	0.266
20	0.268	0.313	0.297	0.295	0.308	0.322
50	0.377	0.449	0.421	0.402	0.430	0.437
100	0.516	0.598	0.557	0.529	0.555	0.540
Pr	0.317	0.334	0.371	0.343	0.357	0.416
Mixtures with SBS Polymer-modified Binder						
Time (sec.)	P1 (3.0%)		P2 (4.5%)		P3 (6.0%)	
	F2	F4	F2	F4	F2	F4
1	0.092	0.126	0.077	0.140	0.116	0.182
2	0.109	0.145	0.095	0.164	0.140	0.223
5	0.138	0.185	0.121	0.198	0.187	0.288
10	0.171	0.220	0.156	0.246	0.227	0.344
20	0.209	0.268	0.187	0.304	0.297	0.407
50	0.292	0.364	0.269	0.424	0.367	0.535
100	0.388	0.476	0.335	0.512	0.440	0.658
Pr	0.428	0.452	0.489	0.303	0.299	0.433

Table B-4: Creep compliance test results at 5°C (1/psi)

Mixtures for Gradation Effects						
Time (sec.)	Control		G1		G2	
	F2	F4	F2	F4	F2	F4
1	6.44E-07	8.29E-07	6.85E-07	8.07E-07	8.60E-07	9.01E-07
2	8.09E-07	1.02E-06	8.74E-07	9.48E-07	1.05E-06	1.12E-06
5	1.09E-06	1.36E-06	1.18E-06	1.26E-06	1.38E-06	1.49E-06
10	1.36E-06	1.69E-06	1.52E-06	1.59E-06	1.72E-06	1.83E-06
20	1.85E-06	2.16E-06	2.04E-06	2.04E-06	2.13E-06	2.22E-06
50	2.60E-06	3.09E-06	2.90E-06	2.77E-06	2.96E-06	3.01E-06
100	3.55E-06	4.12E-06	3.84E-06	3.64E-06	3.83E-06	3.73E-06
Pr	0.317	0.334	0.371	0.343	0.357	0.416
Mixtures with SBS Polymer-modified Binder						
Time (sec.)	P1 (3.0%)		P2 (4.5%)		P3 (6.0%)	
	F2	F4	F2	F4	F2	F4
1	6.33E-07	8.70E-07	5.28E-07	9.62E-07	7.99E-07	1.25E-06
2	7.52E-07	9.97E-07	6.52E-07	1.13E-06	9.68E-07	1.54E-06
5	9.51E-07	1.27E-06	8.31E-07	1.37E-06	1.29E-06	1.98E-06
10	1.18E-06	1.51E-06	1.08E-06	1.70E-06	1.57E-06	2.37E-06
20	1.44E-06	1.85E-06	1.29E-06	2.09E-06	2.05E-06	2.80E-06
50	2.01E-06	2.51E-06	1.85E-06	2.92E-06	2.53E-06	3.69E-06
100	2.67E-06	3.28E-06	2.31E-06	3.53E-06	3.04E-06	4.54E-06
Pr	0.428	0.452	0.489	0.303	0.299	0.433

Table B-5: Creep compliance test results at 25°C (1/GPa)

Mixtures for Gradation Effects						
	Control		G1		G2	
Time (sec.)	F2	F4	F2	F4	F2	F4
1	0.692	0.699	0.744	0.839	0.794	1.108
2	0.899	0.962	1.045	1.146	1.075	1.547
5	1.420	1.400	1.547	1.662	1.546	2.285
10	1.954	1.819	2.107	2.257	2.192	3.023
20	2.535	2.420	2.854	2.997	2.905	3.885
50	3.626	3.259	4.159	4.359	4.206	5.282
100	4.733	4.028	5.604	5.778	5.509	6.534
Pr	0.338	0.358	0.269	0.265	0.304	0.357
Mixtures with SBS Polymer-modified Binder						
	P1 (3.0%)		P2 (4.5%)		P3 (6.0%)	
Time (sec.)	F2	F4	F2	F4	F2	F4
1	0.488	0.542	0.709	0.824	1.126	0.881
2	0.669	0.734	1.006	1.077	1.460	1.117
5	1.054	1.084	1.540	1.542	1.932	1.589
10	1.463	1.460	2.066	1.968	2.413	2.020
20	1.916	2.056	2.724	2.524	3.043	2.575
50	2.754	2.854	3.780	3.426	4.043	3.532
100	3.625	3.679	4.725	4.278	4.938	4.305
Pr	0.352	0.352	0.374	0.246	0.305	0.372

Table B-6: Creep compliance test results at 25°C (1/psi)

Mixtures for Gradation Effects						
	Control		G1		G2	
Time (sec.)	F2	F4	F2	F4	F2	F4
1	4.77E-06	4.82E-06	5.13E-06	5.78E-06	5.47E-06	7.64E-06
2	6.20E-06	6.63E-06	7.21E-06	7.90E-06	7.41E-06	1.07E-05
5	9.79E-06	9.65E-06	1.07E-05	1.15E-05	1.07E-05	1.58E-05
10	1.35E-05	1.25E-05	1.45E-05	1.56E-05	1.51E-05	2.08E-05
20	1.75E-05	1.67E-05	1.97E-05	2.07E-05	2.00E-05	2.68E-05
50	2.50E-05	2.25E-05	2.87E-05	3.01E-05	2.90E-05	3.64E-05
100	3.26E-05	2.78E-05	3.86E-05	3.98E-05	3.80E-05	4.51E-05
Pr	0.338	0.358	0.269	0.265	0.304	0.357
Mixtures with SBS Polymer-modified Binder						
	P1 (3.0%)		P2 (4.5%)		P3 (6.0%)	
Time (sec.)	F2	F4	F2	F4	F2	F4
1	3.37E-06	3.74E-06	4.89E-06	5.68E-06	7.76E-06	6.07E-06
2	4.61E-06	5.06E-06	6.94E-06	7.43E-06	1.01E-05	7.70E-06
5	7.27E-06	7.47E-06	1.06E-05	1.06E-05	1.33E-05	1.10E-05
10	1.01E-05	1.01E-05	1.42E-05	1.36E-05	1.66E-05	1.39E-05
20	1.32E-05	1.42E-05	1.88E-05	1.74E-05	2.10E-05	1.78E-05
50	1.90E-05	1.97E-05	2.61E-05	2.36E-05	2.79E-05	2.44E-05
100	3.625	3.679	4.725	4.278	4.938	4.305
Pr	0.352	0.352	0.374	0.246	0.305	0.372

Table B-7: Creep compliance test results at 40°C (1/GPa)

Mixtures for Gradation Effects						
	Control		G1		G2	
Time (sec.)	F2	F4	F2	F4	F2	F4
1	3.994	2.266	1.734	1.670	1.976	1.616
2	5.019	2.727	2.242	2.196	2.565	2.195
5	6.800	3.588	3.294	3.400	3.597	2.965
10	8.073	4.468	4.178	4.377	4.585	3.696
20	9.383	5.543	5.055	5.374	5.812	4.706
50	11.049	7.884	7.134	7.139	8.153	6.305
100	12.721	9.516	8.817	8.764	10.921	7.950
Pr	0.291	0.325	0.268	0.312	0.298	0.306
Mixtures with SBS Polymer-modified Binder						
	P1 (3.0%)		P2 (4.5%)		P3 (6.0%)	
Time (sec.)	F2	F4	F2	F4	F2	F4
1	1.357	1.562	1.931	2.080	3.628	1.899
2	1.793	1.840	2.476	2.655	4.147	2.268
5	2.671	2.370	3.323	3.495	4.980	2.972
10	3.457	2.783	4.142	4.897	5.742	3.506
20	4.490	3.299	4.910	6.384	6.669	4.034
50	6.033	4.175	6.089	8.189	8.137	5.179
100	8.108	5.423	7.359	9.983	9.533	6.128
Pr	0.373	0.396	0.383	0.272	0.291	0.418

Table B-8: Creep compliance test results at 40°C (1/psi)

Mixtures for Gradation Effects						
	Control		G1		G2	
Time (sec.)	F2	F4	F2	F4	F2	F4
1	2.75E-05	1.56E-05	1.20E-05	1.15E-05	1.36E-05	1.11E-05
2	3.46E-05	1.88E-05	1.55E-05	1.51E-05	1.77E-05	1.51E-05
5	4.69E-05	2.47E-05	2.27E-05	2.34E-05	2.48E-05	2.04E-05
10	5.57E-05	3.08E-05	2.88E-05	3.02E-05	3.16E-05	2.55E-05
20	6.47E-05	3.82E-05	3.48E-05	3.71E-05	4.01E-05	3.24E-05
50	7.62E-05	5.44E-05	4.92E-05	4.92E-05	5.62E-05	4.35E-05
100	8.77E-05	6.56E-05	6.08E-05	6.04E-05	7.53E-05	5.48E-05
Pr	0.291	0.325	0.268	0.312	0.298	0.306
Mixtures with SBS Polymer-modified Binder						
	P1 (3.0%)		P2 (4.5%)		P3 (6.0%)	
Time (sec.)	F2	F4	F2	F4	F2	F4
1	9.36E-06	1.08E-05	1.33E-05	1.43E-05	2.50E-05	1.31E-05
2	1.24E-05	1.27E-05	1.71E-05	1.83E-05	2.86E-05	1.56E-05
5	1.84E-05	1.63E-05	2.29E-05	2.41E-05	3.43E-05	2.05E-05
10	2.38E-05	1.92E-05	2.86E-05	3.38E-05	3.96E-05	2.42E-05
20	3.10E-05	2.27E-05	3.39E-05	4.40E-05	4.60E-05	2.78E-05
50	4.16E-05	2.88E-05	4.20E-05	5.65E-05	5.61E-05	3.57E-05
100	5.59E-05	3.74E-05	5.07E-05	6.88E-05	6.57E-05	4.22E-05
Pr	0.373	0.396	0.383	0.272	0.291	0.418

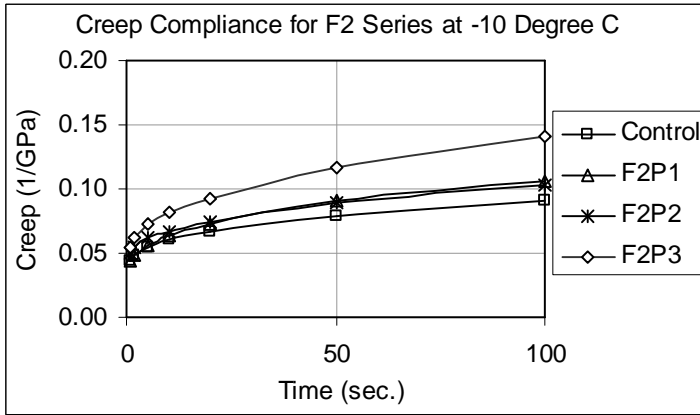


Figure B-1: Creep compliance of F2 control and all polymer-modified levels at -10°C.

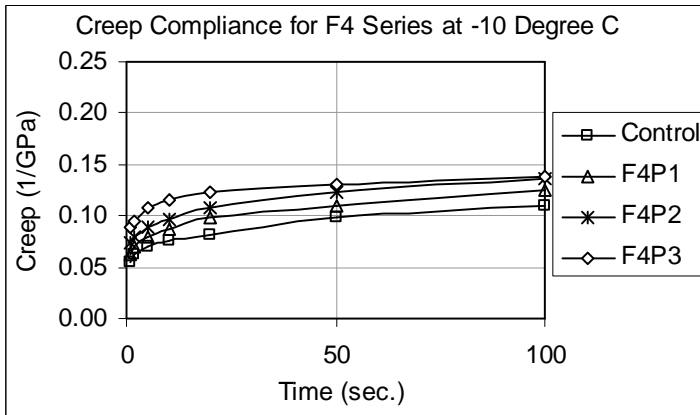


Figure B-2: Creep compliance of F4 control and all polymer-modified levels at -10°C.

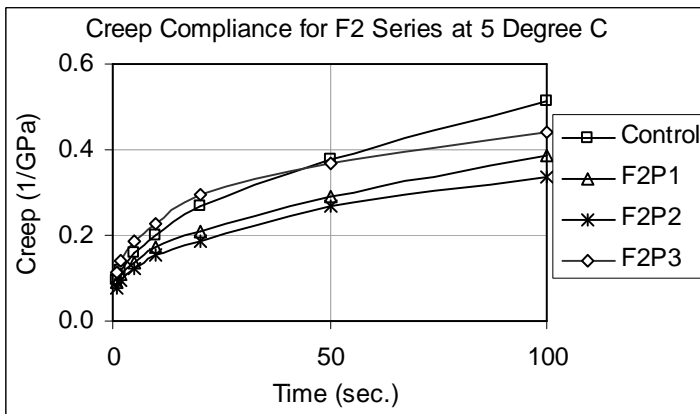


Figure B-3: Creep compliance of F2 control and all polymer-modified levels at 5°C.

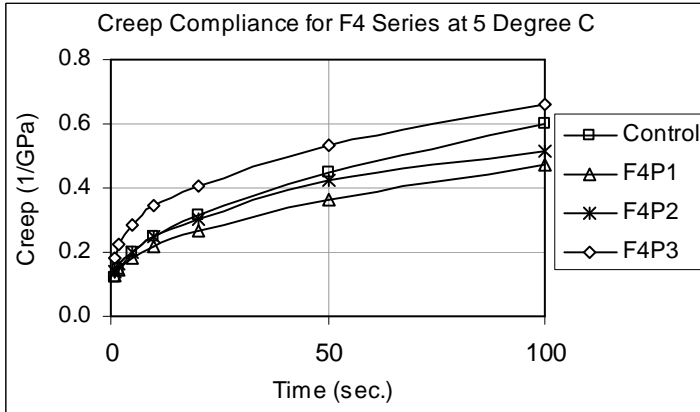


Figure B-4: Creep compliance of F4 control and all polymer-modified levels at 5°C.

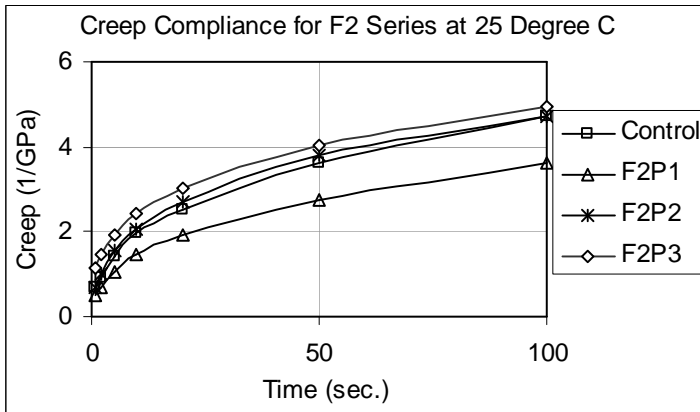


Figure B-5: Creep compliance of F2 control and all polymer-modified levels at 25°C.

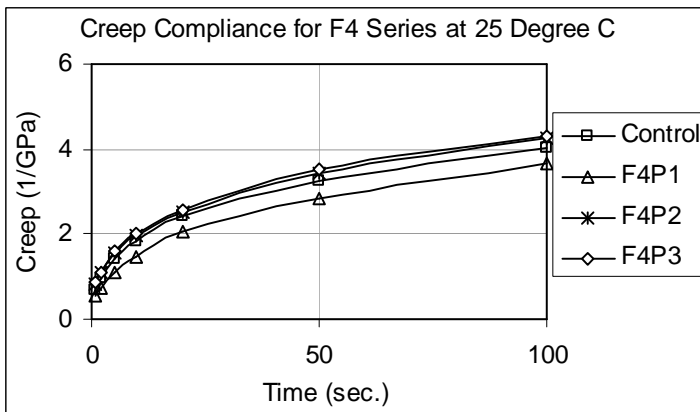


Figure B-6: Creep compliance of F4 control and all polymer-modified levels at 25°C.

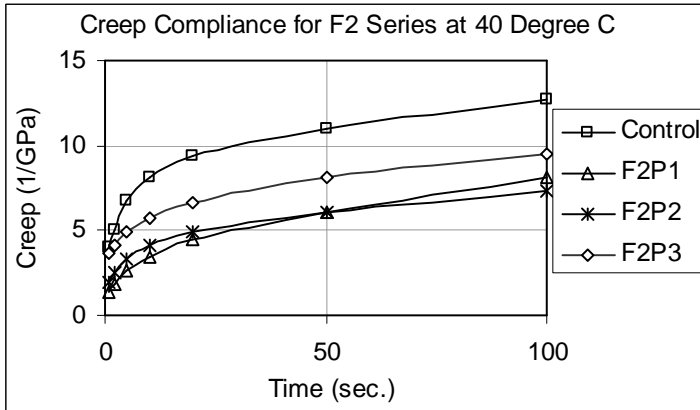


Figure B-7: Creep compliance of F2 control and all polymer-modified levels at 40°C.

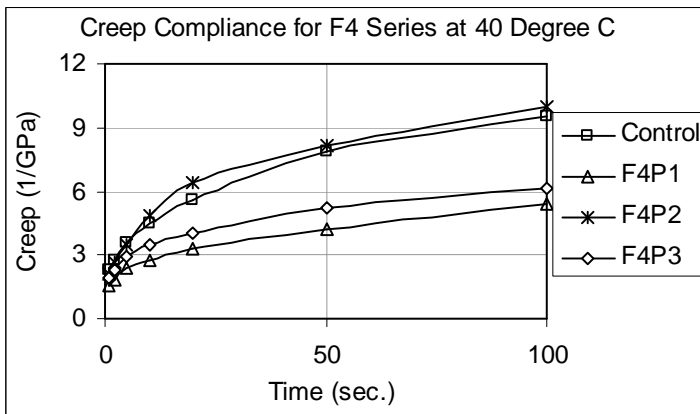


Figure B-8: Creep compliance of F4 control and all polymer-modified levels at 40°C.

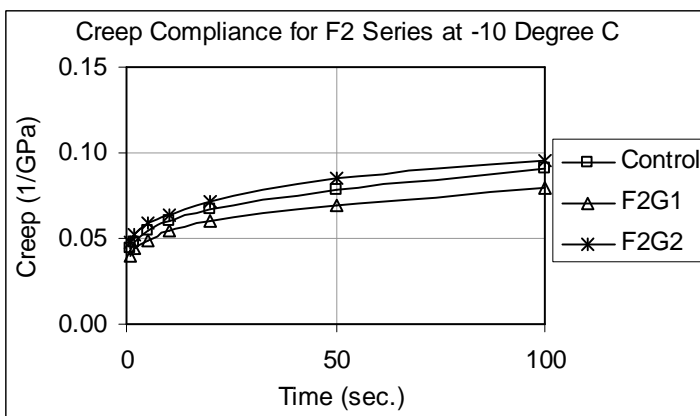


Figure B-9: Creep compliance of F2 control and modified gradation levels at -10°C.

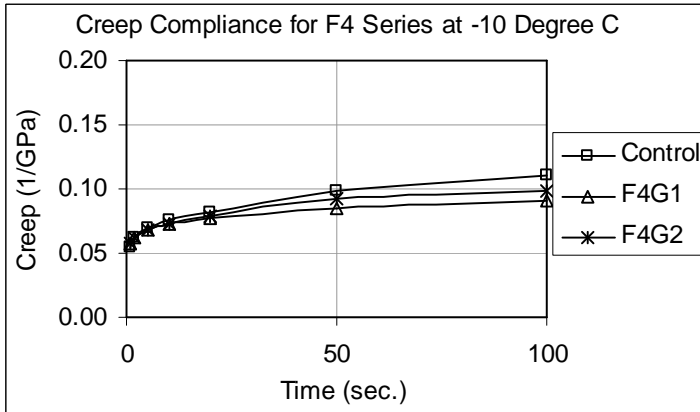


Figure B-10: Creep compliance of F4 control and modified gradation levels at -10°C.

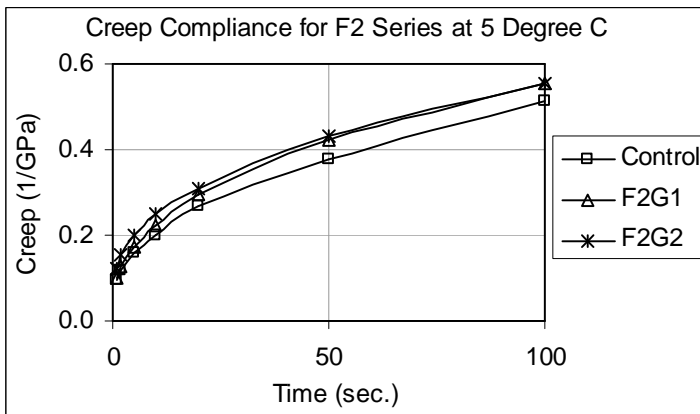


Figure B-11: Creep compliance of F2 control and modified gradation levels at 5°C.

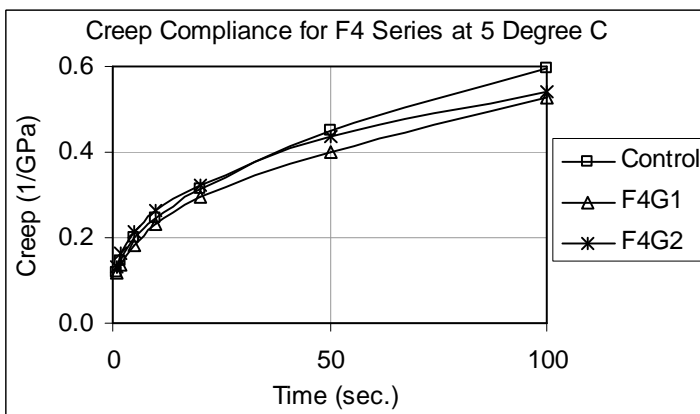


Figure B-12: Creep compliance of F4 control and modified gradation levels at 5°C.

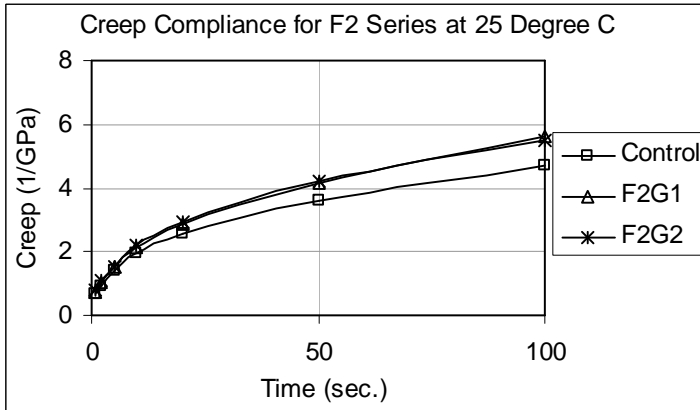


Figure B-13: Creep compliance of F2 control and modified gradation levels at 25°C.

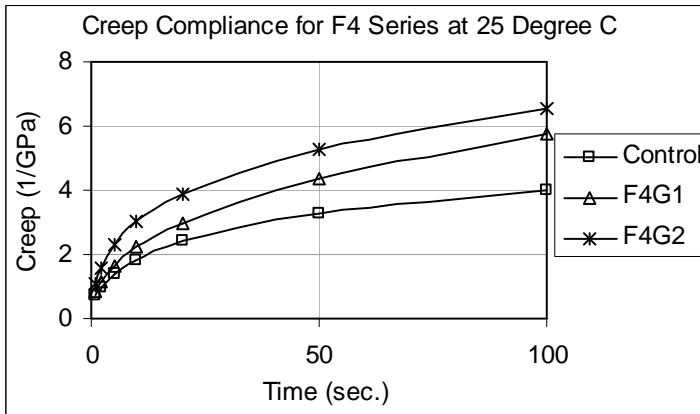


Figure B-14: Creep compliance of F4 control and modified gradation levels at 25°C.

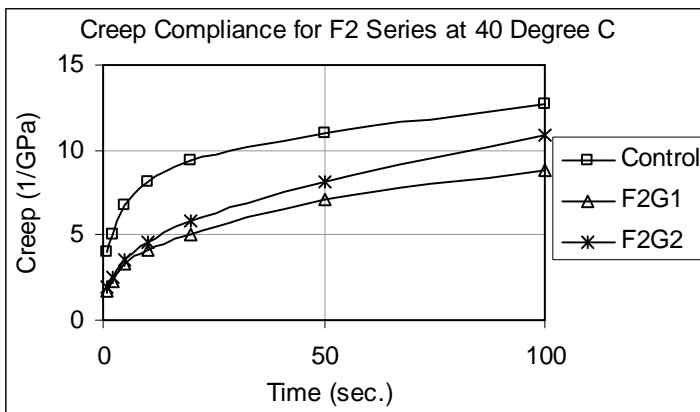


Figure B-15: Creep compliance of F2 control and modified gradation levels at 40°C.

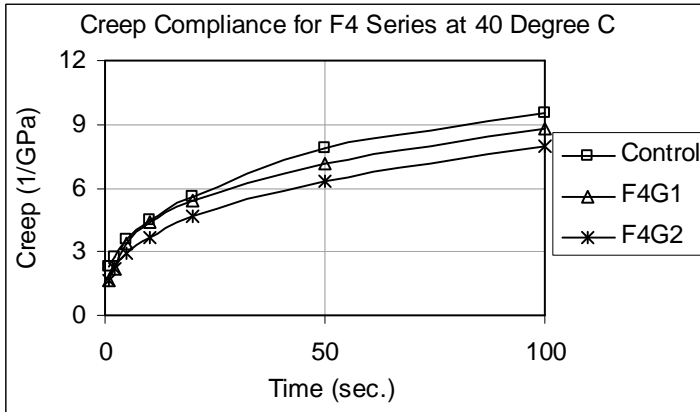


Figure B-16: Creep compliance of F4 control and modified gradation levels at 40°C.

REFERENCES

1. AASHTO, "Guide for Design of Pavement Structures," American Association of State Highway and Transportation Officials (AASHTO), Washington, D.C., 1993.
2. AASHTO TP 31, "Standard Test Method for Determining the Resilient Modulus of Bituminous Mixtures by Indirect Tension," American Association of State Highway and Transportation Officials (AASHTO), Washington, D.C., 1996.
3. Aglan, H.A., "Polymer Modifiers for Improved Performance of Asphalt," *Asphalt Science and Technology*, edited by Arthur Usmani, Marcel Dekker, Inc., New York, 1997, pp. 197-216.
4. American Society for Testing and Materials, *1994 Annual Book of ASTM Standards*, Vol. 04.04, Rubber, Natural and Synthetic-General Test Methods, 1994.
5. American Society for Testing and Materials, ASTM D 4123, "Standard Test Method for Indirect Tension Test for Resilient Modulus of Bituminous Mixture," ASTM International, West Conshohocken, PA, 1982.
6. Asphalt Institute and the Heritage Group, "The Bailey Method: Achieving Volumetrics and HMA Compactability," Asphalt Institute Educational Course and Seminar Materials, Lexington, KY, 2005.
7. Asphalt Institute, "Superpave Level I Mix Design," Asphalt Institute, Lexington, KY, Report No. SP-2, 1995.
8. Asphalt Institute, "Superpave Mix Design," Superpave Series No. 2 (SP-02), Asphalt Institute, Lexington, KY, 2001.
9. Bahia, H.U. and D.A. Anderson, "Strategic Highway Research Program Binder Rheological Parameters: Background and Comparison with Conventional Properties," *Transportation Research Record*, No. 1488, 1995, pp. 32-39.
10. Barksdale, R. D., J. Alba, N. P. Khosla, R. Kim, P. C. Lambe, and M. S. Rahman, "Laboratory Determination of Resilient Modulus for Flexible Pavement Design," NCHRP Program 1-28 Project, TRB, Washington, D.C., 1997.
11. Birgisson, B. and B. Ruth, "Development of Tentative Guidelines for the Selection of Aggregate Gradations for Hot-Mix Asphalt," American Society for Testing and Materials (ASTM), STP 1412, 2001.
12. Birgisson, B., R. Roque and G. Page, "Evaluation of Water Damage Using Hot Mix Asphalt Fracture Mechanics," *Journal of the Association of Asphalt Paving Technologists*, Vol. 72, 2003, pp. 424-462.

13. Birgisson, B., R. Roque, J. Kim, L.V. Pham, "The Use of Complex Modulus to Characterize the Performance of Asphalt Mixtures and Pavements in Florida", Final Report, BC-354-22, Florida Department of Transportation, Tallahassee, Florida, 2004.
14. Birgisson, B., R. Roque, G.C. Page, "Performance-Based Fracture Criterion for Evaluation of Moisture Susceptibility in Hot-Mix Asphalt," Transportation Research Record: Journal of the Transportation Research Board, No. 1891, TRB, National Research Council, Washington, D.C., 2004, pp. 55-61.
15. Brule, B., Y. Brion and A. Tanguy, "Paving Asphalt Polymer Blends: Relationships between Composition, Structure and Properties," Proceedings of the Association of Asphalt Paving Technologists, Vol. 57, 1988, pp. 41-64.
16. Buttlar, W. G. and R. Roque, "Development and Evaluation of the Strategic Highway Research Program Measurement and Analysis System for Indirect Tensile Testing at Low Temperatures," Transportation Research Record: Journal of the Transportation Research Board, No. 1454, Washington, D.C., 1994, pp. 163-171.
17. Button, J.W., "Summary of Asphalt Additive Performance at Selected Sites," Transportation Research Record, No. 1342, TRB, National Research Council, Washington, D.C., 1992, pp. 67-75.
18. Carpenter, S.H. and S. Shen, "Dissipated Energy Approach to Study Hot-Mix Asphalt Healing in Fatigue," Transportation Research Record: Journal of the Transportation Research Board, No. 1970, TRB, National Research Council, Washington, D.C., 2006, pp.178-185.
19. Carpenter, SH. and T. VanDam, "Laboratory Performance Comparisons of Polymer-Modified and Unmodified Asphalt Concrete Mixtures," Transportation Research Record No. 1115, TRB, National Research Council, Washington, D.C., 1987, pp. 62-74.
20. Chen, J. and C. Huang, "Fundamental Characterization of SBS-Modified Asphalt Mixed with Sulfur," Journal of Applied Polymer Science, Vol. 103, 2007, pp. 2817-2825.
21. Chen, J., M. Liao and C. Lin, "Determination of Polymer Content in Modified Bitumen," *Materials and Structures*, Vol. 36, 2003, pp. 594-598.
22. Chen, J., M. Liao and M. Shiah, "Asphalt Modified by Styrene-Butadiene-Styrene Triblock Copolymer: Morphology and Model," *Journal of Materials in Civil Engineering*, ASCE, May/June 2002, pp. 224-229.
23. Chowdhury, A., J. Grau, J. Button and D. Little, "Effect of Aggregate Gradation on Permanent Deformation of Superpave HMA," Proceedings of the 80th Annual Meeting

of Transportation Research Board, TRB, National Research Council, Washington, D.C., 2001.

24. Collins, J.H., M.G. Bouldin, R. Gellens and A. Berker, "Improved Performance of Paving Asphalts by Polymer Modifications," Proceedings of the Association of Asphalt Paving Technologists, Vol. 60, 1991, pp. 43-79.
25. Diani, E., M.D. Via, and M.G. Cavaliere, "Chemistry and Technology of SBS Modifier," *Asphalt Science and Technology*, edited by Arthur Usmani, Marcel Dekker, Inc., New York, 1997, pp. 279-295.
26. Drescher, A., D.E. Newcomb, and W. Zhang, "Interpretation of Indirect Tension Test Based on Viscoelasticity," Transportation Research Record, No. 1590, TRB, National Research Council, Washington, D.C., 1997, pp. 45-52.
27. Ekingen, E. R., "Determining Gradation and Creep Effects in Mixtures Using the Complex Modulus Test," Master's Thesis, Department of Civil Engineering, University of Florida, Gainesville, Florida, 2004.
28. Federal Highway Administration, "Background of Superpave Asphalt Mixture Design and Analysis," FHWA Report Number FHWA-SA-95-003, Washington, D.C., 1995.
29. Federal Highway Administration, "Superpave Asphalt Mixture Design: Illustrated Level I Lab Methods," FHWA Report Number FHWA-SA-95-004, Washington, D.C., 1995.
30. Foster, C.R., "Development of Marshall Procedures for Designing Asphalt Paving Mixtures," National Asphalt Pavement Association, NAPA IS84, Maryland, 1982.
31. Fuller, W.B. and S. Thompson, "The Laws of Proportioning Concrete," Journal of Transportation Division, ASCE, Vol. 59, 1907, pp. 67-143.
32. Goode, J.F., and L.A. Lufsey, "A New Graphical Chart for Evaluating Aggregate Gradations," Proceedings of the Association of Asphalt Paving Technologists, Volume 31, 1962, pp. 176-207.
33. Hines, M.L., "Asphalt Cement Performance Improved by Styrelf-Laboratory and Field Data," Koch Materials Company, 1993.
34. Hondoros, G., "Evaluation of Poisson's Ratio and the Modulus of Materials of a Low Tensile Resistance by the Brazilian (Indirect Tensile) Test with Particular Reference to Concrete," Australian Journal of Applied Science, Vol. 10, No. 3, 1959, pp. 243-268.
35. Huang, Y., *Pavement Analysis and Design*, Second Edition, "Appendix A: Theory of Viscoelasticity," Pearson Education, Inc., New Jersey, 2004.

36. Huber G.A. and T. Shuler, "Providing Sufficient Void Space for Asphalt Cement: Relationship of Mineral Aggregate Void and Aggregate Gradation," *Effects of Aggregates and Mineral Fillers on Asphalt Mixtures Performance*, American Society for Testing and Materials (ASTM), SPT 1147, Philadelphia, 1992.
37. Huffman, J.E., "The Use of Ground Vulcanized Rubber in Asphalt, Asphalt Pavement Construction: New Materials and Techniques," American Society for Testing and Materials (ASTM), SPT 724, Philadelphia, 1980, pp. 3-12.
38. Hveem, F.N., "Gradation of Mineral Aggregate for Dense-Graded Bituminous Mixtures," *Proceedings of the Association of Asphalt Paving Technologists*, Vol. 11, 1940, pp. 315-339.
39. Jones, S.D., K. Mahboub, R. Anderson and H. Bahia, "Applicability of Superpave to Modified Asphalts – A Mixture Study," *Transportation Research Record 1630*, TRB, National Research Council, Washington, D.C., 1998, pp. 42-50.
40. Kandhal, P. and R. Mallick, "Effect of Mix Gradation on Rutting Potential of Dense-Graded Asphalt Mixtures," *Transportation Research Record 1767*, TRB, National Research Council, Washington, D.C., 2001, pp. 146-151.
41. Kennedy, T. W., "Characterization of Asphalt Pavement Materials Using the Indirect Tensile Test," *Proceedings of the Association of Asphalt Paving Technologists*, Vol. 46, 1977, pp. 132-150.
42. Kennedy, T.W., H. Torshizi and D. Jones IV, "Mix Design Procedures and Considerations for Polymer-Modified Asphalt Compatibility and Stability," *Center for Transportation Research, Research Report 492-1F, Project 3-9-87/1-492*, The University of Texas at Austin, Austin, Texas, 1992.
43. Khattak, M.J. and G.Y. Baladi, "Engineering Properties of Polymer-Modified Asphalt Mixtures," *Transportation Research Record*, No. 1638, TRB, National Research Council, Washington, D.C., 1998, pp. 12-22.
44. Khattak, M.J. and G.Y. Baladi, "Fatigue and Permanent Deformation Models for Polymer-Modified Asphalt Mixtures," *Transportation Research Record*, No. 1767, TRB, National Research Council, Washington, D.C., 2001, pp. 135-145.
45. Kim, B., R. Roque, and B. Birgisson, "Laboratory Evaluation of the Effect of SBS Modifier on Cracking Resistance of Asphalt Mixtures," *Transportation Research Record: Journal of the Transportation Research Board*, TRR 1829, TRB, National Research Council, Washington, D.C., 2003, pp. 8-15.

46. Kim, J., "Accurate Determination of Dissipated Creep Strain Energy and Its Effect on Load - and Temperature - Induced Cracking of Asphalt Pavement," Ph.D. Dissertation, University of Florida, Gainesville, Florida, 2005.
47. King, G.N., H. Muncy, and J. Prudhomme, "Polymer Modification: Binder's Effect on Mix Properties," Proceedings of the Association of Asphalt Paving Technologists, Vol. 55, 1986, pp. 519-540.
48. King, G.N., H.W. King, O. Harders, W. Arand and P. Planche, "Influence of Asphalt Grade and Polymer Concentration on the Low Temperature Performance of Polymer Modified Asphalt," Proceedings of the Association of Asphalt Paving Technologists, Vol. 62, 1993, pp. 1-22.
49. Lalwani, S., A. Abushihada and A. Halasa, "Reclaimed Rubber-Asphalt Blends Measurement of Rheological Properties to Access Toughness, Resiliency, Consistency and Temperature Sensitivity," Proceedings of the Association of Asphalt Paving Technologists, Vol. 51, 1982, pp. 562-579.
50. Lu, X, U. Isacsson and J. Ekblad, "Low-temperature Properties of Styrene-butadiene-styrene Polymer Modified Bitumens," *Construction and Building Materials*, Vol.12, Issue 8, 1998, pp. 405-414.
51. McGennis, R.B., S. Shuler, and H.U. Bahia, "Background of Superpave Asphalt Binder Test Methods," FHWA, Report No. FHWA-SA-94-069, Washington, D.C., 1994.
52. National Cooperative Highway Research Program, Project 1-37A-2002 "Mechanistic-Empirical (M-E) Pavement Design Guide (Draft)," NCHRP, Washington, D.C., 2004.
53. National Cooperative Highway Research Program, Project 9-29 "Simple Performance Tester for Superpave Mix Design," First Article: "Development and Evaluation," NCHRP Report 513, Washington, D.C., 2003.
54. Nijboer, L.W., "Plasticity as a Factor in the Design of Dense Bituminous Road Carpets" Elsevier Publishing Company Inc., New York, NY, 1948.
55. Papazian, H. S., "The Response of Linear Viscoelastic Materials in the Frequency Domain with Emphasis on Asphaltic Concrete," (1st) International Conference on the Structural Design of Asphalt Pavements, University of Michigan, 1962, pp. 454-463.
56. Pradhan, M. M. and J. D. Armijo, "Assessing Effects of Commercial Modifiers on Montana Asphalts by Conventional Testing Methods," Transportation Research Record, No. 1417, TRB, National Research Council, Washington, D.C., 1993, pp. 84-92.
57. Quintus, H., J. Mallela and M. Buncher, "Quantification of Effect of Polymer-Modified Asphalt on Flexible Pavement Performance" Transportation Research Record: Journal

of the Transportation Research Board, No. 2001, TRB, National Research Council, Washington, D.C., 2007, pp. 141-154.

58. Roberts, R.L., P.S. Kandhal, E.R. Brown, D. Lee, and T.W. Kennedy, *Hot Mix Asphalt Materials, Mixture Design, and Construction*, National Center for Asphalt Technology (NCAT), National Asphalt Pavement Association (NAPA), Research and Education Foundation, Lanham, Maryland, 1996.
59. Roque, R. and W. G. Buttlar, "The Development of a Measurement and Analysis System to Accurately Determine Asphalt Concrete Properties Using the Indirect Tensile Mode," *Journal of the Association of Asphalt Paving Technologists*, Vol. 61, 1992, pp. 304-332.
60. Roque, R., B. Birgisson and S. Kim, "Development of Mix Design Guidelines for Improved Performance of Asphalt Mixtures" Final Report, BD-545, RPWO#16, Florida Department of Transportation, Tallahassee, Florida, 2006.
61. Roque, R., B. Birgisson, Z. Zhang, B. Sangpetngam, and T. Grant, "Implementation of SHRP Indirect Tension Tester to Mitigate Cracking in Asphalt Pavements and Overlays" Final Report, BA-546, Florida Department of Transportation, Tallahassee, Florida, 2002.
62. Roque, R., B. Birgisson, C. Drakos, and B. Dietrich, "Development and Field Evaluation of Energy-Based Criteria for Top-down Cracking Performance of Hot Mix Asphalt," *Journal of the Association of Asphalt Paving Technologists*, Vol. 73, 2004, pp. 229-260.
63. Roque, R., B. Birgisson, B. Sangpetngam, Z. Zhang, "Hot Mix Asphalt Fracture Mechanics: A Fundamental Crack Growth Law for Asphalt Mixtures" *Journal of the Association of Asphalt Paving Technologists*, Vol. 71, 2002, pp. 816-828.
64. Ruth B.E., R. Roque, and B. Nukunya, "Aggregate Gradation Characterization Factors and Their Relationships to Fracture Energy and Failure Strain of Asphalt Mixtures" *Journal of the Association of Asphalt Paving Technologists*, Vol. 71, 2002, pp. 310-344.
65. Schapery, R.A., "Viscoelastic Behavior and Analysis of Composite Materials," Report MM 72-3, Mechanics and Materials Research Center, Texas A&M University, College Station, Texas, 1972.
66. Scofield, L.A., "The History, Development, and Performance of Asphalt Rubber at ADOT," Special Report, Report Number AZ-SP-8902, Arizona Department of Transportation, Materials Section, Phoenix, Arizona, 1989.
67. Shen, S. and S.H. Carpenter, "Application of the Dissipated Energy Concept in Fatigue Endurance Limit Testing," *Transportation Research Record: Journal of the*

Transportation Research Board, No. 1929, TRB, National Research Council, Washington, D.C., 2005, pp. 165-173.

68. Shih, C., "Evaluation of Asphalt Additives for Improved Cracking and Rutting Resistance of Asphalt Paving Mixtures," Ph.D. Dissertation, University of Florida, Gainesville, Florida, 1996.
69. SHRP-LTPP Protocol P07, "Test Method for Determining the Creep Compliance, Resilient Modulus, and Strength of Asphalt Materials Using the Indirect Tensile Test Device," SHRP, National Research Council, Washington, D.C., 2001.
70. Terrel, R.L. and J.L. Walter, "Modified Asphalt Pavement Materials - The European Experience," Proceedings of the Association of Asphalt Paving Technologists, Vol. 55, 1986, pp. 482-518.
71. The Asphalt Institute, "Mix Design Methods for Asphalt Concrete and Other Hot Mix Types," Manual Series No. 2 (MS-2), Maryland, 1984.
72. The Asphalt Institute, "Mix Design Methods for Asphalt Concrete and Other Hot Mix Types" Manual Series No. 2 (MS-2), Sixth Edition, Lexington, KY, 1993.
73. The Asphalt Institute, "Performance Graded Asphalts Binder Specification and Testing," Superpave Series No.1 (SP-1), Lexington, KY, 1994.
74. Transportation Research Board, "Superior Performing Asphalt Pavements (Superpave): The Product of the SHRP Asphalt Research Program," TRB Report Number SHRP-A-410, National Research Council, Washington, D.C., 1994.
75. Usmani, A.M., "Polymer Science and Technology," *Asphalt Science and Technology*, Marcel Dekker Inc., New York, NY, 1997, pp. 307-336.
76. Vallerga, B.A., and W.R. Lovering, "Evolution of the Hveem Stabilometer Method of Designing Asphalt Paving Mixtures," Proceedings of the Association of Asphalt Paving Technologists, Vol. 54, 1985, pp. 243 - 265.
77. Vavrik, W.R., W.J. Pine, G. Huber, and S.H. Carpenter, "The Bailey Method of Gradation Evaluation: The Influence of Aggregate Gradation and Packing Characteristics on Voids in the Mineral Aggregate," *Journal of the Association of Asphalt Paving Technologists*, Vol. 70, 2001, pp. 132-175.
78. Verhaeghe, B.M.J.A., F.C. Rust, R.M. Vos and A.T. Visser, "Properties of Polymer- and Fiber-Modified Porous Asphalt Mixes," Proceedings of the 6th Conference on Asphalt Pavements for Southern Africa, Vol. 1, Cape Town, South Africa, 1994, pp. III-262-280.

79. Villiers C., "Sensitivity of Superpave Mixtures for Development of Performance-Related Specifications," Ph.D. Dissertation, University of Florida, Gainesville, Florida, 2004.
80. Warren, R.S., R.B. McGennis, and H.U. Bahia, "Superpave Asphalt Binder Test Methods — An Illustrated Overview," Report No. FHWA-SA-94-068, Federal Highway Administration, Washington, D.C., 1994.
81. Wagon, V. and B. Brule, "The Structure of Polymer Modified Binders and Corresponding Asphalt Mixtures," Proceedings of the Association of Asphalt Paving Technologists, Vol. 68, 1999, pp. 64-88.
82. White, T.D., "Marshall Procedures for Design and Quality Control of Asphalt Mixtures," Proceedings of the Association of Asphalt Paving Technologists, Vol. 54, 1985, pp. 265-284.
83. Witczak, M. W., I. Hafez, H. Ayres, & K. Kaloush, "Comparative Study of MSHA Asphalt Mixtures Using Advanced Dynamic Material Characterization Tests," Maryland Department of Transportation, Maryland Port 532 Administration, Department of Civil Engineering, University of Maryland, College Park, MD, 1996.
84. Witczak, M. W., R. Bonaquist, H. Von Quintus, and K. Kaloush, "Specimen Geometry and Aggregate Size Effects in Uniaxial Compression and Constant Height Shear Test," Journal of the Association of Asphalt Paving Technologists, Vol. 69, 2000, pp. 733-782.
85. Witczak, M. W., K. Kaloush, T. Pellinen and M. El-Basyouny, "Simple Performance Test for Superpave Mix Design," NCHRP Report 465, National Cooperative Highway Research Program, TRB, National Research Council, Washington, D.C., 2002.
86. Witczak, M. W., "Laboratory Determination of Resilient Modulus for Flexible Pavement," NCHRP Research Results Digest, No. 285, TRB, National Research Council, Washington, D.C., 2004.
87. Yoder, E.J. and M.W. Witczak, *Principles of Pavement Design*, Second Edition, John Wiley & Sons, Inc., New York, NY, 1975.
88. Zhang, W., A. Drescher, and D. E. Newcomb, "Viscoelastic Analysis of Diametral Compression on Asphalt Concrete," Journal of Engineering Mechanics, Vol. 123, ASCE, 1997, pp. 596-603.
89. Zhang, Z., "Identification of Suitable Crack Growth Law for Asphalt Mixtures Using the Superpave Indirect Tensile Test (IDT)," Ph.D. Dissertation, University of Florida, Gainesville, Florida, 2000.

90. Zhang, Z., R. Roque, and B. Birgisson, "Identification and Verification of a Suitable Crack Growth Law for Asphalt Mixtures," *Journal of the Association of Asphalt Paving Technologists*, Vol. 70, 2001, pp. 206-241.